SOME ASPECTS OF THE NUMERICAL SOLUTION OF EQUILIBRIUM PROBLEMS IN FINITE ELASTICITY

by

G A DUFFETT B.Sc(Eng), M.Sc(Eng)

A thesis submitted in fulfilment of the requirements for the degree of Doctor of Philosophy

Department of Civil Engineering
University of Cape Town

August 1985

ABSTRACT

Analytical and computational aspects of solution paths for nonlinear equations are examined, with emphasis on problems in which there are many parameters. The solution to problems of this type is described by an equilibrium hypersurface and methods are presented which allow for the determination of the various features of this surface. These include methods for following numerically any curve on the primary surface, and for determining on such a curve all the singular points (both limit and bifurcation points). Further methods are then presented which allow branching onto secondary paths (subsets of secondary surfaces) from bifurcation points in order to trace out these paths and so determine the bifurcation behaviour of the problem considered. To complete the analysis of the equilibrium surface methods are developed to trace the loci of singular points. The locus of a bifurcation point determines the intersection of the primary and secondary equilibrium surfaces while the loci of limit points allow for the determination of regions of stable and unstable behaviour on the equilibrium surface.

These methods are applicable to any system of nonlinear equations but the particular application here is to systems of equations obtained from the finite element approximation of boundary-value problems in elasticity. Attention is restricted to plane boundary-value problems involving incompressible hyperelastic materials. The strain-energy function used to characterise these materials is based on a symmetric function of the principal stretches.

All of the above ideas are investigated numerically for the problem of a pressurised rubber cylinder subjected to axial extension. This problem contains two identifiable loading parameters and exhibits complex limit and bifurcation behaviour, which is studied in some detail.

DECLARATION

I, Gino Alan Duffett, hereby declare that this thesis is essentially my own work and that no part of it has been submitted for a degree at any other university.

Signed by candidate

Signature Removed

G A DUFFETT

August 1985

ACKNOWLEDGEMENTS

I wish to express my gratitude to the following

My supervisor, Professor B D Reddy, for his guidance, patience and encouragement throughout this work.

My postgraduate colleagues, especially Dave Hawla, Colin Mercer and Luis Resende, for many useful discussions concerning the research work.

The staff of the Computer Centre of the University of Cape Town for keeping the UNIVAC going during periods of intensive computation.

The Council of Scientific and Industrial Research for their financial assistance.

Mrs Shirley Breed for her accurate and speedy typing of the manuscript.

My parents and friends for their encouragement and continuous support during this work.

CONTENTS

CHAPTER 1

INTRODUCTION

In this introduction we present reviews of methods for the solution of nonlinear equations, and of the finite element approximation of boundary-value problems in finite elasticity. We then give a brief account of the objectives of this thesis.

Solution of nonlinear equations

There has been for many years a sustained interest in both theoretical and practical aspects of the solution of nonlinear equations of the form

$$f(u,\lambda) = 0 \tag{1.1}$$

in which u belongs to some space U (most generally a Banach space), λ is a real parameter and f is a map from $U \times R$ to another space V. The solution to equation (1.1) comprises equilibrium paths or branches that can be defined in the space $U \times R$. A brief history and digest of methods developed to obtain these paths is given by ALLGOWER and GEORG (1980).

In some applications certain quantities are naturally identified as parameters (FINK and RHEINBOLDT (1984)); for example, in structural analysis we may have load intensities, prescribed displacements, imperfection amplitudes or material constants : these parameters are usually used to control the solution process and to parameterise the solution arc. Depending on the choice of parameter, however, the solution arc may contain points at which the (Frechet) derivative of f with respect to u vanishes : these points are called singular points and it can be shown that such points are either limit points or bifurcation points (KELLER (1977) and RIKS (1979)) (see Figure 1.1). A self-contained account of the analysis of the behaviour of the solution path in the vicinity of singular points is given by DECKER and KELLER (1981). In their three papers BREZZI, RAPPAZ and RAVIART (1980, 1981a, 1981b) give a complete analysis of approximate solutions to nonlinear problems including solution paths, limit points and bifurcation points.

Since we will be concerned with systems of equations for which $U = V = R^n$ in (1.1), we concentrate henceforth on various aspects of this special case. Continuation methods employing Newton-Raphson iteration (also called Newton methods) have been widely used (ORTEGA and RHEINBOLDT (1970)) in the numerical computation of solution paths of nonlinear equations of the form (1.1). These methods use information at a known point on the solution path to compute a predictor to the next point on this path; this predictor is then corrected using Newton-Raphson iteration until the solution point on the path is obtained. The complete solution path is traced out in this manner. These methods, in their standard or modified forms (see for example STRICKLIN, HAISLER and VON RIESEMAN (1973), BATHE and CIMENTO (1980), ZHANG and OWEN (1982) and

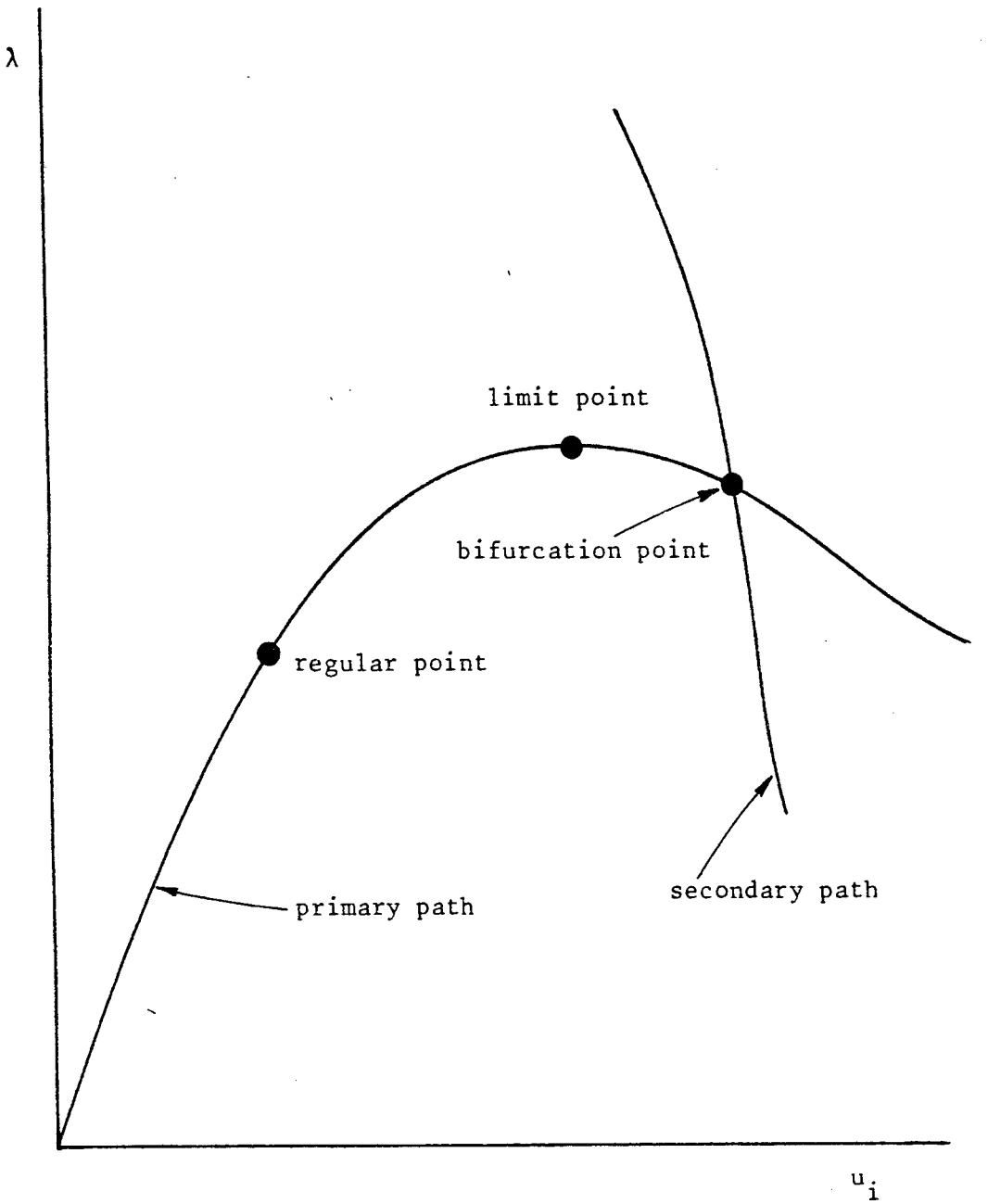

Figure 1.1 Solution paths for $f(u,\lambda) = 0$.

CRISFIELD (1979, 1984)), have been found generally to be very efficient, but they are unable to be used without certain adaptations for general problems in which singular behaviour may occur. In order to overcome the problems inherent in these Newton methods various methods have been developed (see for example THURSTON (1969), WELLFORD and DIB (1976, 1980), BERGAN (1980), BERGAN et al (1978), KARAMANLIDIS, HONECKER and KNOTHE (1981), BARTOZ and DHATT (1979), POWELL and SIMONS (1981)), but lack of generality has led to their use being rather limited. The "homotopy methods" of RHEINBOLDT (1981), KAMAT, WATSON and VENKAYYA (1983) and WATSON et al (1983, 1985) and "arc-length" methods, however, provide a more general alternative for the tracing of solution paths in which singular behaviour may occur. These methods are similar in spirit but "homotopy methods" rely on ordinary differential equation techniques (KAMAT et al (1983)) while generalisation of the Newton method gives us the "arc-length" methods.

Currently the most popular means of generalising the Newton method so that it may deal effectively with problems having singularities, is the inflation procedure proposed independently by RIKS (1972, 1979) and WEMPNER (1971) for finite-dimensional problems and by KELLER (1977) for problems in which f is a map from one Banach space to another. This method introduces some parameterisation of the solution path (usually the approximate arc-length) with an additional constraint equation which effectively relates the variables to this parameter. We thus seek solutions to the system of nonlinear equations of the form

$$\begin{aligned} f(u,\lambda) &= 0 \quad , \\ h(u,\lambda,s) &= 0 \quad , \end{aligned} \tag{1.2}$$

in which s is used to parameterise the solution path, u and λ are now the unknown variables and h represents the additional (arc-length) constraint equation. The various methods that have been proposed differ in their definition of this constraint equation (Figure 1.2); for example the solution may be constrained to lie on a hyperplane (RIKS (1979), WEMPNER (1971)), on a hypersurface (KELLER (1977)) which may be spherical (CRISFIELD (1981)) or on a hyperelliptic surface (PADOVAN and TOVICHAKCHAIKUL (1982)). WATSON and HOLZER (1983) have shown that quadratic convergence is achieved using the method of CRISFIELD (1981). These methods have subsequently been modified by various authors (RAMM (1981), WASZCZYSZYN (1983), BATHE and DVORKIN (1983), CRISFIELD (1982, 1983) and FRIED (1984)) in order to improve overall efficiency and to render the method more suitable for use in large general purpose computer programs. ABBOTT (1980) presents a routine that computes solutions to equations (1.2) using these methods. A key feature of these inflation procedures is the ease with which they allow for continuation of the solution path through limit and bifurcation points, thus providing a useful tool for the stability analysis of structural systems. Theoretical aspects and further numerical algorithms for continuation methods are discussed in some detail by RHEINBOLDT (1980).

A further improvement that most curve-following techniques have in common (ALLGOWER and GEORG (1980)) is that of automatically selecting increment sizes : strong motivation for this is given by SCHWETLICK (1984) and also by BROCKMAN (1984). This improvement provides increments that are neither unnecessarily small (and hence uneconomical) nor so large that convergence is slow or non-existent. Many methods

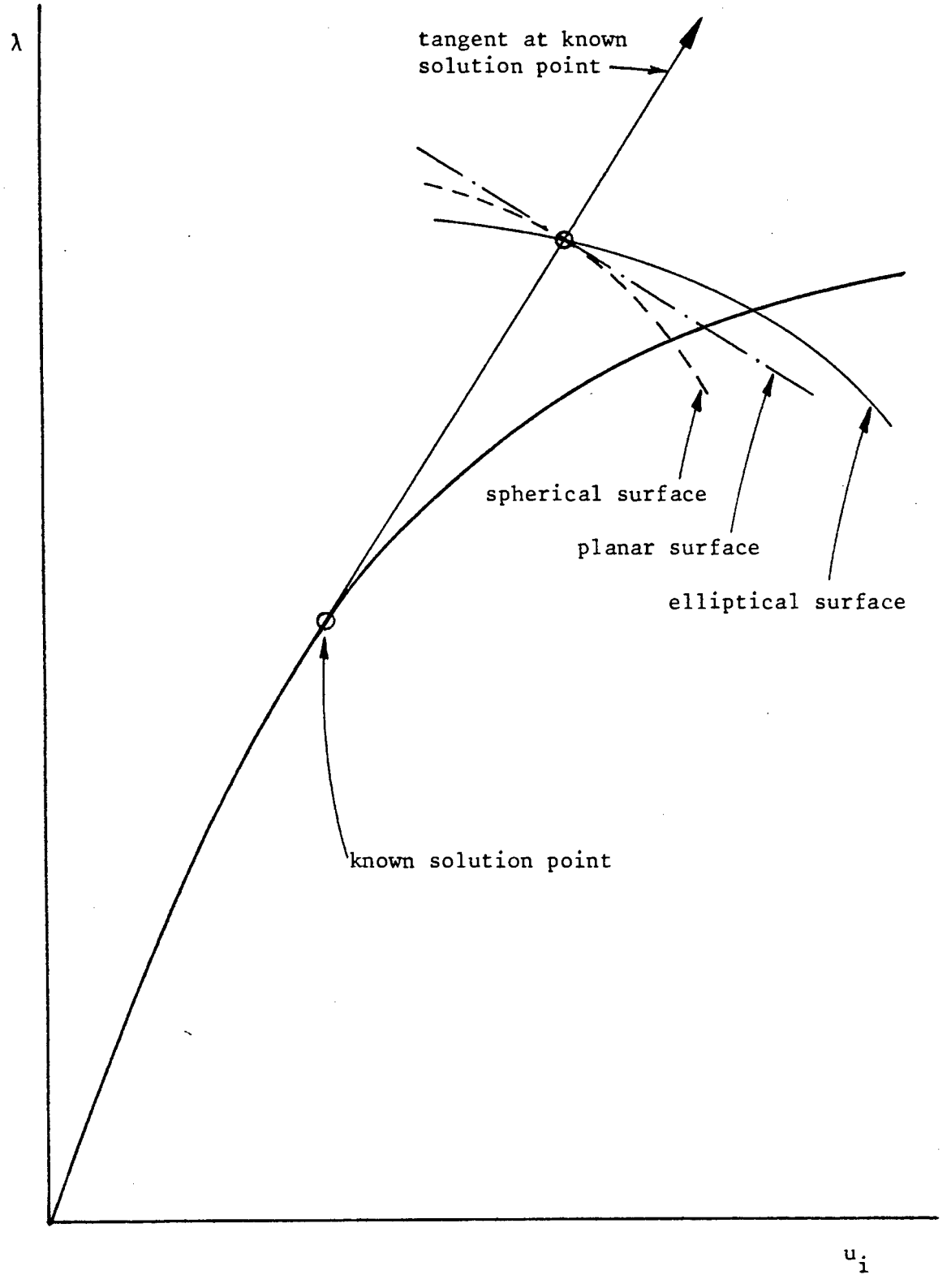

Figure 1.2 Arc-length method showing various intersecting surfaces.

have been proposed to automatically select increment sizes : they include simple methods based on numerical experience (ABAQUS Theoretical Manual (1982)), the methods proposed by CRISFIELD (1980, 1981), RAMM (1981), BERGAN (1980) and BERGAN et al (1978) as well as the more complex methods proposed by SCHMIDT (1978), RHEINBOLDT (1980), DEN HEIJER and RHEINBOLDT (1981) and DEUFLHARD (1979). All of these schemes provide large increments in regions of small curvature of the solution arc and small increments in regions where there is greater curvature and thus enhance the efficiency of the continuation procedures into which they are incorporated.

The analysis of singular (limit or bifurcation point) behaviour is often very important, particularly in structural systems. RIKS (1984) surveys some methods that are used for the analysis of singular points; two aspects are almost always considered : the determination of singular points on the solution paths and also the determination of the secondary branch that intersects with the primary solution path at a bifurcation point. Frequently only the initial behaviour along this secondary branch may be required. SEYDEL (1979) and MOORE and SPENCE (1980) use so-called "direct" methods to compute these singular points, but many authors (SIMPSON (1975), KELLER (1977, 1981), FUJIKAKE (1985)) use continuation methods for locating the singular points and then further methods for computing it accurately. This approach seems more popular since the solution path is required in most cases anyway. When the singular point is a simple bifurcation point we know that two non-tangential solution arcs intersect at this point (DECKER and KELLER (1981)) and frequently this secondary (or bifurcation) branch is also required (Figure 1.1). This may be a singular point at which many

paths intersect (DECKER and KELLER (1980)) but such points do not concern us. In order to change branches at bifurcation points we require methods to compute an initial point on the secondary path; then using continuation we are able to trace out this secondary arc. Many methods for obtaining this initial point have been proposed (KELLER (1977), RHEINBOLDT (1978), RIKS (1979) and SEYDEL (1983)); these methods all use some initial guess of the tangent to the secondary path at the bifurcation point, in order to compute the predictor to the initial point on the secondary path. WEBER (1985) has proposed a multigrid iteration technique and MEHRA and CARROLL (1978) search for the secondary branch in a plane through the bifurcation point; they have used this method in their studies on the stability of aircraft in flight. KUBICEK and KLIC (1983) discuss different possibilities for the intersecting branches at simple bifurcation points.

Multi-parameter systems

In many applications it is not uncommon to encounter systems of equations in which there are two or more parameters. For example, finite element approximations of nonlinear boundary-value problems in structural mechanics frequently lead to such systems, the parameters representing different material and geometric constants and/or prescribed values of load, displacement or temperature, and so on. The equations governing these problems are similar to equation (1.1) but λ now represents a vector in the real parameter space R^m. The solution to these problems is no longer a path but rather a surface in $U \times R^m$ and we are thus interested in determining various features of

this surface. For these multi-parameter problems we may use continuation methods : (i) to follow numerically any curve on the surface specified by a particular combination of parameters; (ii) to determine on this curve all the singular points; (iii) to determine the secondary paths intersecting this curve at the bifurcation points; and (iv) to trace the locus on the surface of any singular point we may find on this curve. These analyses combine to give us a description of the complete equilibrium surface (BABUSKA and RHEINBOLDT (1982)).

It is customary, when there are many parameters, to assign (m-1) conditions involving the m parameters so that the system reduces to one having a single independent parameter; for example, (m-1) of the parameters may simply be held fixed (FINK and RHEINBOLDT (1984)). By varying the values of the fixed parameters it is possible to trace out a family of solution paths and thus determine the shape of the equilibrium surface. It is also possible to determine all the singular points encountered along these paths. Note, of course, that the occurrence of singular points and their determination depend upon the parameters that are chosen (FINK and RHEINBOLDT (1984)). The loci of limit points trace out the crests and troughs of the equilibrium surface and hence are of use in determining regions of stable and unstable behaviour (BABUSKA and RHEINBOLDT (1982)). RHEINBOLDT (1982) presents a method for determining these "critical boundaries" on the equilibrium surface.

Finite element approximation of problems in nonlinear elasticity

All of the above methods are applicable to any system of nonlinear equations, though the application we are interested in is to systems of equations obtained from the finite element approximation of nonlinear boundary-value problems in elasticity. Reviews of work in this field can be found in ODEN (1972), CESCOTTO, FREY and MASSONNET (1980), SHIELD (1983) and others. Much attention has been given to boundary-value problems involving incompressible hyperelastic materials in which there has been practical (see for example KLINGBEIL and SHIELD (1966), HAGGBLAD and SUNDBERG (1983) and BAPAT and BATRA (1984)) and also much theoretical interest. Of course, elastic bodies are really slightly compressible but the assumption is usually made that rubbers and rubberlike materials undergo no volume change. When this is done, the incompressibility constraint must be enforced in some manner. Many formulations have been proposed which enforce this constraint and thus allow for finite element analysis of these elastic bodies. We have, for example, mixed formulations in which hydrostatic pressure is included as a variable (ODEN and KEY (1970), SCHARNHORST and PIAN (1978), BATRA (1980), MALKUS (1980), RUAS (1981), GLOWINSKI and LE TALLEC (1982, 1984)) and the penalty or displacement formulations (CESCOTTO and FONDER (1979), JANKOVICH et al (1981), SIMO and TAYLOR (1982)). Some of these methods as well as others have been reviewed by CESCOTTO and FONDER (1979), ALY (1981) and ODEN and KIKUCHI (1982), the last giving special attention to reduced integration-penalty methods. Both of the basic methods (mixed or penalty) are widely used and neither method appears, from the literature, to be indisputably more advantageous than the

other. Penalty methods have the advantage that the pressure is not present as a variable, but they can be unstable unless a careful choice is made of element types and integration schemes.

The form of the strain-energy function which governs the constitutive laws for isotropic hyperelastic materials such as rubber has also aroused much interest in recent years. A review of the elastic behaviour of rubberlike solids is given by TRELOAR (1973) and OGDEN (1982); also included are discussions on strain-energy functions for incompressible and compressible rubberlike materials. Further discussions on the forms of the strain-energy function for isotropic incompressible elastic materials are given by ODEN and KEY (1972) and SHIELD (1983). In almost all applications to date the strain-energy function is written in terms of the principal invariants of the Green-Saint Venant (or left Cauchy-Green) deformation tensor. OGDEN (1972a), however, developed a strain-energy function for an incompressible isotropic hyperelastic material which is written as a symmetric function of the three principal components of stretch. The strain-energy function takes the simple form of a summation over a finite number of terms and is thus very general and applicable to a wide range of rubberlike materials. This form includes as a special case the often-used neo-Hookean and Mooney-Rivlin approximations. Good correlation between theory and experiment is obtained for this class of strain-energy function which OGDEN (1972b, 1976, 1978) has since extended to allow for volume changes. HAUGHTON and OGDEN (1978a,b, 1979a,b), HAUGHTON (1980), OGDEN and CHADWICK (1972), OGDEN et al (1973) and CHADWICK et al (1977) have used this form of strain-energy function extensively in their analyses of rubberlike tubes, cylinders and

spheres, in which they analyse equilibrium behaviour and also give specific results for limiting and bifurcating problems.

The finite element analysis of incompressible nonlinear elastic solids has been limited mainly to the study of stable solution paths using the well-known Newton methods; comprehensive summaries of this work are given by ODEN (1972) and ALY (1981), while DUFFETT and REDDY (1983) use OGDEN'S (1972a) strain-energy function in a general-purpose finite element program for static problems. These methods, as we have discussed before, break down near singular points and are thus not suitable for a complete analysis (SANDIDGE and ODEN (1974)). However, the inflation procedures proposed by RIKS (1979), KELLER (1977) and WEMPNER (1971) are easily included into finite element programs and thus allow us to analyse a wide range of problems in which singular behaviour may occur. This has been done by many authors mentioned here for limit point analysis of elastic structures. Recently ENDO, ODEN, BECKER and MILLER (1984) have used these methods for limit point (and contact) analysis of rubber solids. The bifurcation problem however, has not received as much attention : KIKUCHI (1978) has investigated finite element approximations to simple bifurcation problems, but there appears to be little work done on the tracing of branches intersecting at bifurcation points in finite element analysis programs (see RIKS (1979)).

Objectives

The objective of this thesis is to develop a finite element analysis of isotropic incompressible hyperelastic bodies which will enable us to determine complete equilibrium surfaces (that is, both primary and secondary) for problems in which there are many parameters. A general description of these surfaces may be obtained by tracing a few primary paths, determining the singular points on these curves and then tracing the bifurcation branches and loci of the singular points from these primary paths (see Figure 1.3); we thus present general methods which can be used to carry out these computations.

The solution paths to multi-parameter problems may be obtained by simply fixing (m-1) parameters, thus reducing the system to one having a single parameter (FINK and RHEINBOLDT (1984)). However, we take the alternative route of adding to the original system of equations an additional (m-1) equations; the choice of the equations is of course arbitrary, and this flexibility allows us to choose equations which will give us the solution path of interest. The solution path is thus governed in general by the system

$$\begin{aligned} f(u,\lambda) &= 0 \quad , \\ h(u,\lambda,s) &= 0 \quad , \\ g(u,\lambda) &= 0 \quad , \end{aligned} \tag{1.3}$$

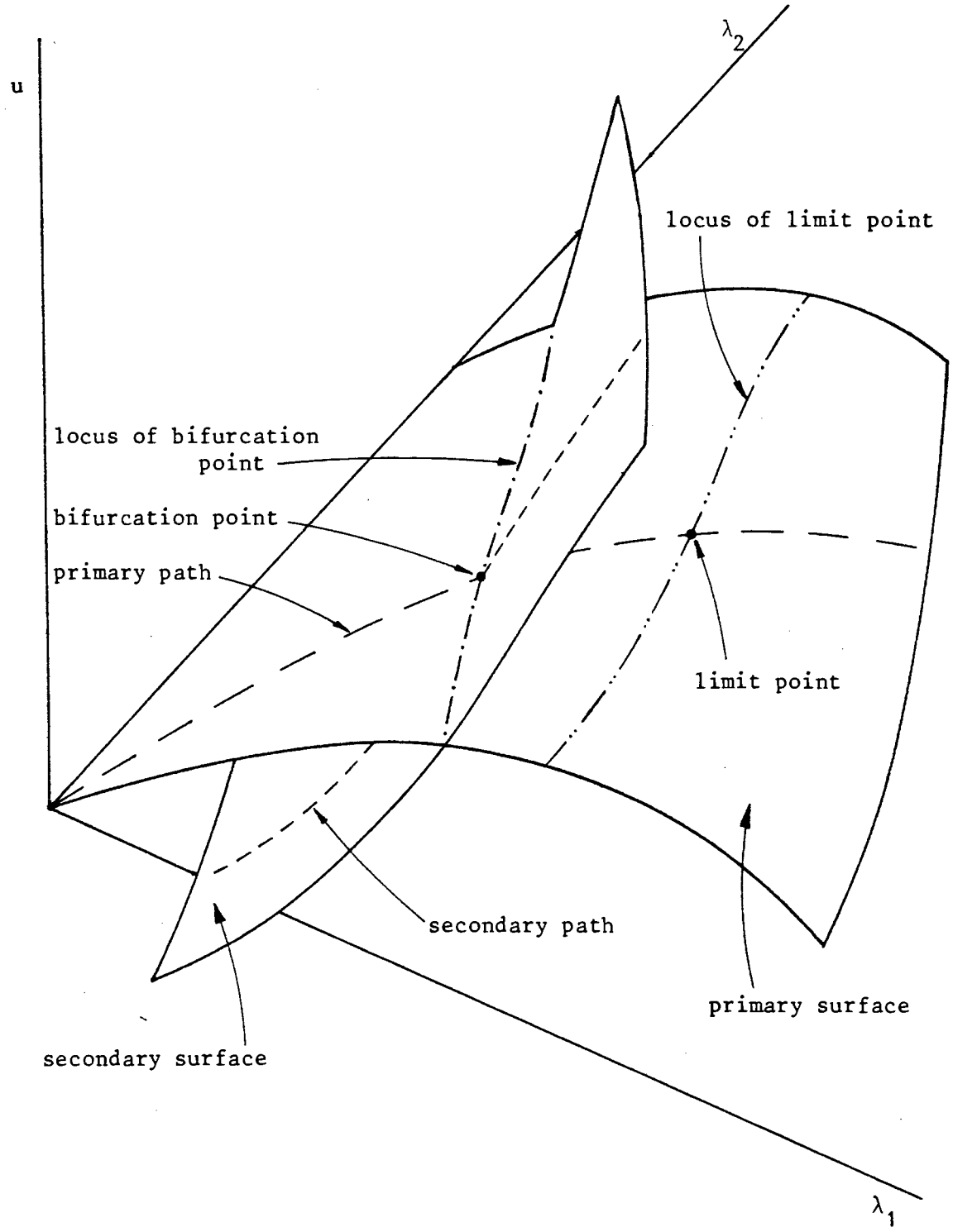

Figure 1.3 Primary and secondary equilibrium surfaces for 2 parameter problem (n=1, m=2) showing solution paths of interest.

where λ is now a vector in R^m and g represents the additional (m-1) constraint equations. Note, of course, that the systems of equations (1.1) and (1.2) are merely subsets of equations (1.3). The solution path of interest is thus an intersection between the complete equilibrium surface (as yet unknown) and the surfaces formed by the constraint equations in the space $U \times R^m$ (Figure 1.4). We examine two possibilities for these constraint equations : prescribing a piecewise-linear path in parameter space for multi-parameter problems and determining loci of singular points for 2-parameter problems. For multi-parameter problems the relationship between the parameters, given by the piecewise-linear paths, determines the direction that the solution arc must follow.

As we trace our required solution path, using the continuation methods discussed previously, we locate and also characterise all singular points that are found along this arc. We are then able to return to the vicinity of each of these singular points in turn, compute the (approximate) singular point, and then, if required, either trace the secondary paths (from bifurcation points) or trace the locus of the singular point (from limit or bifurcation points).

Tracing of the secondary paths from the computed bifurcation points is done using the methods discussed previously; these paths are, in general, also dependent upon the m parameters and are thus subsets of surfaces in the solution space $U \times R^m$. The locus of a bifurcation point is therefore the intersection between the primary equilibrium surface and the secondary (bifurcated) surface. The tracing of the locus of a singular point is carried out by following the solution path

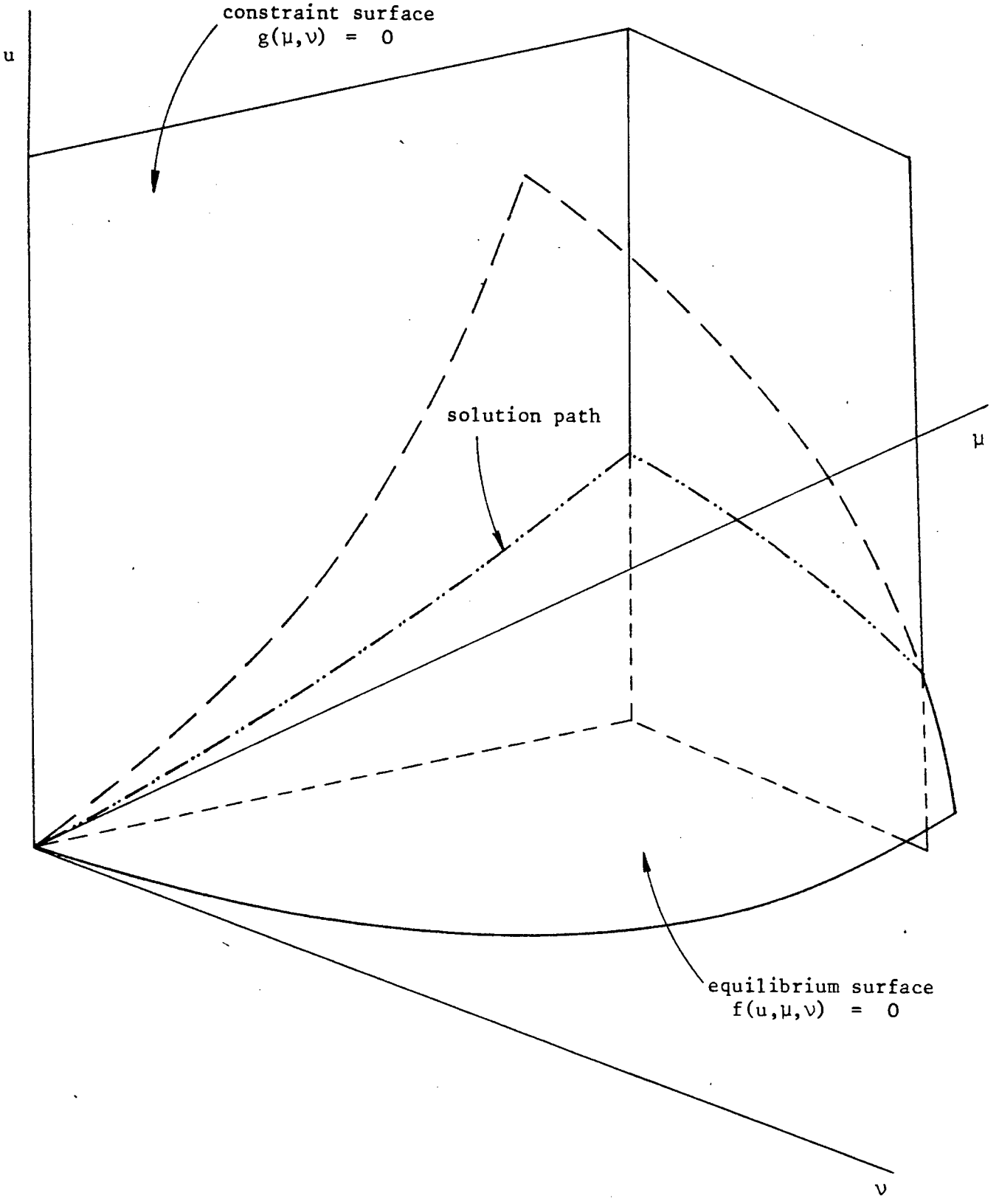

Figure 1.4 Intersection of equilibrium surface with the constraint surfaces for a problem with n=1, m=2 .

governed by the system (1.3) where, normally, we have only 2 parameters and the constraint equation g constrains the solution to lie on a path of singular points.

Our attention is restricted to plane boundary-value problems and we use a mixed formulation in which the incompressibility constraint is satisfied in an average sense over each finite element (THOMPSON (1975)). The strain-energy function developed by OGDEN (1972a) is used to characterise the isotropic elastic material. This strain-energy function is written as a summation over a finite number of terms involving the three principal components of stretch. It is very general and applicable to a wide range of rubberlike materials, which makes its inclusion in a program of the kind developed here, very desirable. Some preliminary work in this direction has been carried out by DUFFETT and REDDY (1983).

The layout is basically in four parts : nonlinear elasticity, systems of nonlinear equations, computation of solutions and an application of the methods. In chapter 2, after briefly describing our notation, we present basic results from continuum mechanics and formulate the boundary-value problem of elasticity (section 2.1). The boundary conditions applicable to our problems include prescribed displacements, prescribed tractions and prescribed pressures which are dependent upon the deformation of the body (HIBBITT (1979) and ALY (1981)). First-order and second-order elastic moduli are discussed in sections 2.2 and 2.3; here use is made of the work presented by CHADWICK and OGDEN (1971a,b) and OGDEN (1974), for the components of these moduli referred to principal axes. In section 2.4 we obtain the first- and

second-order elastic moduli for OGDEN'S (1972a) strain-energy functions; we show too, for plane problems, that the moduli relative to an arbitrary set of axes can be written simply in terms of the moduli relative to the principal axes. Finite element approximations are introduced into our boundary-value problem in section 2.5 and the equilibrium equation together with the incompressibility constraint equation result in a system of nonlinear equations that we require to be solved.

In chapter 3 we examine analytical and computational aspects of solution paths for these systems of nonlinear equations. Firstly, in section 3.1, we review the theory relating to singular points of systems of equations that have a single parameter (DECKER and KELLER (1980, 1981)). The inflation procedures proposed by RIKS (1979), KELLER (1977) and WEMPNER (1971) and some modifications are also reviewed in this section. Secondly, we consider systems of equations with many parameters in section 3.2. Drawing on the results in section 3.1 we investigate the nature of singular points and how these are affected by singularities in the additional set of equations relating these parameters to each other. We extend the inflation procedure to multi-parameter problems and then illustrate these ideas by developing, in section 3.2.3, a set of equations which are appropriate when the parameters are related to each other in a piecewise-linear manner. Another application of this inflated system is that of tracing the locus of a singular point for problems that have two parameters. The aim here is to constrain the system so that the solution follows a path of singular points; this constraint is discussed in section 3.2.4.

The ideas and the formulations in the two previous chapters are used together in chapter 4 where we present numerical methods of solution for our inflated systems of equations. We use a predictor-corrector method for continuation along a solution path, the corrector process using the Newton-Raphson iteration method which is described in general terms in section 4.1.1 and applied to our inflated system of equations in section 4.1.2. Here we also show that the computation of most of the coefficients required for this process may be done for each finite element and then assembled into a global system of equations which is then solved. We thus discuss the element computations for the equilibrium equations (including incompressibility constraints) which are common to all the analyses in section 4.1.3. In section 4.2 we deal with computations required for singular problems; here we present the computations for the arc-length constraint equation (section 4.2.1) as well as the methods used for the location of singular points (section 4.2.2) and those required to compute the initial regular point on a secondary branch from a bifurcation point (section 4.2.3). The methods discussed in sections 4.1 and 4.2 can therefore be used for a complete analysis of single-parameter problems, including location of singular points and tracing of secondary paths. Sections 4.3 and 4.4. relate to two aspects of multi-parameter problems. The computations required for the piecewise-linear parameter constraint equations are presented in section 4.3.1 and the method used to ensure that the solution follows the correct path prescribed by the relationship between the parameters is given in section 4.3.2. The computations for the Newton-Raphson coefficients in sections 4.2 and 4.3 are done on a global level as this is much simpler for these equations. However, in section 4.4.1 the computations described for the singular point locus constraint equation are done at the element level. These computations are very computer-

intensive, but this is justifiable since many solution paths would have to be traced in order to obtain the same result. The method by which we begin tracing this locus is discussed in section 4.4.2.

Other general computational procedures which are required for all the different analyses described above are outlined in section 4.5. In particular, we discuss scaling of the system of equations so that the dimensions of all quantities in the solution space are approximately of the same order of magnitude (section 4.5.1), and we also discuss the method proposed by KELLER (1977) for solving a system of simultaneous equations by exploiting the symmetry in some part of the system (section 4.5.2). Lastly, in section 4.6, we describe some methods of automatic incrementation which attempt to improve the efficiency of continuation methods by ensuring that the increment sizes are neither too small nor too large along the solution arc.

To complete this study we apply the methods presented here to a problem studied in detail by HAUGHTON and OGDEN (1979b), that of a pressurised rubber cylinder subjected to extension along its axis. This example has been chosen since it contains two identifiable loading parameters and also exhibits complex limit point and bifurcation behaviour which can be studied in some depth. In chapter 5 we present results and related discussion pertaining to the computation of the equilibrium surface, the tracing out of any prescribed path on it and the location of singular points on the path. We also present results and discussion for the tracing of secondary paths from bifurcation points which show some interesting bifurcation behaviour, and the tracing of the loci of singular points.

CHAPTER 2

EQUATIONS OF NONLINEAR ELASTICITY

This chapter describes the derivation of a system of nonlinear algebraic equations which arise from a finite element approximation of the boundary-value problem of elasticity. Firstly, after a brief description of our notation, we summarise some basic results from continuum mechanics and proceed to define our boundary-value problem of elasticity in section 2.1. First-order elastic moduli required for the constitutive relations of incompressible materials are discussed in section 2.2 while second-order moduli are discussed in section 2.3. In these sections extensive use is made of results obtained by CHADWICK and OGDEN (1971a,b) and OGDEN (1974) for components of these moduli referred to principal axes. We then obtain these moduli for plane problems in section 2.4 for a class of strain-energy functions derived by OGDEN (1972a) and express the relationships between the moduli relative to an arbitrary set of axes, and those relative to the principal axes, in compact matrix form. In section 2.5 we describe the finite element approximation to our boundary-value problem and obtain a set of nonlinear algebraic equations from which the solution to our problem is obtained using the methods described in the following chapters.

Notation

Throughout this thesis both invariant and indicial notation will be used where appropriate. Thus vectors, which will be denoted by lower

case letters where possible, will be written, for example, as $\underset{\sim}{b}$ while the components relative to a fixed orthonormal basis will be written as b_i or b_α . We will use lower case Roman letters for sub- and superscripts when the range of the sub- or superscript is from 1 to 3 but lower case Greek symbols will be used when the range is only from 1 to 2. This also applies to second and higher order tensors which will generally be denoted by upper case letters so that, for example, we have a second order tensor $\underset{\sim}{T}$ with components T_{ij} (9 components) or $T_{\alpha\beta}$ (4 components).

The indicial notation allows us to adopt the summation convention in which summation is implied over repeated sub- and superscripts. For example, the dot product in three dimensions can be written as

$$a = \underset{\sim}{b}\cdot\underset{\sim}{c} \quad \text{or} \quad a = \sum_{i=1}^{3} b_i c_i \quad \text{or} \quad a = b_i c_i \ ; \tag{2.1}$$

in two dimensions the subscript i in (2.1) is simply replaced by a lower case Greek letter. The vector product is written as

$$\underset{\sim}{r} = \underset{\sim}{s} \wedge \underset{\sim}{t} \ . \tag{2.2}$$

The scalar product of two tensors $\underset{\sim}{T}$ and $\underset{\sim}{S}$ is defined by

$$\underset{\sim}{T}\cdot\underset{\sim}{S} = T_{ij}S_{ij} \tag{2.3}$$

The Kronecker delta is another symbol that will be used in conjunction with the index notation. It is defined by

$$\delta_{ij} = \begin{cases} 1 \text{ if } i = j \\ 0 \text{ if } i \neq j \end{cases} , \tag{2.4a}$$

in three dimensions and by

$$\delta_{\alpha\beta} = \begin{cases} 1 \text{ if } \alpha = \beta \\ 0 \text{ if } \alpha \neq \beta \end{cases} \tag{2.4b}$$

in two dimensions. The invariant form of the Kronecker delta is the Identity tensor which is written as $\underset{\sim}{I}$.

The gradient of a vector field $\underset{\sim}{u}(X_i)$ is defined by

$$\text{Grad } \underset{\sim}{u} \equiv (\partial u_i / \partial X_j)\, \underset{\sim}{e}_i \otimes \underset{\sim}{e}_j \quad , \tag{2.5}$$

and the divergence of a tensor field $\underset{\sim}{S}(X_i)$ is defined by

$$\text{Div } \underset{\sim}{S} \equiv (\partial S_{ij} / \partial X_j)\, \underset{\sim}{e}_i \quad . \tag{2.6}$$

2.1 Kinematics, stresses and the boundary-value problem of elasticity

We identify a body with a region Ω which it occupies in some fixed reference configuration at time t_o, say. The current position of a material particle is given by the spatial coordinates $\underset{\sim}{x} = \underset{\sim}{x}(\underset{\sim}{X},t)$ where $\underset{\sim}{X}$ is the position occupied by the particle in the reference configuration. Clearly $\underset{\sim}{x}(\underset{\sim}{X},t_o) = \underset{\sim}{X}$. In rectangular Cartesian coordinates the components of $\underset{\sim}{x}$ will be given by

$$x_j = x_j(X_1,X_2,X_3,t) \quad , \quad j = 1,2,3 \tag{2.7}$$

where X_1, X_2 and X_3 are the material coordinates in the reference configuration. For plane problems (plane strain, plane stress) we use the (X,Y,Z) coordinate system while for axisymmetric problems the (r,Z,Θ) coordinate system is used. The material and spatial coordinates will be measured with respect to a fixed set of axes with orthonormal basis $\underset{\sim}{e}_i$. The deformation gradient $\underset{\sim}{F}$ is then defined by

$$\underset{\sim}{F} \equiv \text{Grad}\, \underset{\sim}{x} = (\partial x_i/\partial X_j)\, \underset{\sim}{e}_i \otimes \underset{\sim}{e}_j \quad . \tag{2.8}$$

We assume that $\underset{\sim}{F}$ possesses an inverse and we write

$$J \equiv \det \underset{\sim}{F} \neq 0 \quad . \tag{2.9}$$

Since the displacement field $\underset{\sim}{u}$ is defined by $\underset{\sim}{u} = \underset{\sim}{x} - \underset{\sim}{X}$ it follows that

$$\underset{\sim}{F}(\underset{\sim}{u}) = \text{Grad } \underset{\sim}{u} + \underset{\sim}{I} \quad . \tag{2.10}$$

We will only be dealing with plane deformations (plane strain, plane stress and axisymmetric problems) where the plane of deformation coincides with the X_1X_2 plane of the Cartesian coordinates system so we may write

$$\underset{\sim}{F} = (\partial x_\alpha / \partial X_\beta)\, \underset{\sim}{e}_\alpha \otimes \underset{\sim}{e}_\beta + F_{33} \underset{\sim}{e}_3 \otimes \underset{\sim}{e}_3 \quad , \tag{2.11}$$

where

$$F_{33} = 1 \qquad \text{for plane strain,} \tag{2.12a}$$

$$F_{33} = 1 + \partial u_3 / \partial X_3 \qquad \text{for plane stress,} \tag{2.12b}$$

$$F_{33} = 1 + u_1 / X_1 \qquad \text{for axisymmetry.} \tag{2.12c}$$

The left and right Cauchy-Green deformation tensors $\underset{\sim}{B}$ and $\underset{\sim}{C}$, and the Lagrangian strain tensor $\underset{\sim}{E}$, are defined by

$$\underset{\sim}{B} = \underset{\sim}{F}\underset{\sim}{F}^t \quad , \quad \underset{\sim}{C} = \underset{\sim}{F}^t\underset{\sim}{F} \quad , \quad \underset{\sim}{E} = \tfrac{1}{2}(\underset{\sim}{C} - \underset{\sim}{I}) \quad . \tag{2.13}$$

Both $\underset{\sim}{B}$ and $\underset{\sim}{C}$ are positive definite symmetric tensors, and so they possess orthonormal triads $\underset{\sim}{q}_i$ and $\underset{\sim}{p}_i$ respectively, of proper vectors. The proper numbers corresponding to $\underset{\sim}{q}_i$ and $\underset{\sim}{p}_i$ coincide and are equal to the squares of the <u>principal stretches</u> a_i ; that is,

$$\underset{\sim}{B}\underset{\sim}{q}_i = a_i^2 \underset{\sim}{q}_i \quad , \quad \underset{\sim}{C}\underset{\sim}{p}_i = a_i^2 \underset{\sim}{p}_i \quad \text{(no sum on } i\text{)} \quad . \tag{2.14}$$

Furthermore, $\underset{\sim}{p}_i$ and $\underset{\sim}{q}_i$ define the local directions of the <u>principal axes</u> in the reference and current configurations respectively.

Later on it will be necessary to define the principal directions in the <u>current configuration</u> at various points within a body, for <u>plane deformations</u>. That is, given $\underset{\sim}{B}$, we require a_i and $\underset{\sim}{q}_i$ in (2.14). For the plane deformations described above we find that $\underset{\sim}{q}_3 = \underset{\sim}{e}_3$ and $a_3^2 = B_{33}$ so the problem reduces to the eigenvalue problem

$$(B_{\alpha\beta} - a^2\delta_{\alpha\beta})\, q_\beta = 0 \quad , \tag{2.15}$$

for which a non-trivial solution exists if and only if

$$\det (B_{\alpha\beta} - a^2\delta_{\alpha\beta}) = 0 \tag{2.16a}$$

$$\text{or} \quad a_1^2 \, , \, a_2^2 = \tfrac{1}{2}\left[(B_{11} + B_{22}) \pm \{(B_{11} - B_{22})^2 + 4B_{12}^2\}^{1/2}\right] \quad . \tag{2.16b}$$

The corresponding unit proper vectors are found from (2.14) and are

$$\underset{\sim}{q}_1 = \left[\underset{\sim}{e}_1 + \frac{a_1^2 - B_{11}}{B_{12}} \underset{\sim}{e}_2 \right] \frac{B_{12}}{\{B_{12}^2 + (a_1^2 - B_{11})^2\}^{1/2}} , \tag{2.17a}$$

$$\underset{\sim}{q}_2 = \frac{\underset{\sim}{e}_3 \wedge \underset{\sim}{q}_1}{\| \underset{\sim}{e}_3 \wedge \underset{\sim}{q}_1 \|} . \tag{2.17b}$$

Rates of change of kinematic quantities in the current configuration are measured by the velocity vector $\dot{\underset{\sim}{u}} \equiv \dot{\underset{\sim}{x}}$, a superimposed dot denoting the material derivative with respect to time. The velocity gradient $\underset{\sim}{H}$, deformation rate $\underset{\sim}{D}$ and spin tensor $\underset{\sim}{W}$ are defined by

$$\underset{\sim}{H} \equiv \operatorname{grad} \dot{\underset{\sim}{u}} = (\partial \dot{u}_i / \partial x_j) \, \underset{\sim}{e}_i \otimes \underset{\sim}{e}_j , \tag{2.18}$$

$$2\underset{\sim}{D} = \underset{\sim}{H} + \underset{\sim}{H}^t , \quad 2\underset{\sim}{W} = \underset{\sim}{H} - \underset{\sim}{H}^t . \tag{2.19}$$

It is a simple matter to show that

$$\dot{\underset{\sim}{F}} = \underset{\sim\sim}{H}\underset{\sim}{F} , \quad \dot{J} = J \operatorname{div} \dot{\underset{\sim}{u}} . \tag{2.20}$$

The ratio $d\bar{V}/dV$ of current volume to initial volume of an elemental cube is equal to J and so we have, from $(2.20)_2$

$$J = 1 \quad \text{and} \quad \operatorname{div} \dot{\underset{\sim}{u}} = 0 \tag{2.21}$$

for <u>incompressible</u> materials.

For problems in which inertial effects are negligible, balance of linear and angular momentum lead to the equilibrium equations

$$\operatorname{div} \underset{\sim}{\sigma} \equiv (\partial \sigma_{ij}/\partial x_j)\, \underset{\sim}{e}_i = \underset{\sim}{0} \quad , \qquad \underset{\sim}{\sigma} = \underset{\sim}{\sigma}^t \qquad \text{in } \bar{\Omega} \tag{2.22}$$

in the absence of body forces, where $\underset{\sim}{\sigma}$ is the Cauchy stress tensor and $\bar{\Omega}$ is the set of points currently occupied by the body. Two other stress measures of importance are the first and second Piola-Kirchhoff stress tensors $\underset{\sim}{S}$ and $\underset{\sim}{T}$ defined by

$$\underset{\sim}{S} = J\underset{\sim}{\sigma}\underset{\sim}{F}^{-t} \quad , \quad \underset{\sim}{T} = J\underset{\sim}{F}^{-1}\underset{\sim}{\sigma}\underset{\sim}{F}^{-t} \quad ; \tag{2.23}$$

note that $\underset{\sim}{T}$ is symmetric while $\underset{\sim}{S}$ is not. The total force acting on a surface element of area $d\bar{A}$ with unit normal $\bar{\underset{\sim}{n}}$ in the current configuration is

$$\bar{\underset{\sim}{t}}\, d\bar{A} = \underset{\sim}{\sigma}^t \bar{\underset{\sim}{n}}\, d\bar{A} = \underset{\sim}{S}\underset{\sim}{n}\, dA = \underset{\sim}{t}\, dA \tag{2.24}$$

where $\bar{\underset{\sim}{t}}$ is the surface traction vector, $\underset{\sim}{n}$ and dA are the unit normal and area, respectively, of the surface element in the reference configuration, and $\underset{\sim}{t}$ may be described as the <u>current</u> force per unit <u>reference</u> area acting on the element. The physical interpretation of $\underset{\sim}{S}$ is thus clear from (2.24).

In the reference configuration the equilibrium equations become, using (2.22) and $(2.23)_1$,

$$\operatorname{Div} \underset{\sim}{S} \equiv (\partial S_{ij}/\partial X_j)\, \underset{\sim}{e}_i = \underset{\sim}{0} \quad , \quad \underset{\sim}{S}\underset{\sim}{F}^t = \underset{\sim}{F}\underset{\sim}{S}^t \quad \text{in } \Omega \quad . \tag{2.25}$$

Boundary conditions on the surface Γ are (Figure 2.1)

$$\underset{\sim}{u} = \lambda_1 \underset{\sim}{a} \quad \text{on} \quad \Gamma_u \qquad \text{(prescribed displacements)} , \tag{2.26a}$$

$$\underset{\sim\sim}{S}\underset{\sim}{n} = \lambda_2 \underset{\sim}{b} \quad \text{on} \quad \Gamma_t \qquad \text{(prescribed tractions)} , \tag{2.26b}$$

$$\underset{\sim\sim}{S}\underset{\sim}{n} = - \lambda_3 J \underset{\sim}{F}^{-t} \underset{\sim}{n} \quad \text{on} \quad \Gamma_p \qquad \text{(prescribed pressures)} ,$$

$$\left(\text{or } \underset{\sim\sim}{\sigma}\underset{\sim}{\bar{n}} = - \lambda_3 \underset{\sim}{\bar{n}} \quad \text{on} \quad \bar{\Gamma}_p\right) \tag{2.26c}$$

where

$$\Gamma_u \cup \Gamma_t \cup \Gamma_p = \Gamma , \tag{2.27a}$$

$$\Gamma_u \cap \Gamma_t \cap \Gamma_p = \phi \tag{2.27b}$$

and λ_i, $i = 1,2,3$ is a set of independent parameters. Note that λ_3 represents pressure per unit <u>current</u> area and that this pressure acts in an opposite direction to the outward normal on the surface. We can easily generalise these boundary conditions to <u>any number</u> of different displacements, tractions and pressures, and hence <u>any number</u> of independent parameters. For clarity, though, and since the procedures for dealing with each type of boundary condition are the same, we consider the special case as given in (2.26).

We shall be dealing exclusively with <u>elastic</u> materials, for which the stress is completely determined by the deformation :

$$\underset{\sim}{\sigma} = \hat{\underset{\sim}{\sigma}}(\underset{\sim}{F}) \quad \text{or} \quad \underset{\sim}{S} = \hat{\underset{\sim}{S}}(\underset{\sim}{F}) \quad . \tag{2.28}$$

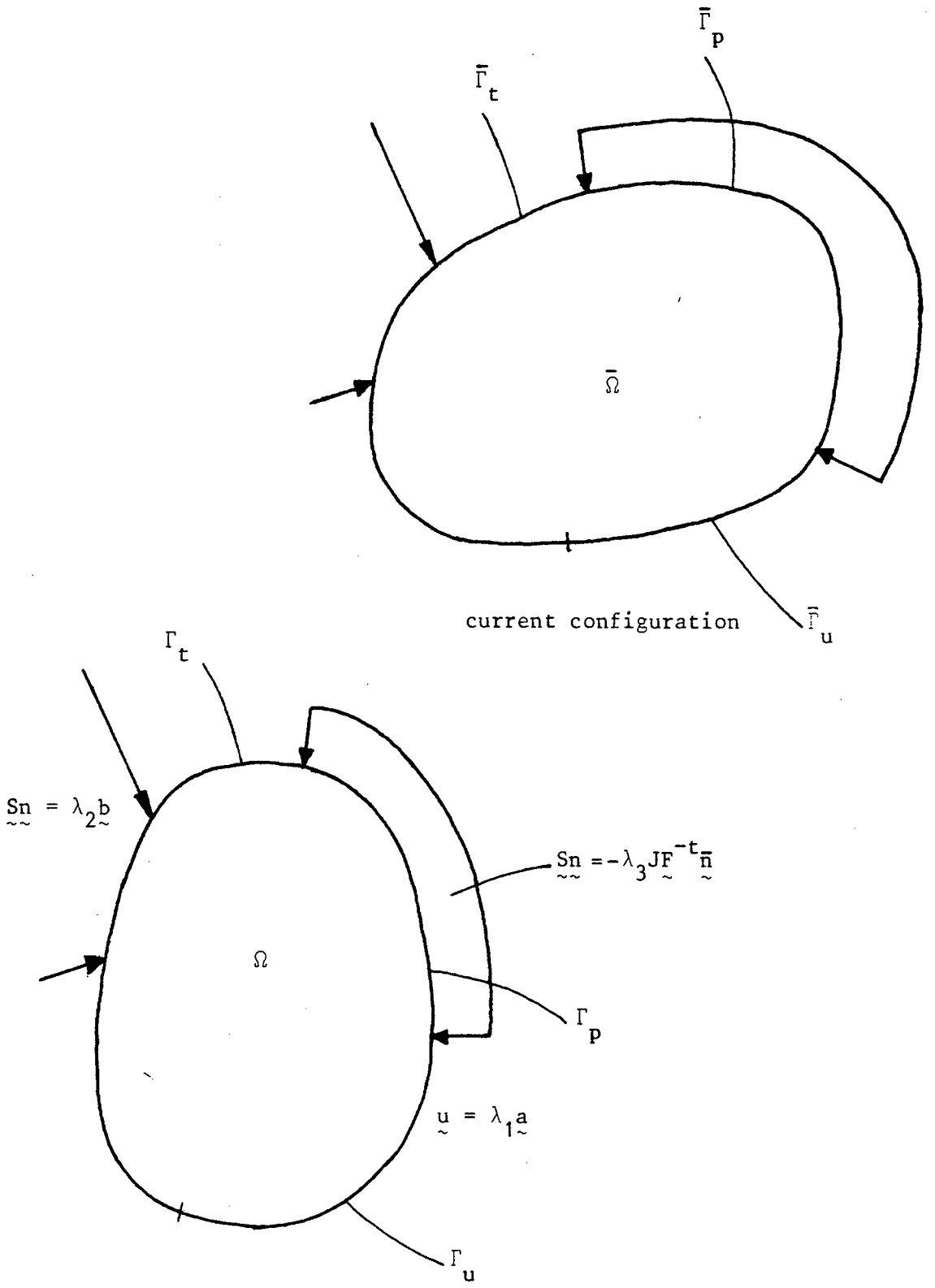

Figure 2.1 Boundary-value problem description.

As a consequence of the principle of material frame indifference (GURTIN (1981)) the constitutive equations can be written in the alternative (reduced) form

$$\underset{\sim}{T} = \hat{\underset{\sim}{T}}(\underset{\sim}{E}) \quad . \tag{2.29}$$

An elastic material is hyperelastic if there exists a scalar strain energy function $W(\underset{\sim}{F})$ such that

$$\hat{\underset{\sim}{S}}(\underset{\sim}{F}) = \partial W/\partial \underset{\sim}{F} \quad \text{or} \quad \hat{\underset{\sim}{\sigma}}(\underset{\sim}{F}) = J^{-1}(\partial W/\partial \underset{\sim}{F})\ \underset{\sim}{F}^{t} \quad . \tag{2.30}$$

The results (2.28) to (2.30) remain valid for incompressible materials, but the stress is determined by the deformation only to within an arbitrary hydrostatic pressure p, so that

$$\underset{\sim}{\sigma} = \hat{\underset{\sim}{\sigma}}(\underset{\sim}{F}) - p\underset{\sim}{I} \quad , \quad \underset{\sim}{T} = \hat{\underset{\sim}{T}}(\underset{\sim}{E}) - p\underset{\sim}{C}^{-1} \tag{2.31}$$

using $(2.23)_2$. If the material is hyperelastic $\hat{\underset{\sim}{\sigma}}$ and $\hat{\underset{\sim}{T}}$ in (2.28) and (2.29) respectively are expressible as derivatives of W with respect to $\underset{\sim}{F}$ or $\underset{\sim}{E}$.

The boundary-value problem for nonlinear elasticity can now be stated : given an elastic body which occupies a bounded region Ω in the reference configuration, suppose that displacements, tractions and pressures are prescribed on parts Γ_u, Γ_t and Γ_p of the boundary surface Γ . We are required to find the displacement field $\underset{\sim}{u}$ which satisfies the equations of equilibrium (2.25), the constitutive relations (2.28) or (2.29) and the boundary conditions (2.26) .

The problem described by equations (2.25) to (2.29) is rendered more suitable for solution by the finite element method if it is recast in a weak or variational form. To do this, consider

$$I = \int_{\Gamma} \underset{\sim}{t}.\underset{\sim}{v}\, dA = \int_{\Gamma} \underset{\sim}{\underset{\sim}{S}n}.\underset{\sim}{v}\, dA \tag{2.32}$$

where $\underset{\sim}{v}$ is an arbitrary vector field. Using the divergence therorem, (2.32) becomes

$$I = \int_{\Omega} \text{Div}\,(\underset{\sim}{\underset{\sim}{S}}^{t}\underset{\sim}{v})\, dV \tag{2.33a}$$

$$= \int_{\Omega} \{(\text{Div}\,\underset{\sim}{\underset{\sim}{S}}).\underset{\sim}{v} + \underset{\sim}{\underset{\sim}{S}}.\text{Grad}\,\underset{\sim}{v}\}\, dV \tag{2.33b}$$

$$= \int_{\Omega} \underset{\sim}{\underset{\sim}{S}}.\text{Grad}\,\underset{\sim}{v}\, dV \tag{2.33c}$$

using $(2.25)_1$. Making use of the boundary conditions (2.26) in (2.32) and the constitutive equation $(2.28)_2$, we obtain the weak form

$$\int_{\Omega} \hat{\underset{\sim}{\underset{\sim}{S}}}(\underset{\sim}{\underset{\sim}{F}}).\text{Grad}\,\underset{\sim}{v}\, dV - \int_{\Gamma_u} \underset{\sim}{t}.\underset{\sim}{v}\, dA - \lambda_2 \int_{\Gamma_t} \underset{\sim}{b}.\underset{\sim}{v}\, dA + \lambda_3 \int_{\bar{\Gamma}_p} \underset{\sim}{\bar{n}}.\underset{\sim}{v}\, d\bar{A} = 0 \quad . \tag{2.34}$$

If the material is incompressible, $\hat{\underset{\sim}{\underset{\sim}{S}}}(\underset{\sim}{\underset{\sim}{F}})$ in (2.34) has to be replaced by $\hat{\underset{\sim}{\underset{\sim}{S}}}(\underset{\sim}{\underset{\sim}{F}}) - p\underset{\sim}{\underset{\sim}{F}}^{-t}$ using (2.23), (2.31) and (2.21) . With the exception of plane stress for which the terms p are absent (p can be determined explicitly since the stress perpendicular to the plane is zero; see, for example, section 4.1.3 and Appendix 4A), (2.34) has to be

supplemented by the condition of incompressibility $(2.21)_1$ which must be put into a weak form as well. By carrying out these extensions the variational boundary-value problem becomes : find $\underset{\sim}{u} \in V$ and $p \in Q$ such that

$$\int_{\Omega} [\hat{\underset{\sim}{S}}(\underset{\sim}{F}) - p\underset{\sim}{F}^{-t}].\text{Grad } \underset{\sim}{v} \, dV - \int_{\Gamma_u} \underset{\sim}{t}.\underset{\sim}{v} \, dA$$

$$- \lambda_2 \int_{\Gamma_t} \underset{\sim}{b}.\underset{\sim}{v} \, dA + \lambda_3 \int_{\bar{\Gamma}_p} \bar{\underset{\sim}{n}}.\underset{\sim}{v} \, d\bar{A} = 0 \quad , \tag{2.35a}$$

$$\int_{\Omega} q(J-1) \, dV = 0 \quad , \tag{2.35b}$$

for all $\underset{\sim}{v} \in W$ and $q \in Q$, where

$$V = \{ \underset{\sim}{u} \in H^1(\Omega) \ , \ \underset{\sim}{u} = \lambda_1 \underset{\sim}{a} \text{ on } \Gamma_u \} \quad , \tag{2.36a}$$

$$W = \{ \underset{\sim}{v} \in H^1(\Omega) \ , \ \underset{\sim}{v} = \underset{\sim}{0} \text{ on } \Gamma_u \} \quad , \tag{2.36b}$$

$$Q = L^2(\Omega) \quad . \tag{2.37}$$

2.2 First-order elastic moduli for incompressible materials

Later on it will be necessary to know the components of the fourth-order tensor $\underset{\sim}{L} \equiv \partial \hat{\underset{\sim}{T}} / \partial \underset{\sim}{E}$, relative to the principal axes of the deformation. These components or first-order elasticities are best obtained by considering the rate form of the constitutive relation

$$\underset{\sim}{T} = \hat{\underset{\sim}{T}}(\underset{\sim}{E}) - p\underset{\sim}{C}^{-1} \quad , \tag{2.38}$$

that is

$$\dot{\underset{\sim}{T}} = \underset{\sim}{L}[\dot{\underset{\sim}{E}}] - \dot{p}\underset{\sim}{C}^{-1} + 2p\underset{\sim}{F}^{-1}\underset{\sim}{D}\underset{\sim}{F}^{-t} \quad , \tag{2.39}$$

where

$$\underset{\sim}{L} = \partial\hat{\underset{\sim}{T}}/\partial\underset{\sim}{E} \quad <=> \quad L_{ijkl} = \partial\hat{T}_{ij}/\partial E_{kl} \quad . \tag{2.40}$$

From (2.23) and (2.20), (2.21) we have

$$\dot{\underset{\sim}{T}} = \underset{\sim}{F}^{-1} (\dot{\underset{\sim}{\sigma}} - \underset{\sim}{H}\underset{\sim}{\sigma} - \underset{\sim}{\sigma}\underset{\sim}{H}^{t}) \underset{\sim}{F}^{-t} \quad . \tag{2.41}$$

Suppose that we now choose as the reference configuration the current configuration of the material : then if the corresponding value of $\dot{\underset{\sim}{T}}$ is denoted $\dot{\underset{\sim}{T}}^{o}$, we have, from (2.41) and setting $\underset{\sim}{F} = \underset{\sim}{I}$,

$$\dot{\underset{\sim}{T}}^{o} = \dot{\underset{\sim}{\sigma}} - \underset{\sim}{H}\underset{\sim}{\sigma} - \underset{\sim}{\sigma}\underset{\sim}{H}^{t} \tag{2.42}$$

which implies that

$$\dot{\underset{\sim}{T}} = \underset{\sim}{F}^{-1}\dot{\underset{\sim}{T}}^{o}\underset{\sim}{F}^{-t} \quad . \tag{2.43}$$

Also, $\underset{\sim}{D} = \dot{\underset{\sim}{E}}^{o}$ and $\dot{\underset{\sim}{E}} = \underset{\sim}{F}^{t}\dot{\underset{\sim}{E}}^{o}\underset{\sim}{F}$, so if we write

$$\dot{\underset{\sim}{T}}^{o} = \underset{\sim}{C}[\dot{\underset{\sim}{E}}^{o}] - \dot{p}\underset{\sim}{I} + 2p\dot{\underset{\sim}{E}}^{o} \tag{2.44}$$

then it follows from (2.39), (2.43) and (2.44) that

$$\underset{\sim}{C}[.] = \underset{\sim}{F}\,\underset{\sim}{L}[\underset{\sim}{F}^{t}(.)\underset{\sim}{F}]\,\underset{\sim}{F}^{t} \quad , \tag{2.45a}$$

or in component form

$$C_{ijkl} = F_{ip}F_{jq}F_{kr}F_{ls}L_{pqrs} \quad . \tag{2.45b}$$

For hyperelastic materials the elasticities L_{ijkl} and C_{ijkl} have the symmetry properties

$$i \leftrightarrow j \quad , \quad k \leftrightarrow l \quad , \quad ij \leftrightarrow kl \quad . \tag{2.46}$$

These results have been given by CHADWICK and OGDEN (1971a) for compressible materials and by OGDEN (1974) for incompressible materials possessing any (or no) degree of material symmetry.

Considerable simplification results if the material is <u>isotropic</u> : when this is the case then $\underset{\sim}{T}$ is a coaxial function of $\underset{\sim}{E}$ and the non-zero components $\bar{L}_{ijkl}$ of $\underset{\sim}{L}$ referred to the <u>common principal axes</u> of $\underset{\sim}{T}$ and $\underset{\sim}{E}$ are (CHADWICK and OGDEN (1971b))

$$\bar{L}_{iijj} = \partial\hat{T}_i/\partial E_j \quad , \tag{2.47a}$$

$$\bar{L}_{ijij} = \tfrac{1}{2}(\hat{T}_i - \hat{T}_j)/(E_i - E_j) \quad , \quad i\neq j,\ E_i \neq E_j \quad , \tag{2.47b}$$

where $\hat{T}_i$ and E_i are the proper numbers of $\hat{\underset{\sim}{T}}$ and $\underset{\sim}{E}$. In the event that two proper numbers of $\underset{\sim}{E}$ are equal, a limiting procedure applied to (2.47b) yields

$$\bar{L}_{ijij} = \tfrac{1}{2}(\partial\hat{T}_i/\partial E_i - \partial\hat{T}_j/\partial E_i) \quad , \quad i\neq j, \; E_i=E_j \quad . \tag{2.47c}$$

The components of $\hat{\underset{\sim}{T}}$ and $\underset{\sim}{E}$ relative to the principal axes in the reference configuration are given by

$$\hat{T}_i = a_i^{-2}\hat{\sigma}_i \quad , \quad 2E_i = a_i^2 - 1 \quad , \tag{2.48}$$

where $\hat{\sigma}_i$ and a_i are the components of principal Cauchy stress and stretch, respectively. It is now a straightforward matter to obtain the following corresponding results for the components of $\underset{\sim}{C}$ relative to the principal axes in the current configuration, using (2.45b), (2.47) and (2.48) :

$$\bar{C}_{iijj} = a_j\partial\hat{\sigma}_i/\partial a_j - 2\delta_{ij}\hat{\sigma}_i \quad ,$$

$$a_i\neq a_j\neq a_k \quad , \quad a_i=a_j\neq a_k \quad \text{or all a's equal} \quad , \tag{2.49a}$$

$$\bar{C}_{ijij} = \begin{cases} \dfrac{a_j^2\hat{\sigma}_i - a_i^2\hat{\sigma}_j}{a_i^2 - a_j^2} \quad , \; i\neq j \quad , \; a_i\neq a_j\neq a_k \quad , & (2.49b) \\ \\ -\hat{\sigma}_i + \tfrac{1}{2}a_i(\partial\hat{\sigma}_i/\partial a_i - \partial\hat{\sigma}_j/\partial a_i) \quad , \\ i\neq j \quad , \quad a_i=a_j\neq a_k \text{ or all a's equal} \quad . & (2.49c) \end{cases}$$

OGDEN (1974) has given the results (2.49a,b) while (2.49c) is new (DUFFETT and REDDY (1983)) and is based on a similar result for compressible materials (CHADWICK and OGDEN (1971b)).

The components C_{ijkl} of $\underset{\sim}{C}$ relative to <u>any</u> orthonormal basis $\underset{\sim}{e}_i$ are related to the components $\bar{C}_{ijkl}$ relative to the principal basis $\underset{\sim}{q}_i$ (see (2.17)) by

$$C_{ijkl} = Q_{ip}Q_{jq}Q_{kr}Q_{ls}\bar{C}_{pqrs} \tag{2.50}$$

where

$$Q_{ip} = \underset{\sim}{e}_i \cdot \underset{\sim}{q}_p \ . \tag{2.51}$$

For <u>plane</u> problems the matrix of $\underset{\sim}{Q}$ is

$$[Q] = \begin{bmatrix} \cos\theta & -\sin\theta & 0 \\ \sin\theta & \cos\theta & 0 \\ 0 & 0 & 1 \end{bmatrix} \tag{2.52}$$

where $\theta = \cos^{-1}(\underset{\sim}{e}_1 \cdot \underset{\sim}{q}_1)$. In Section 2.4.1 we shall give explicit results for (2.50), for a particular class of strain-energy functions.

2.3 Second-order elastic moduli for incompressible materials

It will also be necessary to know the components of the sixth-order tensor

$$\underset{\sim}{\mathcal{L}} \equiv \partial^2\hat{\underset{\sim}{T}}/\partial\underset{\sim}{E}^2 \quad <=> \quad \mathcal{L}_{ijklmn} = \partial^2\hat{T}_{ij}/\partial E_{kl}\partial E_{mn} \quad , \qquad (2.53)$$

relative to the principal axes of deformation. These second-order elasticities are obtained by considering a second material derivative with respect to time of the constitutive relation (2.38) . Thus, from (2.39) , we have

$$\begin{aligned}\ddot{\underset{\sim}{T}} &= \underset{\sim}{\mathcal{L}}[\dot{\underset{\sim}{E}},\dot{\underset{\sim}{E}}] + \underset{\sim}{L}[\ddot{\underset{\sim}{E}}] - \ddot{p}\underset{\sim}{C}^{-1} + 4\dot{p}\underset{\sim}{F}^{-1}\underset{\sim}{D}\underset{\sim}{F}^{-t} \\ &\quad - 2p\underset{\sim}{F}^{-1}(\underset{\sim}{L}\underset{\sim}{D} + \underset{\sim}{D}\underset{\sim}{L}^t - \dot{\underset{\sim}{D}})\underset{\sim}{F}^{-t} \quad , \qquad (2.54)\end{aligned}$$

where $\underset{\sim}{\mathcal{L}}$ is given in (2.53).

By following similar arguments to those in the previous section we can show that

$$\ddot{\underset{\sim}{T}} = \underset{\sim}{F}^{-1}\ddot{\underset{\sim}{T}}^{o}\underset{\sim}{F}^{-t} \quad ; \qquad (2.55)$$

then if we write

$$\begin{aligned}\ddot{\underset{\sim}{T}}^{o} &= \underset{\sim}{\mathcal{L}}[\dot{\underset{\sim}{E}}^{o},\dot{\underset{\sim}{E}}^{o}] - 2p(\underset{\sim}{L}\dot{\underset{\sim}{E}}^{o} + \dot{\underset{\sim}{E}}^{o}\underset{\sim}{L}^t) + 4\dot{p}\dot{\underset{\sim}{E}}^{o} \\ &\quad + \{\underset{\sim}{C}[\ddot{\underset{\sim}{E}}^{o}] - \ddot{p}\underset{\sim}{I} + 2p\ddot{\underset{\sim}{E}}^{o}\} \qquad (2.56)\end{aligned}$$

it follows from (2.53), (2.55) and (2.56) that

$$\underset{\sim}{\mathcal{C}}[.,.] = \underset{\sim}{F}\,\underset{\sim}{\mathcal{L}}[\underset{\sim}{F}^t(.)\underset{\sim}{F}\,,\ \underset{\sim}{F}^t(.)\underset{\sim}{F}]\,\underset{\sim}{F}^t \qquad (2.57a)$$

or, in component form ,

$$\mathcal{C}_{ijklmn} = F_{ip}F_{jq}F_{kr}F_{ls}F_{mt}F_{nu}\mathcal{L}_{pqrstu} \quad . \qquad (2.57b)$$

Notice the similarity of the last term in equation (2.56) with equation (2.44) . For hyperelastic materials the elasticities $\mathcal{L}_{ijklmn}$ and $\mathcal{C}_{ijklmn}$ have the symmetry properties

$$\begin{aligned} &i \leftrightarrow j \quad , \quad k \leftrightarrow l \quad , \quad m \leftrightarrow n \quad , \\ &ij \leftrightarrow kl \quad , \quad ij \leftrightarrow mn \quad , \quad kl \leftrightarrow mn \quad . \end{aligned} \qquad (2.58)$$

These results have also been given by CHADWICK and OGDEN (1971a) for compressible materials and by OGDEN (1974) for incompressible materials possessing any (or no) degree of material symmetry.

As with the first-order elasticities considerable simplification results if the material is <u>isotropic</u>. The non-zero components of $\underset{\sim}{\mathcal{L}}$ referred to the common principal axes of $\underset{\sim}{E}$ and $\underset{\sim}{T}$ are then (CHADWICK and OGDEN (1971b))

$$\bar{\mathcal{L}}_{iijjkk} = \partial \bar{L}_{iijj}/\partial E_k \quad , \tag{2.59a}$$

$$\bar{\mathcal{L}}_{ijijkk} = \partial \bar{L}_{ijij}/\partial E_k \quad , \quad i \neq j \quad , \tag{2.59b}$$

$$\bar{\mathcal{L}}_{iijkjk} = 1/2\,(\bar{L}_{iijj} - \bar{L}_{iikk})/(E_j - E_k) - \bar{L}_{jkjk}(\delta_{ij} - \delta_{ik})/(E_j - E_k) \quad , \quad j \neq k \, , \; E_j \neq E_k \, , \tag{2.59c}$$

$$\bar{\mathcal{L}}_{ijjkki} = 1/4\,(\bar{L}_{ijij} - \bar{L}_{kiki})/(E_j - E_k) + 1/4\,(\bar{L}_{jkjk} - \bar{L}_{ijij})/(E_k - E_i) \, , \quad i \neq j \neq k \neq i \, , \; E_j \neq E_k \, , \; E_i \neq E_k \, , \tag{2.59d}$$

where E_i are the proper numbers of $\underset{\sim}{E}$. In the event that <u>two proper numbers</u> of $\underset{\sim}{E}$ are <u>equal</u>, limiting procedures applied to (2.59b) and (2.59c) yield

$$\bar{\mathcal{L}}_{ijjiii} = 1/4\,(\partial^2 \hat{T}_i/\partial E_i^2 - \partial^2 \hat{T}_j/\partial E_i^2) \quad , \quad i \neq j, \; E_i = E_j \quad , \tag{2.59e}$$

$$\bar{\mathcal{L}}_{iiijij} = 1/4\,(\partial^2 \hat{T}_i/\partial E_i^2 + \partial^2 \hat{T}_j/\partial E_i^2 - 2\partial^2 \hat{T}_i/\partial E_i \partial E_j) \quad , \quad i \neq j \, , \; E_i = E_j \quad , \tag{2.59f}$$

$$\bar{\mathcal{L}}_{ijijkk} = \tfrac{1}{2}(\partial^2\hat{T}_i/\partial E_i\partial E_k - \partial^2\hat{T}_j/\partial E_i\partial E_k) \quad , \; i\neq j\neq k\neq i, \; E_i=E_j \quad , \tag{2.59g}$$

$$\bar{\mathcal{L}}_{kkijij} = \tfrac{1}{2}(\partial^2\hat{T}_k/\partial E_i^2 - \partial^2\hat{T}_k/\partial E_i\partial E_j) \quad , \; i\neq j\neq k\neq i \; , \; E_i=E_j \quad . \tag{2.59h}$$

When <u>all three proper numbers</u> of $\underset{\sim}{E}$ are <u>equal</u> equations (2.59a) and (2.59e) to (2.59h) continue to hold but (2.59d) is replaced by

$$\bar{\mathcal{L}}_{ijjkki} = \frac{1}{8}(\partial^2\hat{T}_i/\partial E_i^2 - \partial^2\hat{T}_i/\partial E_j^2 + 2\partial^2\hat{T}_i/\partial E_j\partial E_k - 2\partial^2\hat{T}_i/\partial E_i\partial E_j) \quad , \; i\neq j\neq k\neq i \; , \; E_i=E_j=E_k \quad . \tag{2.59i}$$

It is now a straightforward matter to obtain the following corresponding results for the components of $\underset{\sim}{\mathcal{L}}$ relative to the principal axes in the current configuration, using (2.57b), (2.59) and (2.48) :

$$\bar{\mathcal{L}}_{iijjkk} = a_j\partial\bar{C}_{iikk}/\partial a_j - 2(\delta_{ij}+\delta_{jk})\bar{C}_{iikk} \quad , \quad a_i\neq a_j\neq a_k \; , \; a_i=a_j\neq a_k \text{ or all a's equal} \quad , \tag{2.60a}$$

$$\bar{\mathcal{L}}_{ijijkk} = a_k\partial\bar{C}_{ijij}/\partial a_k - 2(\delta_{ik}+\delta_{jk})\bar{C}_{ijij} \quad , \quad i\neq j \; , \; a_i\neq a_j\neq a_k \quad , \tag{2.60b}$$

$$\bar{\mathcal{C}}_{ijijii} = 2\hat{\sigma}_i - \tfrac{1}{4} a_i \partial(5\hat{\sigma}_i - \hat{\sigma}_j)/\partial a_i + \tfrac{1}{4} a_i^2 \partial^2(\hat{\sigma}_i - \hat{\sigma}_j)/\partial a_i^2 \ ,$$

$$i \neq j \ , \ a_i = a_j \neq a_k \text{ or all a's equal} \ , \qquad (2.60c)$$

$$\bar{\mathcal{C}}_{ijijkk} = -a_k \partial\hat{\sigma}_i/\partial a_k + \tfrac{1}{2} a_i a_k \partial^2(\hat{\sigma}_i - \hat{\sigma}_j)/\partial a_i \partial a_k \ ,$$

$$i \neq j \neq k \neq i \ , \ a_i = a_j \neq a_k \text{ or all a's equal} \ , \qquad (2.60d)$$

$$\bar{\mathcal{C}}_{kkijij} = \left[(a_j^2 \bar{C}_{kkii} - a_i^2 \bar{C}_{kkjj}) - 2a_k^2 \bar{C}_{ijij}(\delta_{ki} - \delta_{kj}) \right] / (a_i^2 - a_j^2) \ ,$$

$$i \neq j \ , \ a_i \neq a_j \neq a_k \ , \qquad (2.60e)$$

$$\bar{\mathcal{C}}_{iiijij} = 2\hat{\sigma}_i - \tfrac{1}{4} a_i \partial(5\hat{\sigma}_i + \hat{\sigma}_j)/\partial a_i + \tfrac{1}{4} a_i^2 \partial^2(\hat{\sigma}_i + \hat{\sigma}_j)/\partial a_i^2$$

$$+ a_i \partial\hat{\sigma}_i/\partial a_j - \tfrac{1}{2} a_i^2 \partial^2\hat{\sigma}_i/\partial a_i \partial a_j \ ,$$

$$i \neq j \ , \ a_i = a_j \neq a_k \text{ or all a's equal} \ , \qquad (2.60f)$$

$$\bar{\mathcal{C}}_{kkijij} = \tfrac{1}{2} a_i (a_i \partial^2\hat{\sigma}_k/\partial a_i^2 - a_i \partial^2\hat{\sigma}_k/\partial a_i \partial a_j - \partial\hat{\sigma}_k/\partial a_i) \ ,$$

$$i \neq j \neq k \neq i \ , \ a_i = a_j \neq a_k \text{ or all a's equal} \ , \qquad (2.60g)$$

$$\bar{\mathcal{C}}_{ijjkki} = \tfrac{1}{2} (a_k^2 \bar{C}_{ijij} - a_j^2 \bar{C}_{kiki})/(a_j^2 - a_k^2)$$

$$+ \tfrac{1}{2} (a_i^2 \bar{C}_{jkjk} - a_k^2 \bar{C}_{ijij})/(a_k^2 - a_i^2) \ ,$$

$$i \neq j \neq k \neq i \ , \ a_i \neq a_j \neq a_k \text{ or } a_i = a_j \neq a_k \ , \qquad (2.60h)$$

$$\bar{\mathscr{C}}_{ijjkki} = \hat{\sigma}_i - \tfrac{1}{4}a_i^2(\partial^2\hat{\sigma}_i/\partial a_i\partial a_j - \partial^2\hat{\sigma}_i/\partial a_j\partial a_k)$$
$$+ \tfrac{1}{8}a_i^2(\partial^2\hat{\sigma}_i/\partial a_i^2 - \partial^2\hat{\sigma}_i/\partial a_j^2) - \tfrac{1}{8}a_i(5\partial\hat{\sigma}_i/\partial a_i - 4\partial\hat{\sigma}_i/\partial a_j) \quad ,$$
$$i\neq j\neq k\neq i \quad , \quad a_i=a_j=a_k \quad . \qquad (2.60i)$$

OGDEN (1974) has given the results (2.60a,b,e,h) while the other equations (2.60c,d,f,g,i) are new and based on similar results for compressible materials (CHADWICK and OGDEN (1971b)) .

The components $\mathscr{C}_{ijklmn}$ of $\underset{\sim}{\mathscr{C}}$ relative to any orthonormal basis $\underset{\sim}{e}_i$ are related to the components $\bar{\mathscr{C}}_{ijklmn}$ relative to the principal basis $\underset{\sim}{q}_i$ (equation (2.17)) by

$$\mathscr{C}_{ijklmn} = Q_{ip}Q_{jq}Q_{kr}Q_{ls}Q_{mt}Q_{nu}\bar{\mathscr{C}}_{pqrstu} \quad , \qquad (2.61)$$

where the components Q_{ip} are given in (2.51) and the matrix $\underset{\sim}{Q}$ for plane problems is given in (2.52) . In section 2.4.2 we shall give explicit results for (2.61) , for a particular class of strain-energy functions.

2.4 Ogden's strain energy functions

For isotropic hyperelastic materials, the strain-energy function W is a symmetric function of the three principal stretches a_i . This has been exploited by OGDEN (1972a) who proposed a class of strain-

energy functions for incompressible isotropic elastic materials. In subsequent papers OGDEN (1972b, 1976, 1978) extended his previous results to allow for volume changes. However, we limit ourselves to incompressible materials for which the strain-energy function proposed by OGDEN (1972a) is of the form

$$W(a_i) = \sum_n \mu_n \phi(\alpha_n, a_i) \quad , \quad a_1 a_2 a_3 = 1 \quad , \tag{2.62a}$$

$$\phi(\alpha_n, a_i) = (a_1^{\alpha_n} + a_2^{\alpha_n} + a_3^{\alpha_n} - 3)/\alpha_n \quad , \tag{2.62b}$$

$$\mu_n \alpha_n > 0 \quad \text{for each} \quad n \quad . \tag{2.62c}$$

Here μ_n and α_n are material constants, and the summation in (2.62a) is over a finite number of terms. The principal stresses derived from (2.30) and (2.62) are

$$\hat{\sigma}_i = a_i \partial W / \partial a_i = \sum_n \mu_n a_i^{\alpha_n} \quad . \tag{2.63}$$

It is now an easy matter to compute the components of $\underset{\sim}{C}$ and $\underset{\sim}{\mathscr{C}}$ relative to the principal axes in the current configuration from equations (2.49) and (2.60) respectively, so that the relations (2.50) and (2.61) may be obtained.

2.4.1 First-order elastic moduli for plane problems

The components of $\underset{\sim}{C}$ relative to the principal axes in the current configuration are found from (2.63) and (2.49) ; thus

$$\bar{C}_{iijj} = \delta_{ij} \sum \mu_n a_i^{\alpha_n} (\alpha_n - 2) \quad , \tag{2.64a}$$

$$\bar{C}_{ijij} = \begin{cases} \sum \mu_n (a_j^2 a_i^{\alpha_n} - a_i^2 a_j^{\alpha_n})/(a_i^2 - a_j^2) \quad , \\ \qquad i \neq j \ , \ a_i \neq a_j \neq a_k \quad , \qquad (2.64b) \\ \\ \sum \mu_n a_i^{\alpha_n} (\tfrac{1}{2} \alpha_n - 1) \quad , \\ \qquad i \neq j \ , \ a_i = a_j \neq a_k \text{ or all a's equal} \quad . \qquad (2.64c) \end{cases}$$

There are only <u>four</u> independent moduli $\bar{C}_{ijkl}$ for <u>plane</u> problems using the strain-energy function (2.62), and it turns out that there are only <u>seven</u> independent moduli C_{ijkl} ; hence (2.50) can be written compactly as

$$[C] = \begin{bmatrix} C_{1111} & C_{1122} & C_{1112} \\ & C_{2222} & C_{1222} \\ \text{sym} & & C_{1212} \end{bmatrix} = [P] \, [\bar{C}] \, [P]^t \quad , \quad C_{3333} = \bar{C}_{3333} \ , \tag{2.65}$$

where $[\bar{C}] = \text{diag}\,(\bar{C}_{1111}\ ,\ \bar{C}_{2222}\ ,\ \bar{C}_{1212})$ and

$$[P] = \begin{bmatrix} c^2 & s^2 & -2cs \\ s^2 & c^2 & 2cs \\ cs & -cs & c^2-s^2 \end{bmatrix} \quad , \quad c = \cos\Theta \quad , \quad s = \sin\Theta \quad . \tag{2.66}$$

2.4.2 Second-order elastic moduli for plane problems

The non-zero components of $\underset{\sim}{\mathscr{C}}$ relative to the principal axes in the current configuration are found from (2.63) and (2.60) ; thus

$$\bar{\mathscr{C}}_{iiiiii} = \sum \mu_n a_i^{\alpha_n} (\alpha_n - 2)(\alpha_n - 4) \quad ,$$

$$a_i \neq a_j \neq a_k \ , \ a_i = a_j \neq a_k \text{ or all a's equal} \ , \tag{2.67a}$$

$$\bar{\mathscr{C}}_{ijijii} = \begin{cases} [a_j^2(a_i^2 - a_j^2)\sum \mu_n a_i^{\alpha_n}(\alpha_n - 2) - 2a_i^2 \sum \mu_n (a_j^2 a_i^{\alpha_n} - a_i^2 a_j^{\alpha_n})] \\ \qquad\qquad /(a_i^2 - a_j^2)^2 \quad , \\ \text{or} \\ (a_j^2 \bar{C}_{iiii} - 2a_i^2 \bar{C}_{ijij})/(a_i^2 - a_j^2) \quad , \\ \quad i \neq j \ , \ a_i \neq a_j \neq a_k \quad , \end{cases} \tag{2.67b}$$

$$\begin{cases} \sum \mu_n a_i^{\alpha_n} (2 - \tfrac{3}{2}\alpha_n + \tfrac{1}{4}\alpha_n^2) \quad , \\ \quad i \neq j \ , \ a_i = a_j \neq a_k \text{ or all a's equal} \ , \end{cases} \tag{2.67c}$$

$$\bar{\mathscr{C}}_{ijjkki} = \begin{cases} \sum\mu_n[a_i^{\alpha_n}a_j^2a_k^2(a_k^2-a_j^2) + a_i^2a_j^{\alpha_n}a_k^2(a_i^2-a_k^2) + a_i^2a_j^2a_k^{\alpha_n}(a_j^2-a_i^2)] \\ \quad /[(a_i^2-a_j^2)(a_j^2-a_k^2)(a_k^2-a_i^2)] \quad , \\ \quad i\neq j\neq k\neq i \ , \ a_i\neq a_j\neq a_k \quad , \qquad (2.67d) \\ \\ [a_k^2(2a_k^2-a_j^2-a_i^2)\sum\mu_n a_i^{\alpha_n}(\tfrac{1}{2}\alpha_n-1) - a_j^2\sum\mu_n(a_i^2a_k^{\alpha_n}-a_k^2a_i^{\alpha_n}) \\ \quad + a_i^2\sum\mu_n(a_k^2a_j^{\alpha_n}-a_j^2a_k^{\alpha_n})]/[2(a_j^2-a_k^2)(a_k^2-a_i^2)] \quad , \\ \quad i\neq j\neq k\neq i \ , \ a_i=a_j\neq a_k \quad , \qquad (2.67e) \\ \\ \sum\mu_n a_i^{\alpha_n}(1-\frac{3}{4}\alpha_n+\frac{1}{8}\alpha_n^2) \quad , \\ \quad i\neq j\neq k\neq i \ , \ \text{all a's equal} \quad . \qquad (2.67f) \end{cases}$$

There are only <u>five</u> independent moduli $\bar{\mathscr{C}}_{ijklmn}$ for <u>plane</u> problems using the strain-energy function (2.62), and it turns out that there are only <u>eleven</u> independent moduli $\mathscr{C}_{ijklmn}$ so that (2.61) can be written compactly in matrix form as

$$\begin{Bmatrix} \mathscr{E}_{111111} \\ \mathscr{E}_{222222} \\ \mathscr{E}_{111122} \\ \mathscr{E}_{112222} \\ \mathscr{E}_{111112} \\ \mathscr{E}_{222212} \\ \mathscr{E}_{112212} \\ \mathscr{E}_{111212} \\ \mathscr{E}_{221212} \\ \mathscr{E}_{121212} \end{Bmatrix} = \begin{bmatrix} c^6 & s^6 & 12a & 12b \\ s^6 & c^6 & 12b & 12a \\ a & b & 4b-8a & 4a-8b \\ b & a & 4a-8b & 4b-8a \\ d & -e & 8k-4d & 4e-8k \\ e & -d & 8k-4e & 4d-8k \\ k & -k & 2(d+e)-8k & 8k-2(d+e) \\ a & b & 5b-6a+c^6 & 5a-6b+s^6 \\ b & a & 5a-6b+s^6 & 5b-6a+c^6 \\ k & -k & 3(d+e)-6k & 6k-3(d+e) \end{bmatrix} \begin{Bmatrix} \bar{\mathscr{E}}_{111111} \\ \bar{\mathscr{E}}_{222222} \\ \bar{\mathscr{E}}_{111212} \\ \bar{\mathscr{E}}_{221212} \end{Bmatrix} , \qquad (2.68a)$$

$$\mathscr{E}_{333333} = \bar{\mathscr{E}}_{333333} \quad ,$$

$$c = \cos\theta \quad , \quad s = \sin\theta \quad ,$$

$$a = c^4 s^2 \quad , \quad b = s^4 c^2 \quad , \quad d = c^5 s \quad , \quad e = s^5 c \quad , \quad k = c^3 s^3 \quad ,$$

or as

$$\{\mathscr{E}\} = [R]\,\{\bar{\mathscr{E}}\} \quad . \qquad (2.68b)$$

2.5 Finite element approximations

We construct in this section a finite element approximation of the problem defined by equation (2.35). Consider an approximation Ω_h of the domain Ω (Figure 2.2); Ω_h is the union of a total of E finite elements, the e^{th} element being denoted by Ω^e, so that

$$\Omega_h = \bigcup_{e=1}^{E} \Omega^e \quad , \quad \Omega^e \cap \Omega^f = \phi \quad , \quad e \neq f \quad . \tag{2.69}$$

The mesh parameter h characterises the quality of the approximation ; for each element Ω^e with position vectors $\underset{\sim}{x}$ and $\underset{\sim}{y}$ we define h_e by

$$h_e = \sup \{ \, | \underset{\sim}{x} - \underset{\sim}{y} | \; ; \; \underset{\sim}{x} , \underset{\sim}{y} \in \Omega^e \, \} \tag{2.70}$$

and then h is defined by

$$h = \max_{1 \leq e \leq E} h_e \quad . \tag{2.71}$$

We hope of course that the approximate solutions approach the exact solution as $h \to 0$.

It is assumed subsequently that mesh refinements are uniform in the sense that, for some constant γ ,

$$\rho_e \geq \gamma h_e \quad , \quad e = 1, \ldots, E \quad , \tag{2.72}$$

where ρ_e is the diameter of the largest sphere that can be inscribed in element Ω^e (CAREY and ODEN (1983)).

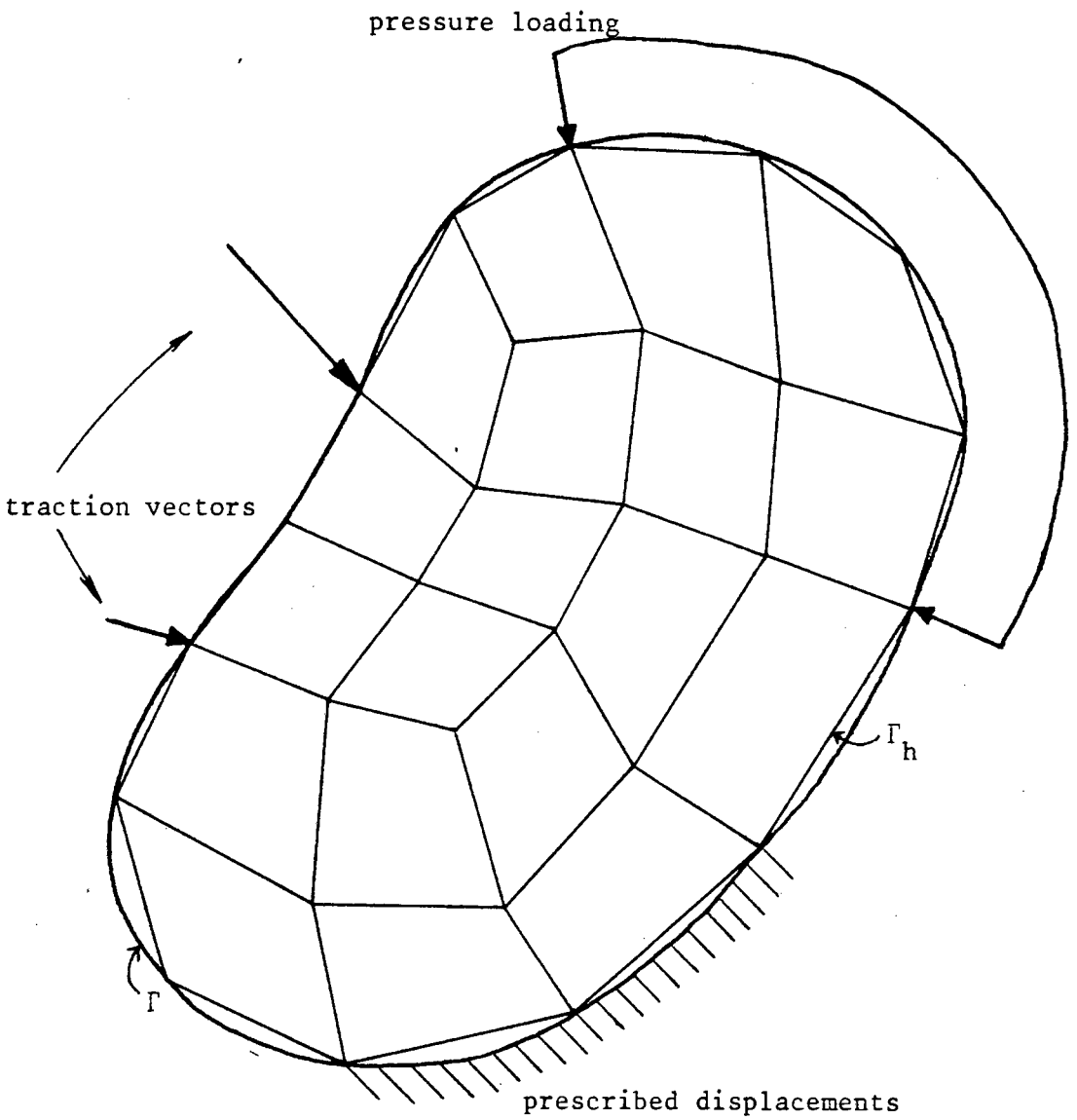

Figure 2.2 Finite element discretisation of the domain Ω by a mesh Ω_h consisting of quadratic elements.

Then instead of working in the infinite-dimensional space of admissible functions V (ODEN and CAREY (1983)) required in section 2.1 we seek approximate solutions in the finite-dimensional subspace V_h of V , which is now defined. Let Ω^e be a typical element and let N_A , A = 1,...,n_e , be a set of linearly independent <u>local</u> interpolation functions defined on Ω^e , with the property

$$N_A(\underset{\sim}{x}^B) = \delta_{AB} \quad , \tag{2.73}$$

where $\underset{\sim}{x}^B$, B = 1,...,n_e are the position vectors of <u>nodes</u> of Ω^e. Let V_h^e be the linear space spanned by the interpolation functions N_A. Then V_h is defined to be the subspace of V consisting of <u>continuous</u> functions $\underset{\sim}{v}_h$ on Ω_h whose restriction to Ω^e lies in V_h^e :

$$V_h = \{ \underset{\sim}{v}_h \mid \underset{\sim}{v}_h \in C^o(\Omega_h) \ , \ \underset{\sim}{v}_h|_{\Omega^e} \in V_h^e \ , \ 1 \leq e \leq E \} \ . \tag{2.74}$$

The subspace W_h is defined in the same manner.

In the case of incompressible materials we require also the finite-dimensional subspace Q_h of Q by defining Q_h^e to be the linear space spanned by the interpolation functions M_K , with the property

$$M_K(\underset{\sim}{x}^L) = \delta_{KL} \ . \tag{2.75}$$

Here K and L range from 1 to n_p, the number of nodes appropriate to Q_h^e. Then Q_h is defined by

$$Q_h = \{ q_h \mid q_h \in C^0(\Omega_h) , q_h|_{\Omega^e} \in Q_h^e , 1 \leq e \leq E \} \quad . (2.76)$$

The discrete variational problem now becomes, from (2.35) : find $\underset{\sim}{u}_h \in V_h$ and $p_h \in Q_h$ such that

$$\int_{\Omega_h} [\hat{\underset{\sim}{S}}(\underset{\sim}{F}(\underset{\sim}{u}_h)) - p_h \underset{\sim}{F}^{-t}(\underset{\sim}{u}_h)] \cdot \text{Grad } \underset{\sim}{v}_h \, dV - \int_{\Gamma_{uh}} \underset{\sim}{t} \cdot \underset{\sim}{v}_h \, dA$$

$$- \lambda_2 \int_{\Gamma_{th}} \underset{\sim}{b} \cdot \underset{\sim}{v}_h \, dA + \lambda_3 \int_{\bar{\Gamma}_{ph}} \bar{\underset{\sim}{n}} \cdot \underset{\sim}{v}_h \, d\bar{A} = 0 \quad , \quad (2.77a)$$

$$\int_{\Omega_h} q_h (J(\underset{\sim}{u}_h) - 1) \, dV = 0 \quad , \quad (2.77b)$$

for all $\underset{\sim}{v}_h \in W_h$ and $q_h \in Q_h$.

Equation (2.77) can now be written (see equation (2.69)) as

$$\sum_{e=1}^{E} \{ \int_{\Omega_h^e} [\hat{\underset{\sim}{S}}(\underset{\sim}{F}(\underset{\sim}{u}_h)) - p_h \underset{\sim}{F}^{-t}(\underset{\sim}{u}_h)] \cdot \text{Grad } \underset{\sim}{v}_h \, dV - \int_{\Gamma_{uh}^e} \underset{\sim}{t} \cdot \underset{\sim}{v}_h \, dA$$

$$- \lambda_2 \int_{\Gamma_{th}^e} \underset{\sim}{b} \cdot \underset{\sim}{v}_h \, dA + \lambda_3 \int_{\bar{\Gamma}_{ph}^e} \bar{\underset{\sim}{n}} \cdot \underset{\sim}{v}_h \, d\bar{A} \} = 0 \quad , \quad (2.78a)$$

$$\sum_{e=1}^{E} \{ \int_{\Omega_h^e} q_h (J(\underset{\sim}{u}_h) - 1) \, dV \} = 0 \quad ; \tag{2.78b}$$

the surface integrals (last three terms in (2.78a)) being included only if part of the boundary of Ω^e coincides with the corresponding boundary of the domain. Hence the entire procedure of formulating the set of nonlinear algebraic equations corresponding to the discrete problem can be carried out at element level and the contributions of all elements can be summed at a subsequent stage.

The restrictions of $\underset{\sim}{u}_h$, $\underset{\sim}{v}_h$ and p_h , q_h to Ω^e are given by

$$\underset{\sim}{u}_h = \underset{\sim}{u}^A N_A(\underset{\sim}{x}) \quad , \quad \underset{\sim}{v}_h = \underset{\sim}{v}^A N_A(\underset{\sim}{x}) \quad , \tag{2.79}$$

$$p_h = p^K M_K(\underset{\sim}{x}) \quad , \quad q_h = q^K M_K(\underset{\sim}{x}) \quad , \tag{2.80}$$

where $\underset{\sim}{u}^A$, $\underset{\sim}{v}^A$ and p^K , q^K are the nodal values of $\underset{\sim}{u}_h$, $\underset{\sim}{v}_h$ and p_h , q_h respectively. Summation over repeated indices is implied : here and henceforth, indices A,B,C range over 1 to n_e, while indices K,L,M range over 1 to n_p. Derivatives of the restrictions with respect to the position vectors $\underset{\sim}{x}$ are

$$\underset{\sim}{u}_{h,j} = \underset{\sim}{u}^A N_{A,j} \quad , \quad \underset{\sim}{v}_{h,j} = \underset{\sim}{v}^A N_{A,j} \quad , \tag{2.81}$$

$$p_{h,j} = p^K M_{K,j} \quad , \quad q_{h,j} = q^K M_{K,j} \quad ; \tag{2.82}$$

thus equations (2.78) become

$$\sum_{e=1}^{E} v_i^{A(e)} \Big\{ \int_{\Omega_h^e} [N_{A,j} \hat{S}_{ij}(\underset{\sim}{u}^B) - p^K M_K F^{-t}_{ij}(\underset{\sim}{u}^B) N_{A,j}] \, dV$$

$$- \int_{\Gamma_{uh}^e} N_A t_i \, dA - \lambda_2 \int_{\Gamma_{th}^e} N_A b_i \, dA + \lambda_3 \int_{\bar{\Gamma}_{ph}^e} N_A \bar{n}_i \, d\bar{A} \Big\} = 0 \, , \tag{2.83a}$$

$$\sum_{e=1}^{E} q^{K(e)} \Big\{ \int_{\Omega_h^e} M_K \, (J(\underset{\sim}{u}^B) - 1) \, dV \Big\} = 0 \, . \tag{2.83b}$$

These equations can be written compactly as

$$\sum_{e=1}^{E} v_i^{A(e)} \, G^i_{A(e)}(\underset{\sim}{u}^B, p^K, \lambda_2, \lambda_3) = 0 \, , \tag{2.84a}$$

$$\sum_{e=1}^{E} q^{K(e)} \, H_{K(e)}(\underset{\sim}{u}^B) = 0 \, . \tag{2.84b}$$

To write the equations in <u>global</u> form we introduce the transformation $\Lambda_a^{A(e)}$, defined by (ODEN and REDDY (1976))

$$\Lambda_a^{A(e)} = \begin{cases} 1 & \text{if node A of element } \Omega^e \text{ is identical} \\ & \quad \text{to node a of the assembled system} \\ 0 & \text{otherwise} \, . \end{cases} \tag{2.85}$$

Then we may write

$$v_i^{A(e)} = \Lambda_a^{A(e)} v_i^a \quad , \qquad q^{K(e)} = \Lambda_k^{K(e)} q^k \quad , \tag{2.86}$$

where v_i^a and q^k are global degrees of freedom. Consequently equations (2.84) become

$$v_i^a G_a^i = 0 \quad , \tag{2.87a}$$

$$q^k H_k = 0 \quad , \tag{2.87b}$$

where

$$G_a^i = \Lambda_a^{A(e)} G_{A(e)}^i \quad , \qquad H_k = \Lambda_k^{K(e)} H_{K(e)} \quad , \tag{2.88}$$

with summation over repeated indices A,K and (e) . Since v_i^a and q^k are arbitrary we end up with the set of nonlinear equations

$$G_a^i(\underset{\sim}{u}, \underset{\sim}{p}, \underset{\sim}{\lambda}) = 0 \quad , \tag{2.89a}$$

$$H_k(\underset{\sim}{u}) = 0 \quad , \tag{2.89b}$$

where $\underset{\sim}{u}$ and $\underset{\sim}{p}$ are vectors of global degrees of freedom and $\underset{\sim}{\lambda}$ is a vector of the parameters λ_i . Properties of equations of the form (2.89) and methods used for their solution are discussed in the following chapters.

CHAPTER 3

SYSTEMS OF NONLINEAR EQUATIONS

In this chapter we examine analytical and computational aspects of solution paths for systems of nonlinear equations. In section 3.1 we discuss results for equations that have a single parameter. These results are then extended in section 3.2 to problems with many parameters.

First, we need to re-examine the concept of a singular solution point for single parameter problems; this is done in section 3.1.1. For problems in which this singular behaviour may occur it has been found that conventional methods, such as the well known Newton methods, are unable to be used without certain adaptations or modifications. Thus various inflation procedures, discussed in section 3.1.2, have been developed to overcome these difficulties. It is also necessary to define properly and investigate the occurrence of singular points in multi-parameter problems : this is done in section 3.2.1, before the aforementioned inflation procedures can be applied (in section 3.2.2) to these problems. Two particular examples of multi-parameter problems are chosen for illustration. First, the problem in which piecewise-linear paths relate the parameters in parameter space is dealt with in section 3.2.3. Then in section 3.2.4 we discuss the problem of tracing the loci of singular points in these multi-parameter problems. More detailed computational aspects and methods will be dealt with in the following chapter.

3.1 Systems of equations with a single parameter

Newton methods have been widely used (ORTEGA and RHEINBOLDT (1970) and RALL (1969)) for the computation of solution paths of systems of nonlinear equations of the form

$$f(u,\lambda) = 0 \quad , \tag{3.1}$$

where $u \in R^n$ is a vector, $\lambda \in R$ is a naturally occurring parameter and f is a map from $R^n \times R$ to R^n. Note that here and throughout this chapter the underlining of symbols with a tilde ($\sim$) to denote a vector or a tensor has been omitted for clarity. These methods, in their standard or modified forms, have been found to be very efficient, but they are unable to be used without certain adaptations for general problems in which singular behaviour may occur. These difficulties and various methods to overcome them are discussed in the following sections.

3.1.1 Singular points

In subsequent sections we shall draw heavily on results established for singular points on solution paths of systems of nonlinear equations with a single parameter. For this reason we summarise here a few of the more important ideas, following closely the work of KELLER (1977) and DECKER and KELLER (1980, 1981).

Consider (3.1) which represents a set of n equations. A point $p = (u_o,\lambda_o)$ on the solution path of (3.1) is said to be

$$\left.\begin{matrix}\text{regular}\\ \\ \text{singular}\end{matrix}\right\} \quad \text{if } f_u \text{ is} \quad \left\{\begin{matrix}\text{nonsingular}\\ \\ \text{singular}\end{matrix}\right. . \qquad (3.2)$$

Here f_u is the matrix with components $\partial f_i/\partial u_j$. If p is a regular point the implicit function theorem (IOOSS and JOSEPH (1980)) guarantees the existence of a unique solution path $u(\lambda)$ in the neighbourhood of p , such that $f(u(\lambda_o),\lambda_o) = 0$ (see Figure 3.1). In the event that f_u is singular, however, the usual procedure of parameterising the path by λ may not work, and it is necessary to introduce another parameter s, say . Then we seek a solution $(u(s),\lambda(s))$ to

$$f(u(s),\lambda(s)) = 0 \quad . \qquad (3.3)$$

It is customary, though by no means necessary, to regard s as a measure of arc-length (Figure 3.1) .

We proceed now to characterise a singular point $(u_o,\lambda_o) \equiv (u(s_o),\lambda(s_o))$. Suppose that f_u has a one-dimensional null space $N(f_u)$ spanned by a vector ϕ . Then the transpose f_u^* of f_u also has a one-dimensional null space $N(f_u^*)$ spanned by a vector ϕ^* ,

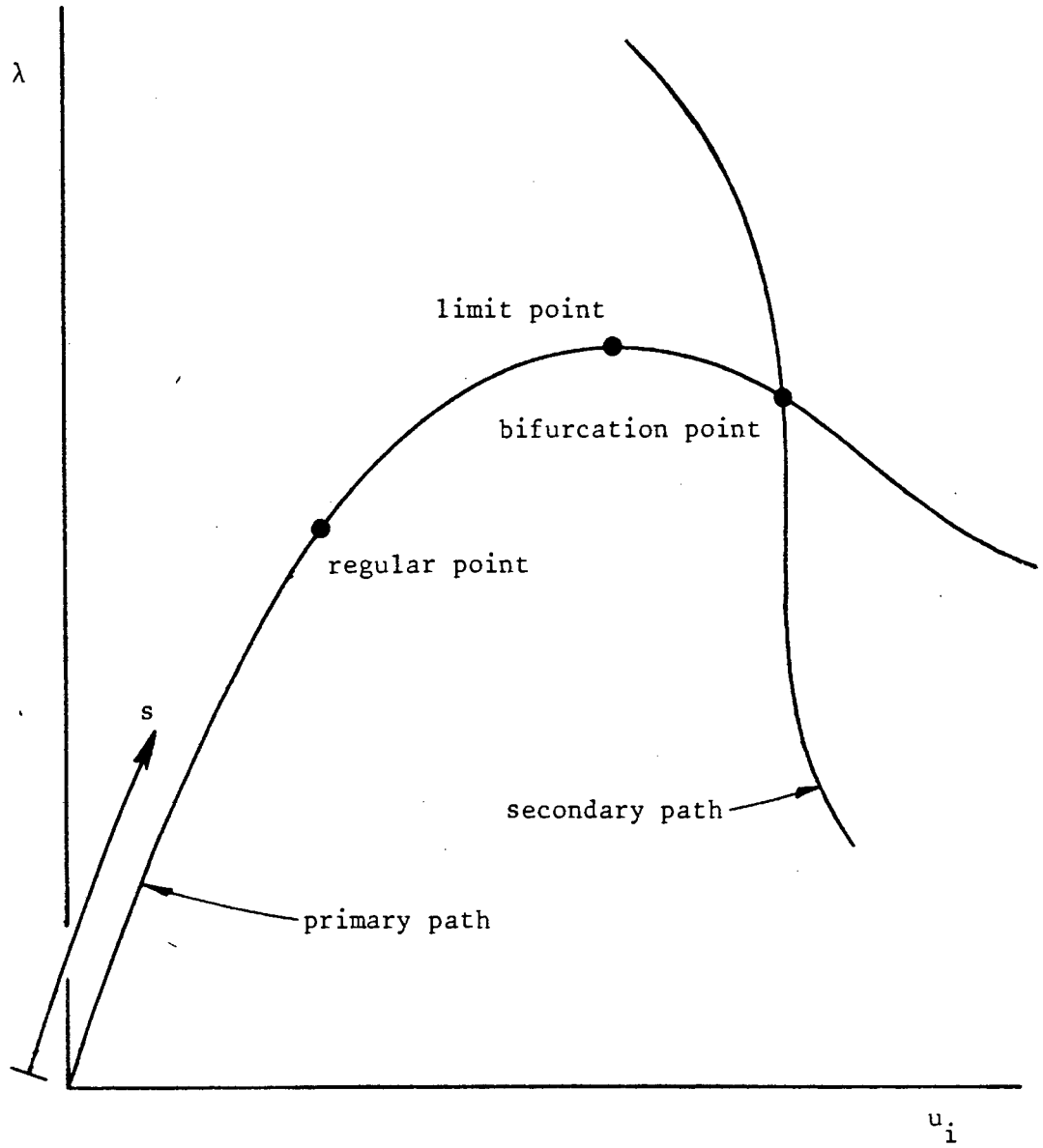

Figure 3.1 Solution paths for $f(u,\lambda) = 0$.

say. Of course, if f_u is symmetric then $\phi^* = \phi$. It is well known (STRANG (1980)) that a necessary condition for the existence of a solution to the equation

$$f_u x = y \quad , \tag{3.4}$$

is that y must be orthogonal to ϕ^* :

$$R(f_u) = \{ y \mid y \in R^n \quad , \quad \phi^* . y = 0 \} \quad , \tag{3.5}$$

where R( ) denotes the range of an operator. When (3.5) holds the (non-unique) general solution of (3.4) is

$$x = \bar{x} + a\phi \quad , \tag{3.6}$$

where $\bar{x}$ is any solution of (3.4) and a is an undetermined constant. The vector $\bar{x}$ is not unique but may be made so by requiring that

$$\bar{x} . \phi^* = 0 \quad . \tag{3.7}$$

In order to determine the nature of the solution path at the singular point we differentiate (3.3) with respect to s and evaluate at p to obtain

$$f_u \dot{u} + f_\lambda \dot{\lambda} = 0 \quad , \tag{3.8}$$

where $(\dot{})\ \equiv\ d(\ )/ds$. For a solution of (3.8) to exist we require from (3.5) that

$$\phi^*.(f_\lambda \dot{\lambda}) \;=\; 0 \quad . \tag{3.9}$$

Two possibilities therefore exist : either

$$\dot{\lambda} \;=\; 0 \quad , \quad \phi^*.f_\lambda \;\neq\; 0 \quad , \tag{3.10}$$

in which case p is called a <u>limit point</u>, or

$$\dot{\lambda} \;\neq\; 0 \quad , \quad \phi^*.f_\lambda \;=\; 0 \quad , \tag{3.11}$$

in which case p is called a <u>bifurcation point</u>. It is not difficult to show (DECKER and KELLER (1980)) that there exists a <u>unique</u> solution arc $(u(s),\lambda(s))$ of (3.3) through a limit point. For a <u>bifurcation point</u> it is necessary to examine the second derivative of (3.3) evaluated at p :

$$f_u \ddot{u} \;+\; f_\lambda \ddot{\lambda} \;+\; f_{uu}\dot{u}\dot{u} \;+\; 2f_{u\lambda}\dot{u}\dot{\lambda} \;+\; f_{\lambda\lambda}\dot{\lambda}\dot{\lambda} \;=\; 0 \quad . \tag{3.12}$$

Equations (3.8) and (3.11) result in the solution

$$\dot{u} \;=\; \bar{a}\bar{\phi} \;+\; a\phi \quad , \quad \dot{\lambda} \;=\; \bar{a} \quad , \tag{3.13}$$

where $\bar{\phi}$ is the solution of $f_u\bar{\phi} + f_\lambda = 0$ and a, $\bar{a}$ are at present undetermined scalars, while equation (3.12) together with an equation which determines the parameter s (this may correspond to an

approximation of the arc length) result in a pair of quadratic equations for a and $\bar{a}$ (see DECKER and KELLER (1980)). For a solution to exist it is necessary that the Jacobian of this pair of algebraic bifurcation equations does not vanish and, if so, then $(a,\bar{a})$ is an isolated root of the algebraic bifurcation equations. These equations can have at most two roots and hence it follows that at most two non-tangential solution arcs intersect at p. RIKS (1979) has also obtained these results for a finite dimensional space. These ideas are illustrated in Figure 3.1.

3.1.2 Inflation procedures

In order to overcome the problems inherent in the use of Newton methods near singular points the following procedure has been proposed independently by KELLER (1977) for problems in Banach spaces and by RIKS (1972,1979) and WEMPNER (1971) for finite-dimensional problems : an additional scalar equation

$$h(u,\lambda,s) = 0 \quad , \tag{3.14}$$

is added to (3.1), so that the simultaneous solution of (3.1) and (3.14) locates a single point on the solution path. Here the scalar s may be regarded as a measure of arc-length as in the previous section. Before discussing features of this procedure we give some examples of (3.14) that have been used in practice.

Suppose that the solution (u_o,λ_o) (not necessarily a singular point) and the tangent $(\dot{u}_o,\dot{\lambda}_o)$ at this point are known ; then RIKS (1979) defines the constraint equation by

$$h(u,\lambda,s) \equiv (u-u_o).\dot{u}_o + (\lambda-\lambda_o)\dot{\lambda}_o - (s-s_o) = 0 \quad . \qquad (3.15)$$

This equation constrains the next solution point to lie on the hyperplane with normal $(\dot{u}_o,\dot{\lambda}_o)$, which is a distance $(s-s_o)$ from the previous known point (Figure 3.2). KELLER (1977) defines a similar constraint of the form

$$h(u,\lambda,s) \equiv \theta(u-u_o).\dot{u}_o + (1-\theta)(\lambda-\lambda_o)\dot{\lambda}_o - (s-s_o) = 0 \quad , \qquad (3.16)$$

where $0 < \theta < 1$.

The constraint equation (3.15) requires for its use the tangent at the previous known point. Evaluation of the tangent may be circumvented though, by using instead the <u>secant</u> vector $(\bar{u},\bar{\lambda}) = (u_o-u_{-1},\lambda_o-\lambda_{-1})$ through the two previous known points (WEMPNER (1971) and RIKS (1979)). Then, instead of (3.15), we have (Figure 3.3)

$$h(u,\lambda,s) \equiv (u-u_o).\bar{u} + (\lambda-\lambda_o)\bar{\lambda} - (s-s_o) = 0 \quad . \qquad (3.17)$$

The constraint equation (3.16) can be modified in the same manner. Yet another possibility that is used by KELLER (1977), in which the

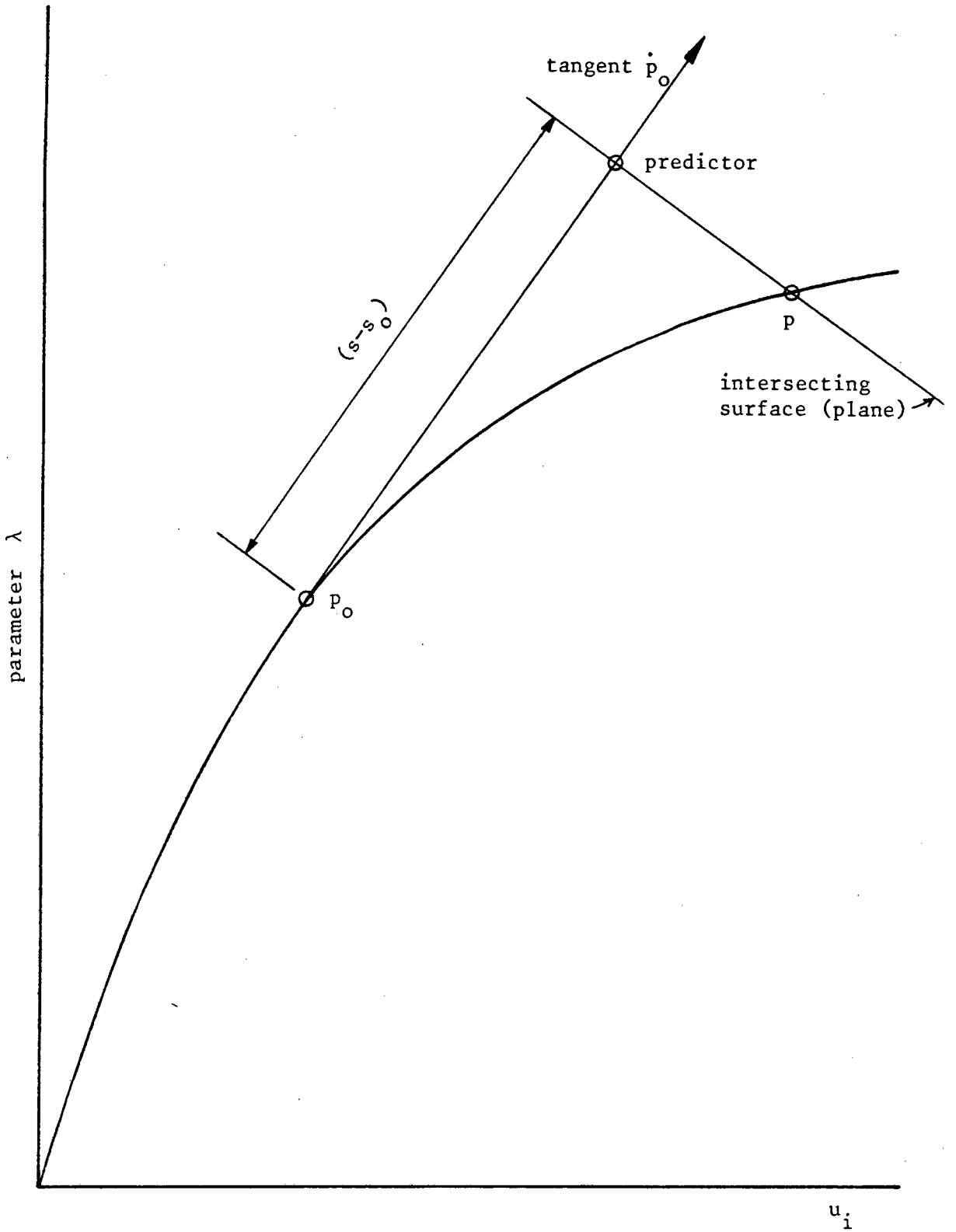

Figure 3.2 Arc-length method with intersecting plane using exact tangent.

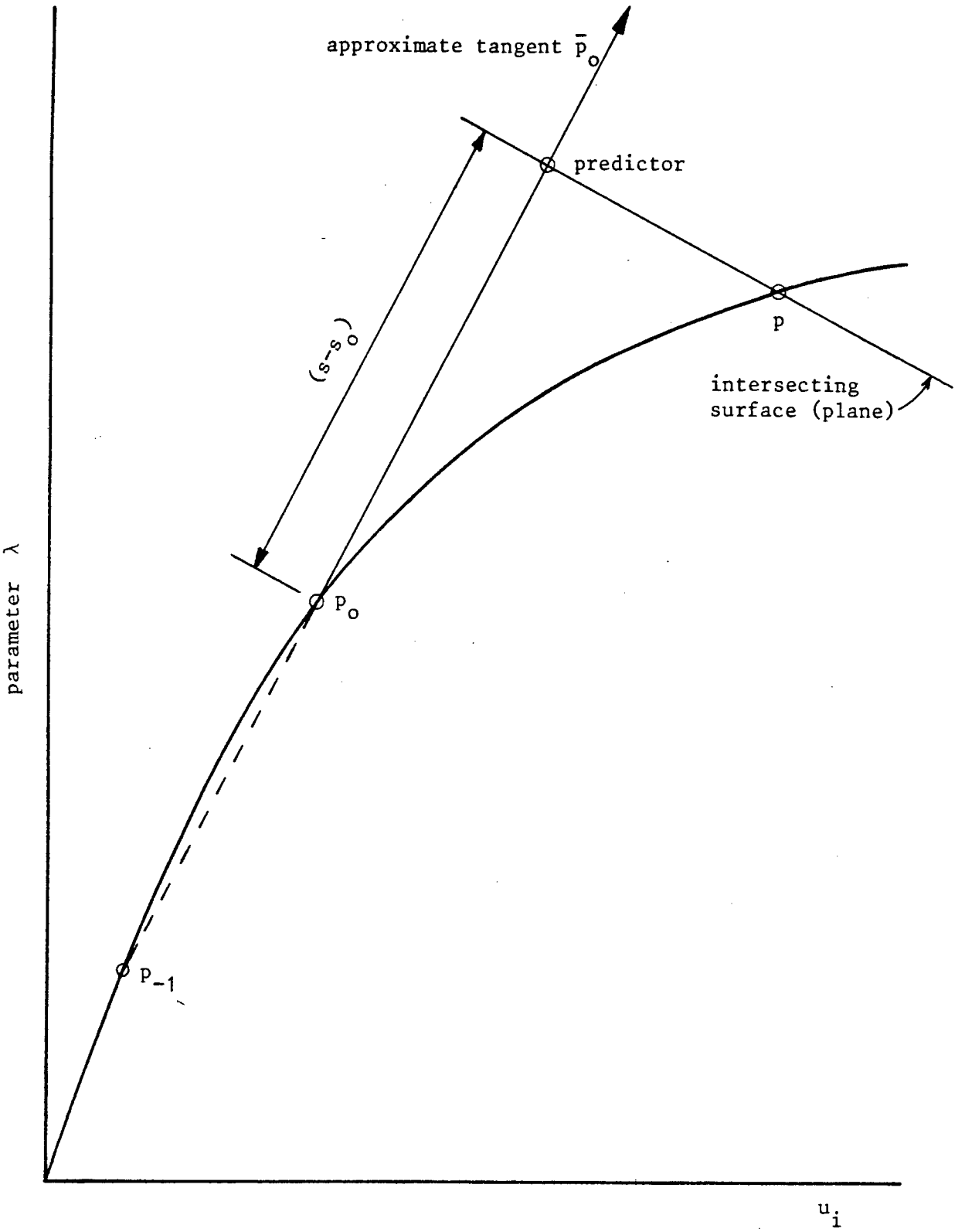

Figure 3.3 Arc-length method with intersecting plane using approximate tangent.

hyperplane in the previous equations is replaced by a hypersurface (Figure 3.4), is

$$h(u,\lambda,s) \equiv \theta(u-u_o).(u-u_o) + (1-\theta)(\lambda-\lambda_o)^2 - (s-s_o)^2 = 0 \quad . \tag{3.18}$$

Instead of using (3.18) CRISFIELD (1981) found it preferable to fix the arc-length in R^n so that the constraint equation is of similar form to (3.18) but with $\theta = 1$. A generalisation of (3.18) is proposed by PADOVAN and TOVICHAKCHAIKUL (1982) who have introduced a hyper-elliptic constraint surface.

The most important advantage to be obtained from working with (3.1) and (3.14) comes from the fact that the matrix

$$A = \begin{bmatrix} f_u & f_\lambda \\ h_u & h_\lambda \end{bmatrix} , \tag{3.19}$$

which is the gradient of $\begin{Bmatrix} f \\ h \end{Bmatrix}$ with respect to $\begin{Bmatrix} u \\ \lambda \end{Bmatrix}$, can be <u>nonsingular</u> even though f_u is <u>singular</u>. We summarise the conditions under which this occurs in the following theorem, which extends a result due to KELLER (1977).

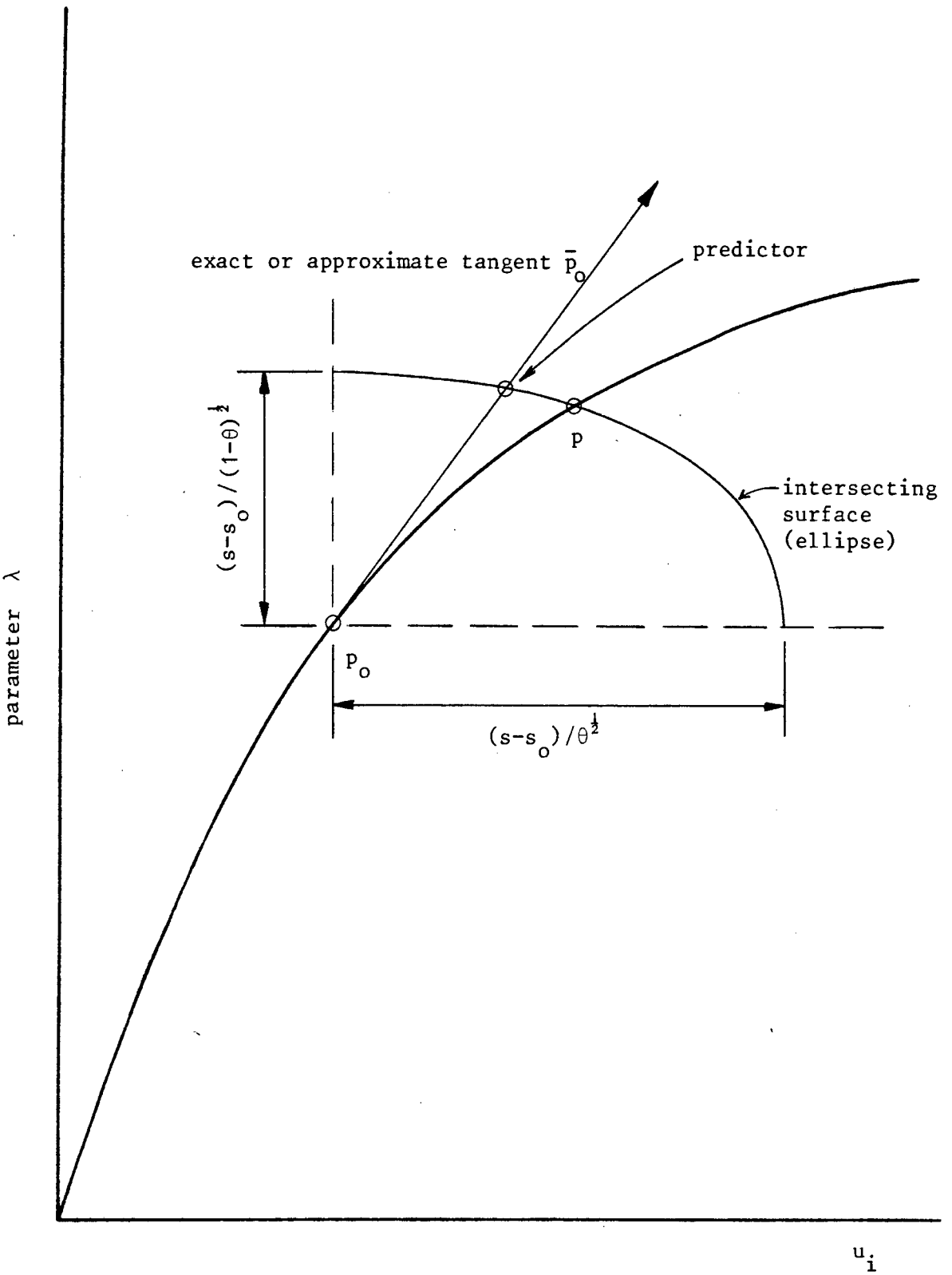

Figure 3.4 Arc-length method with elliptical intersecting surface.

Theorem 3.1

(i) Let (u_o,λ_o) be a regular point or a limit point of $f(u,\lambda) = 0$. Then there exists a unique solution arc $(u(s),\lambda(s))$ in a neighbourhood of (u_o,λ_o), and along this arc A is nonsingular, provided that

$$\dot{u}_o.h_u + \dot{\lambda}_o h_\lambda \neq 0 \quad . \tag{3.20}$$

(ii) If (u_o,λ_o) is a simple bifurcation point of $f(u,\lambda) = 0$, then A is singular.

Proof

Let (u_o,λ_o) be a solution of $f(u,\lambda) = 0$ and let $(\dot{u}_o,\dot{\lambda}_o)$ satisfy the requirements (see equation (3.8))

$$f_u\dot{u}_o + f_\lambda\dot{\lambda}_o = 0 \quad , \tag{3.21a}$$

$$\dot{u}_o.\dot{u}_o + \dot{\lambda}_o^2 > 0 \quad , \tag{3.21b}$$

where we assume that f_u and f_λ have been evaluated at (u_o,λ_o). First we consider (u_o,λ_o) to be a limit point : from equations (3.10) and (3.5) we have $\dot{\lambda}_o = 0$ and $f_\lambda \notin R(f_u)$. This, together with (3.21a) implies that $\dot{u}_o \in N(f_u)$ where $N(\ )$ denotes the null space of an operator :

$$N(f_u) = \{ y \mid y \in R^n \ , \ f_u y = 0 \} \quad . \tag{3.22}$$

Also, since $h_u.\dot{u}_o \neq 0$ and the dimension of $N(f_u) = 1$, we find that $h_u \notin R(f_u^*)$. These results together with those of KELLER (1977, Lemma 2.8 and equation (2.9)) show that A is nonsingular.

Now let (u_o,λ_o) be a <u>regular point</u> : if $\dot{\lambda}_o = 0$ we see from equation (3.21a) that $\dot{u}_o = 0$. This contradicts equation (3.21b) and thus we have $\dot{\lambda}_o \neq 0$ at a regular point. Using KELLER'S (1977, Lemma 2.8) result we find that A is nonsingular if and only if

$$h_\lambda - h_u f_u^{-1} f_\lambda \neq 0 \quad . \tag{3.23}$$

Using equation (3.21a) we rewrite (3.23) as

$$\dot{u}_o.h_u + \dot{\lambda}_o h_\lambda \neq 0 \quad . \quad \square \tag{3.24}$$

We note that KELLER (1977) gives part (i) of this theorem with conditions pertaining to a particular constraint equation h, instead of (3.20) which is valid for any h.

We see then that limit points "disappear" in the inflated system, while bifurcation occurs simultaneously in this system and for $f(u,\lambda)$ alone. The result has important consequences for numerical computations : limit points present no problems, and when tracing out a solution path a standard Newton procedure allows us to "jump" over bifurcation points. The location of bifurcation points can be determined by monitoring det A for a change in sign, and by using a method such as bisection to locate the point exactly.

3.2 Systems of equations with many parameters

In this section we discuss methods for dealing with systems of equations of the form (3.1) containing many parameters. We assume that there are m such parameters, which are related to each other via an arbitrary set of $(m-1)$ constraint equations :

$$g(u,\lambda) = 0 \quad . \tag{3.25}$$

Here, λ now represents an m dimensional vector, and equations (3.25) together with (3.1) allow us to solve for the unknown vectors u and λ. For our purposes, however, it suffices to consider equations such as (3.25) in which there is no dependence on u , i.e.

$$g(\lambda) = 0 \quad , \tag{3.26}$$

where we now have $g : R^m \to R^{m-1}$.

Geometrically, equation (3.26) represents a path in m-dimensional parameter space, and so the discussion in section 3.1 is appropriate here as well. The ideas in section 3.1 are best put to use by singling out one of the variables λ_i as a parameter of the system (3.26). To do this, we write

$$\lambda = (\nu,\mu) \quad , \quad \nu = \lambda_i \in R \quad , \quad \mu = (\lambda_1,\lambda_2,\ldots\lambda_{i-1},\lambda_{i+1},\ldots\lambda_m) \quad . \tag{3.27}$$

Note that the choice of ν is quite arbitrary ; once a variable λ_k, say, has been chosen as the parameter, the remaining variables are labelled $\mu_1 \ldots \mu_{m-1}$ and λ_k is labelled as ν .

Of primary interest here is the extent to which the theory of section 3.1.1 is applicable to a system with many parameters. With this as our goal, we now consider the set of equations

$$f(u,\nu,\mu) = 0 \quad , \tag{3.28a}$$

$$g(\nu,\mu) = 0 \quad , \tag{3.28b}$$

in which the relabelling (3.27) has been carried out. As before (3.28a) is a set of n equations. The situation is depicted in Figure 3.5 for $n = 1$ and $m = 2$; here, the single equations $f = 0$ and $g = 0$ represent surfaces in R^3 and the intersection of these two surfaces gives the required solution curve.

3.2.1 Regular and singular points

The classification of points on the solution path is carried out by considering the matrices $f_u \equiv \partial f/\partial u$ and $g_\mu \equiv \partial g/\partial \mu$. We proceed now to consider the various possibilities at a point (u_o, ν_o, μ_o); these are all summarised in Table 3.1.

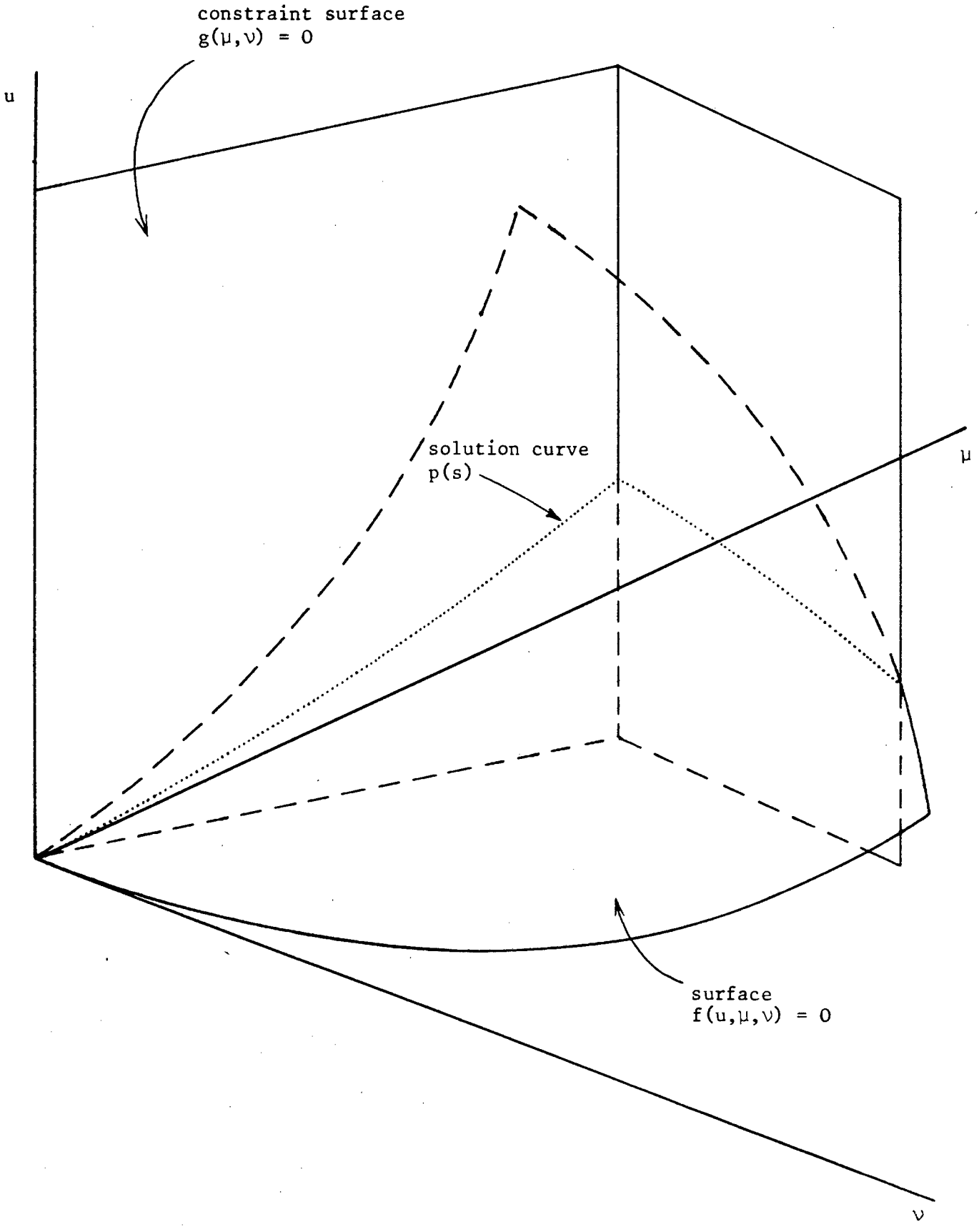

Figure 3.5 Intersection of solution surface with the constraint surfaces for a problem with n=1, m=2.

Criteria		Point in R^{n+1}	Point in R^{m}	Possible Solutions in R^{n+m}
I f_u nonsingular	(i) g_μ nonsingular	regular	regular	1 solution
	(ii) g_μ singular	regular	(a) limit	1 solution
			(b) bifurcation	2 solutions
II f_u singular	(i) g_μ nonsingular	(a) limit	regular	1 solution
		(b) bifurcation	regular	2 solutions
	(ii) g_μ singular	(a) limit	(1) limit	1 solution
			(2) bifurcation	2 solutions
		(b) bifurcation	(1) limit	2 solutions
			(2) bifurcation	4 solutions

Table 3.1 Classification of points on solution paths for nonlinear equations with many parameters (numbering corresponds to that in the text).

I f_u is nonsingular

(i) g_μ is nonsingular

By the implicit function theorem there exists a unique curve $\mu(\nu)$ in a neighbourhood of (ν_o,μ_o), which passes through this point, and is such that $g(\nu,\mu(\nu)) = 0$. Equation (3.28a) thus becomes

$$f(u,\nu,\mu(\nu)) = 0 \quad , \tag{3.29}$$

and since f_u is nonsingular, there is a unique curve $u(\nu)$ which passes through the point (u_o,ν_o) and which satisfies (3.29) in a neighbourhood of this point. There is thus a unique solution to (3.28) in a neighbourhood of (u_o,ν_o,μ_o).

(ii) g_μ is singular

The theory of section 3.1.1 is immediately applicable to (3.28b).

(a) Suppose first that (ν_o,μ_o) is a limit point : then $\dot{\nu}_o = 0$ and $g_\nu.\phi_1^* \neq 0$, where $\phi_1^* \in N(g_\mu^*)$. There exists a unique solution path $(\nu(s),\mu(s))$ through (ν_o,μ_o) with corresponding tangent $(\dot{\nu}_o,\dot{\mu}_o) = (0,\phi_1)$. From (3.28a) we find immediately that

$$f(u,\nu(s),\mu(s)) = 0 \quad , \tag{3.30}$$

and so there exists a unique solution $u(s)$ passing through (u_o,s_o) . This result indicates that the solution path in R^{n+m} may also be parameterised by s.

(b) Secondly, suppose that (ν_o,μ_o) is a bifurcation point : then $\dot{\nu}_o \neq 0$ and $g_\nu.\phi_1^* = 0$. By the theory of section 3.1.1 there are two solution paths which intersect non-tangentially at (ν_o,μ_o); each path may be parameterised by s so we may write $(\nu^{(i)}(s),\mu^{(i)}(s))$ for the paths $i = 1,2$. Thus (3.28a) becomes

$$f(u,\nu^{(i)}(s),\mu^{(i)}(s)) = 0 \quad , \tag{3.31}$$

and so corresponding to each path in parameter space there is a unique solution $u^{(i)}(s)$ of (3.31) in a neighbourhood (u_o,s_o). There are thus two solution curves to (3.28), which intersect at (u_o,ν_o,μ_o) .

II f_u is singular

We assume throughout that $\dim N(f_u^*) = 1$ with $N(f_u^*)$ spanned by ϕ_1^* .

(i) g_μ is nonsingular

Equation (3.29) is again applicable, but this time f_u is singular. However, since (3.29) is in a form such that the results of section 3.1.1 apply, we may conclude that (u_o,ν_o)

is <u>either a limit point or a bifurcation point</u>, depending on which of the criteria

$$\text{(a)} \qquad \dot{\nu}_o = 0 \ , \ (f_\nu + f_\mu \mu_\nu).\phi_1^* \neq 0 \ , \qquad (3.32)$$

(limit point) ,

or

$$\text{(b)} \qquad \dot{\nu}_o \neq 0 \ , \ (f_\nu + f_\mu \mu_\nu).\phi_1^* = 0 \ , \qquad (3.33)$$

(bifurcation point) ,

is satisfied. We note as a matter of interest that if (u_o, ν_o) is a limit point, then since $g_\nu \dot{\nu}_o + g_\mu \dot{\mu}_o = 0$ we find, for $\dot{\nu}_o = 0$ and nonsingular g_μ that $\dot{\mu}_o = 0$. In other words, the projection of the solution path on to the parameter space R^m "stops" at (ν_o, μ_o) . This phenomenon is illustrated in Figure 3.6. As with the case I(ii) there are <u>either one or two solution paths</u> through (u_o, ν_o, μ_o) depending on which of (3.32) or (3.33) holds.

(ii) <u>g_μ is singular</u>

Here we have the situation that singularities exist in f_u and g_μ , so we have to find out how the two sets of singularities react. As will become evident, the solution paths are naturally characterised in terms of two further parameters, rather than one which has been the case up to now.

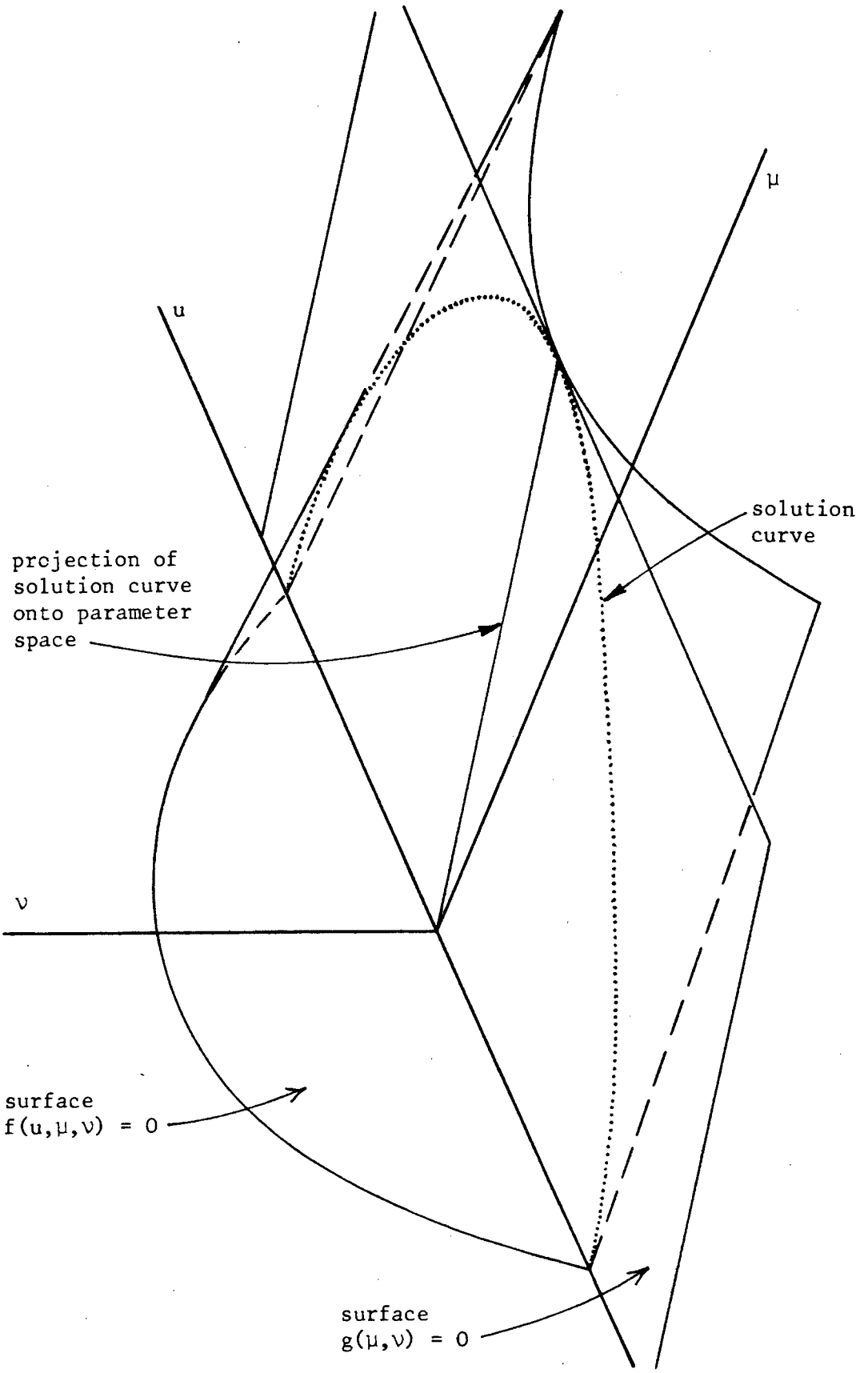

Figure 3.6 Intersection of surfaces for problem with n=1, m=2 showing parameters which "stop" in parameter space (μ,ν).

(1) If (ν_o,μ_o) is a limit point, then as before there is a unique solution path $(\nu(s),\mu(s))$ passing through (ν_o,μ_o), with $d\nu/ds = 0$ and $d\mu/ds \neq 0$. Thus equation (3.30) holds, though this time f_u is singular. We parameterise the solution arc corresponding to (3.30) by a parameter t, and differentiate (3.30) with respect to this parameter; thus

$$f_u\dot{u}_o + (f_\nu\nu_s + f_\mu\mu_s)\dot{s}_o = 0 \quad , \tag{3.34}$$

where $(\dot{})\equiv d(\,)/dt$. In order for a solution to (3.34) to exist it is necessary that

$$\phi_1^*.\underbrace{(f_\nu\nu_s + f_\mu\mu_s)}_{d}\dot{s}_o = 0 \quad . \tag{3.35}$$

Provided this holds, the theory of section 3.1.1 is applicable, this time in the space R^{n+1} to which the point (u_o,t_o) belongs.

(a) If $\dot{s}_o = 0$ and $\phi_1^*.d \neq 0$, we have a limit point at (u_o,s_o); there is thus a unique solution path $(u(t),s(t))$ passing through this point. Hence, when viewed in R^{n+m} we find that there exists a unique solution path

$(u(t),s(t),\nu(s(t)),\mu(s(t)))$

passing through (u_o,ν_o,μ_o).

(b) If $\dot{s}_o \neq 0$ and $\phi_1^* . d = 0$, then (u_o, s_o) is a bifurcation point and there exists a pair of solution paths $(u^{(i)}(t), s^{(i)}(t))$. The solution of (3.34) at (u_o, ν_o, μ_o) thus consists of the pair of paths $(u^{(i)}(t), s^{(i)}(t), \nu^{(i)}(t), \mu^{(i)}(t))$ where $\nu^{(i)}(t) \equiv \nu(s^{(i)}(t))$, with a similar interpretation for $\mu^{(i)}(t)$.

(2) If (ν_o, μ_o) is a bifurcation point, then there exists a pair of solutions $(\nu^{(j)}(s), \mu^{(j)}(s))$ with $j = 1,2$. Equation (3.28a) thus becomes (similar to (3.31))

$$f(u, \nu^{(j)}(s), \mu^{(j)}(s)) = 0 \quad . \tag{3.36}$$

Once again we parameterise the solution of (3.36) by t , and then differentiate (3.36) with respect to t to obtain

$$f_u \dot{u}_o + \underbrace{(f_\nu \nu_s^{(j)} + f_\mu \mu_s^{(j)})}_{d^{(j)}} \dot{s}_o = 0 \quad . \tag{3.37}$$

The discussion following (3.35) is again appropriate, with d replaced by $d^{(j)}$.

(a) If $\dot{s}_o = 0$ and $\phi_1^* . d^{(j)} \neq 0$ we have a limit point at (u_o, s_o), and there is a unique solution $(u^{(j)}(t), s^{(j)}(t))$ passing through this point for each of the two equations $(j = 1,2)$ represented by (3.36). Hence there are two solution arcs $(u^{(j)}(t), s^{(j)}(t), \nu^{(j)}(t), \mu^{(j)}(t))$

passing through (u_o,ν_o,μ_o) . Note that $\nu^{(j)}(t) \equiv \nu(s^{(j)}(t))$ with a similar interpretation for $\mu^{(j)}(t)$.

(b) Finally, if $\dot{s}_o \neq 0$ and $\phi_1^*.d^{(j)} = 0$, then we have a bifurcation point at (u_o,s_o) for each value of j . It follows that there exists, for each j , a pair of solution arcs $(u^{(ij)}(t),s^{(ij)}(t))$ $(i = 1,2)$ passing through (u_o,s_o) . It is thus possible for four solution arcs $(u^{(ij)}(t),s^{(ij)}(t),\nu^{(ij)}(t),\mu^{(ij)}(t))$ to exist. Note, however, that it is quite possible that $\dot{s}_o \neq 0$, $\phi_1^*.d^{(1)} = 0$ but $\phi_1^*.d^{(2)} \neq 0$ (or the other way around); when this is the case then only two solutions occur, corresponding to $\phi_1^*.d^{(1)} = 0$.

3.2.2 Inflation procedure

The inflation procedure discussed in section 3.1.2 may be applied without modification to the class of multi-parameter problems of interest. If the path in R^{n+m} is parameterised by t the inflated system is

$$f(u(t),\nu(t),\mu(t)) = 0 \quad , \tag{3.38a}$$

$$h(u(t),\nu(t),\mu(t),t) = 0 \quad , \tag{3.38b}$$

$$g(\nu(t),\mu(t)) = 0 \quad , \tag{3.38c}$$

where h may be given by any one of the constraint equations discussed in section 3.1.2. By analogy with Theorem 3.1 we may prove the following result.

Theorem 3.2

Let (u_o, ν_o, μ_o) be a regular point of (3.38) or a simple limit point in the sense that I(ii)(a) or II(i)(a) or II(ii)(1)(a) hold (Table 3.1). Then there exists a unique solution arc $(u(t), \nu(t), \mu(t), t)$ of (3.38) through (u_o, ν_o, μ_o) in a neighbourhood of this point, and along the arc the matrix

$$A = \begin{bmatrix} f_u & f_\nu & f_\mu \\ h_u & h_\nu & h_\mu \\ 0 & g_\nu & g_\mu \end{bmatrix} \tag{3.39}$$

is nonsingular, provided that

$$\dot{u}_o . h_u + \dot{\nu}_o . h_\nu + \dot{\mu}_o . h_\mu \neq 0 \tag{3.40}$$

where $(\dot{}) \equiv d(\,)/dt$.

3.2.3 Piecewise-linear paths

We describe here the application of the ideas discussed in section 3.2.1 and 3.2.2 to the situation in which equation (3.26) describes a given piecewise-linear path in R^m such as that shown in Figure 3.7. The aim is to derive a set of equations of the form (3.26) which has the advantage of simplicity, and which furthermore is amenable to both analysis and numerical implementation. This may be achieved by deriving a set of equations whose solution is a number of straight lines, some intersecting, and which contain as a subset the path of interest (see Figure 3.7).

A piecewise-linear path in R^m may be described by the equation

$$\lambda(s) = \lambda^{(p)} + se^{(p)} \quad , \quad s^{(p)} \leq s \leq s^{(p+1)} \, , \quad p = 1,2... \qquad (3.41)$$

in which (p) indexes both paths and junctions (Figure 3.7); λ is a vector in R^m, $\lambda^{(p)}$ is the value of λ at junction (p) and $e^{(p)}$ is the unit vector along path (p). The real variable s parameterises distance along the path (p).

Suppose that there are N paths, so that p ranges from 1 to N, and define for each path (p) the set $A^{(p)}$ of integers by

$$A^{(p)} = \{ k \in Z \mid 1 \leq k \leq m \, , \, e_k^{(p)} \neq 0 \} \, . \qquad (3.42)$$

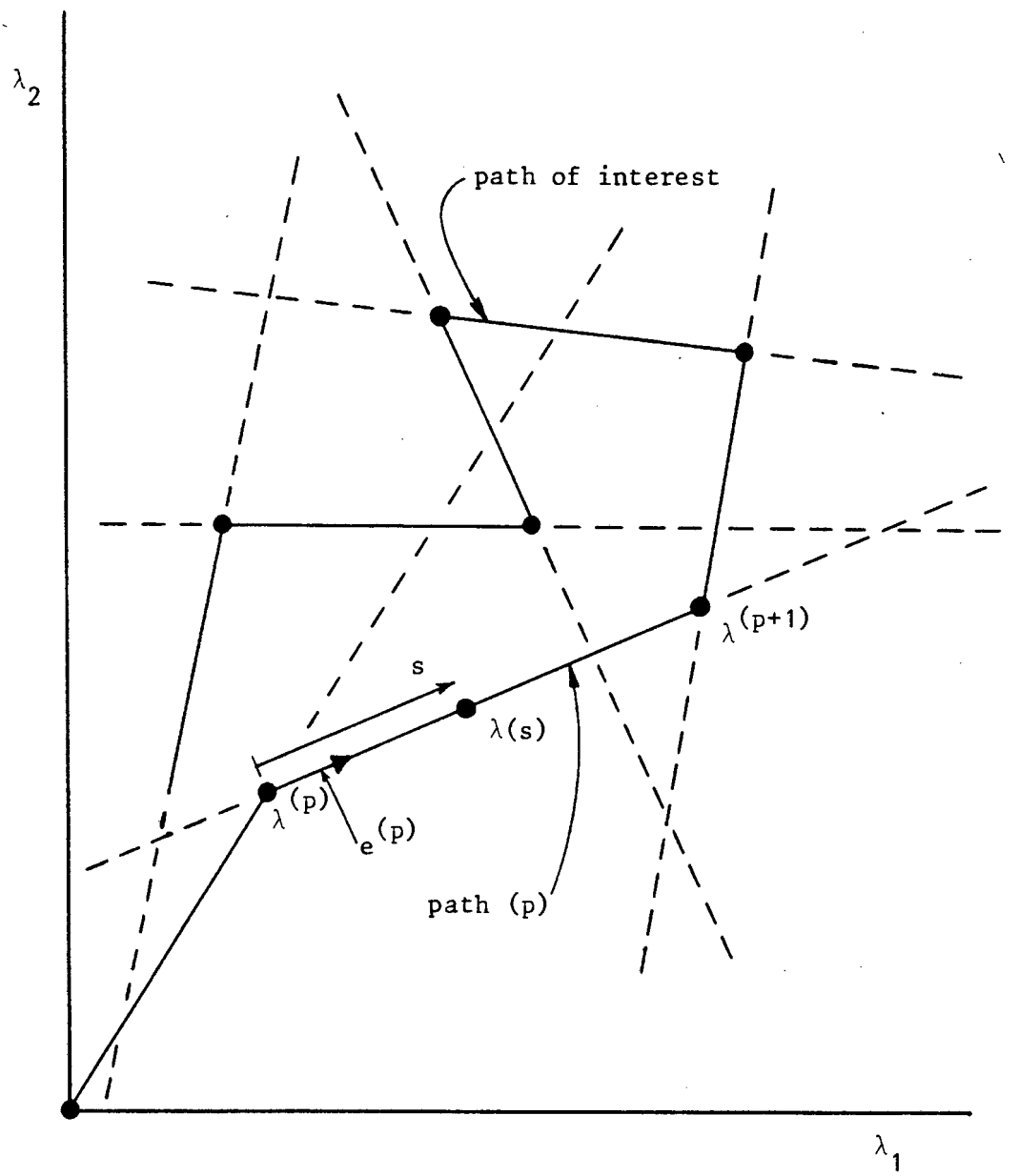

Figure 3.7 Piecewise linear constraint equations for the case when m=2.

That is, $A^{(p)}$ is the set of all integers between 1 and m corresponding to non-zero components of $e^{(p)}$. Obviously $A^{(p)}$ is never empty. Next, define the set B by

$$B = \bigcap_{p=1}^{N} A^{(p)} \quad . \tag{3.43}$$

We assume that B is not empty; of course, it is not difficult to construct examples in which B is null, but if this happens to be the case it can be easily overcome, for example, by a perturbation of one or more of the paths. Finally we set

$$L = \max \{ k \mid k \in B \} \quad . \tag{3.44}$$

That is, L is the largest integer, taken over all the paths, such that $e_L^{(p)} \neq 0$.

Let us consider a simple example to clarify these ideas. A piecewise-linear path is described in Figure 3.8 for which m = 3, N = 4. Using the coordinates of the junctions the unit directional vectors for each path can easily be computed; we obtain

$$\begin{aligned} e^{(1)} &= (0,1,0) \quad , \quad e^{(2)} = (0,1,1)/\sqrt{2} \quad , \\ e^{(3)} &= (1,1,0)/\sqrt{2} \quad , \quad e^{(4)} = (1,1,1)/\sqrt{3} \quad . \end{aligned} \tag{3.45}$$

The integer sets $A^{(p)}$, p = 1 to 4 are now obtained by examining (3.45). We thus find

$$\begin{aligned} A^{(1)} &= \{2\} \quad , \quad A^{(2)} = \{2,3\} \quad , \\ A^{(3)} &= \{1,2\} \quad , \quad A^{(4)} = \{1,2,3\} \quad . \end{aligned} \tag{3.46}$$

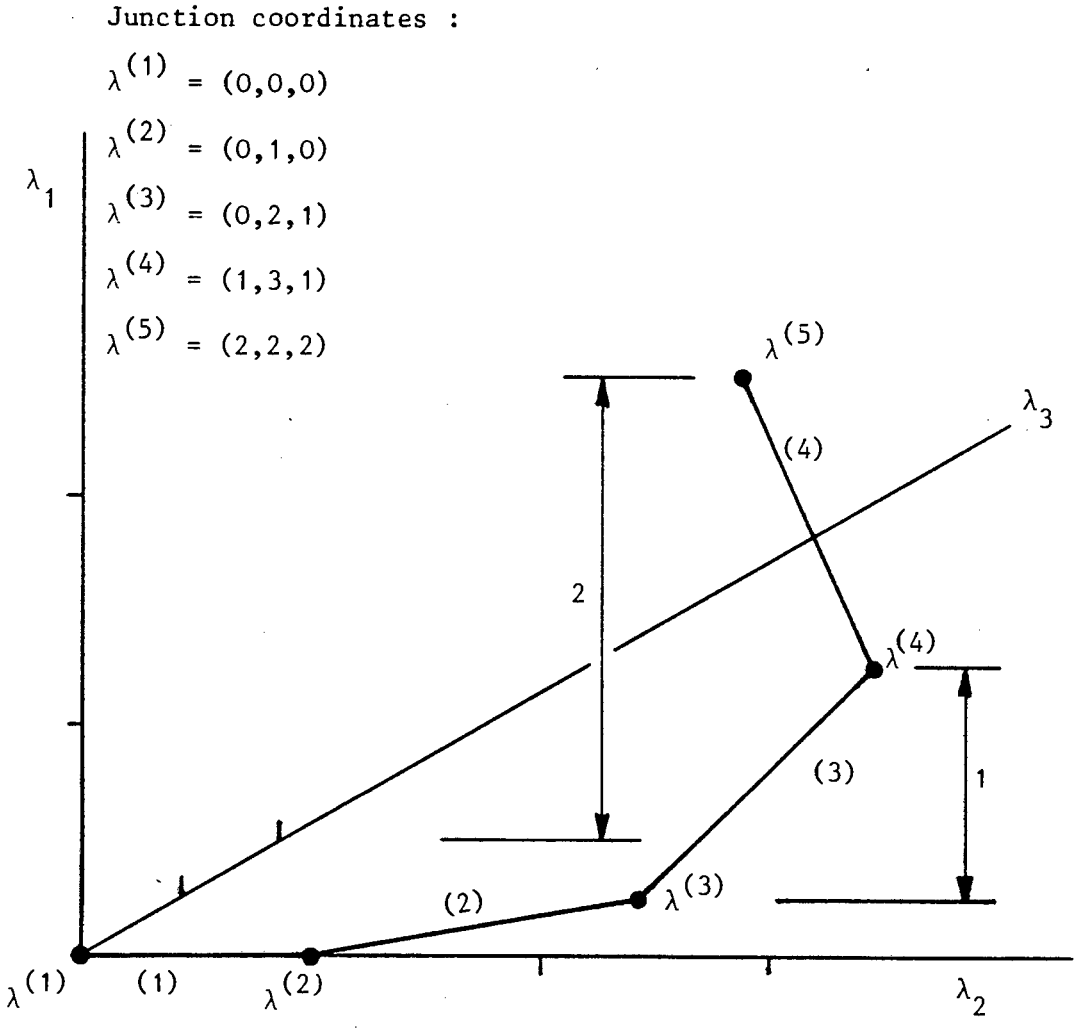

Figure 3.8 Piecewise-linear path for the case when m=3, N=4.

The intersection of these sets (3.46) gives us the set $B = \{ 2 \}$ and thus we have $L = 2$.

With these definitions aside we obtain from the L th component of (3.41)

$$s = (\lambda_L - \lambda_L^{(p)})/e_L^{(p)} \quad ; \tag{3.47}$$

substitution of this result back into (3.41) yields the set of $(m-1)$ equations for path (p) :

$$g_j^{(p)} = (\lambda_L - \lambda_L^{(p)})e_j^{(p)}/e_L^{(p)} - (\lambda_j - \lambda_j^{(p)}) \quad , \qquad j = 1,2, \ldots, (L-1),(L+1), \ldots,m \quad . \tag{3.48}$$

By dropping for the time being any reference to the range of λ for which (3.48) holds, equation (3.48) describes a straight line in R^m of which path (p) is a subset.

We now set (see also equation (3.27))

$$\nu = \lambda_L \text{ and } \mu = (\lambda_1,\lambda_2, \ldots,\lambda_{L-1},\lambda_{L+1},\ldots,\lambda_m) \quad ; \tag{3.49}$$

with this change in notation, equation (3.48) can be written as

$$g_j^{(p)} = (\nu - \nu^{(p)})e_j^{(p)}/e_L^{(p)} - (\mu_j - \mu_j^{(p)}) \quad , \qquad j = 1, \ldots, m-1 \quad . \tag{3.50}$$

Then the set of equations describing all paths is expressible in the form

$$g_j(\nu,\mu) \equiv \prod_{p=1}^{N} g_j^{(p)}(\nu,\mu) = 0 \quad , \quad j = 1, \ldots, m-1 \quad . \tag{3.51}$$

It may happen that $g_j^{(p)} = g_j^{(q)}$ so that (3.51) may contain a quadratic (or higher order) term. Apart from being superflous, this can also cause problems later on in the solution procedure. Whenever $g_j^{(p)} = g_j^{(q)}$, then, we set $g_j^{(q)} = 1$. Similar considerations apply when more than one such equation is identical.

The classification of points on the curve depends on the nature of g_μ. On the curve (p), we have

$$\partial g_i/\partial \mu_j = (g_i^{(1)} g_i^{(2)} \ldots g_i^{(p-1)} g_i^{(p+1)} \ldots g_i^{(N)}) \partial g_i^{(p)}/\partial \mu_j \tag{3.52}$$

by application of the chain rule; the other terms in the chain rule expansion being zero because they contain $g_i^{(p)}$ which is zero on the curve (p). Equation (3.52) may be written more concisely, by considering (3.50) and (3.51), in the form

$$\partial g_i/\partial \mu_j = - (g_i/g_i^{(p)}) \delta_{ij} \tag{3.53}$$

where δ_{ij} is the Kronecker delta. We see immediately from (3.53) that g_μ is a diagonal matrix, and is nonsingular everywhere along path (p) except at its endpoints $(\nu^{(p)}, \mu^{(p)})$ and $(\nu^{(p+1)}, \mu^{(p+1)})$, at which $g_i^{(p-1)}$ and $g_i^{(p+1)}$, hence also g_i, vanish. We recognise these points as bifurcation points.

Solution of the complete inflated problem (3.38) is straightforward (see section 4.1). The only further requirement in the solution algorithm is a means for changing from path (p) to (p+1) when junction (p+1) is reached. This is easily done and is discussed in further detail in section 4.3.2.

3.2.4 Loci of singular points

A further application of the ideas discussed in sections 3.2.1 and 3.2.2 is that of tracing the locus of a singular point for two-parameter problems. The aim here is to constrain the system of equations via an equation of the form (3.25) so that the solution follows a path of singular points in R^{n+2} (see for example Figure 3.9).

From equation (3.2) we see that at a singular point we have

$$D \equiv \det f_u = 0 \quad ; \tag{3.54}$$

this equation is thus the required constraint equation. Derivatives of this equation, which are required in later chapters, can be obtained using

$$C_{ij} \equiv \text{cofactor } (f_u)_{ij} = \frac{\partial D}{\partial (f_u)_{ij}} \tag{3.55}$$

and

$$C_{ij}(f_u)_{jk} = \delta_{ik} D \quad . \tag{3.56}$$

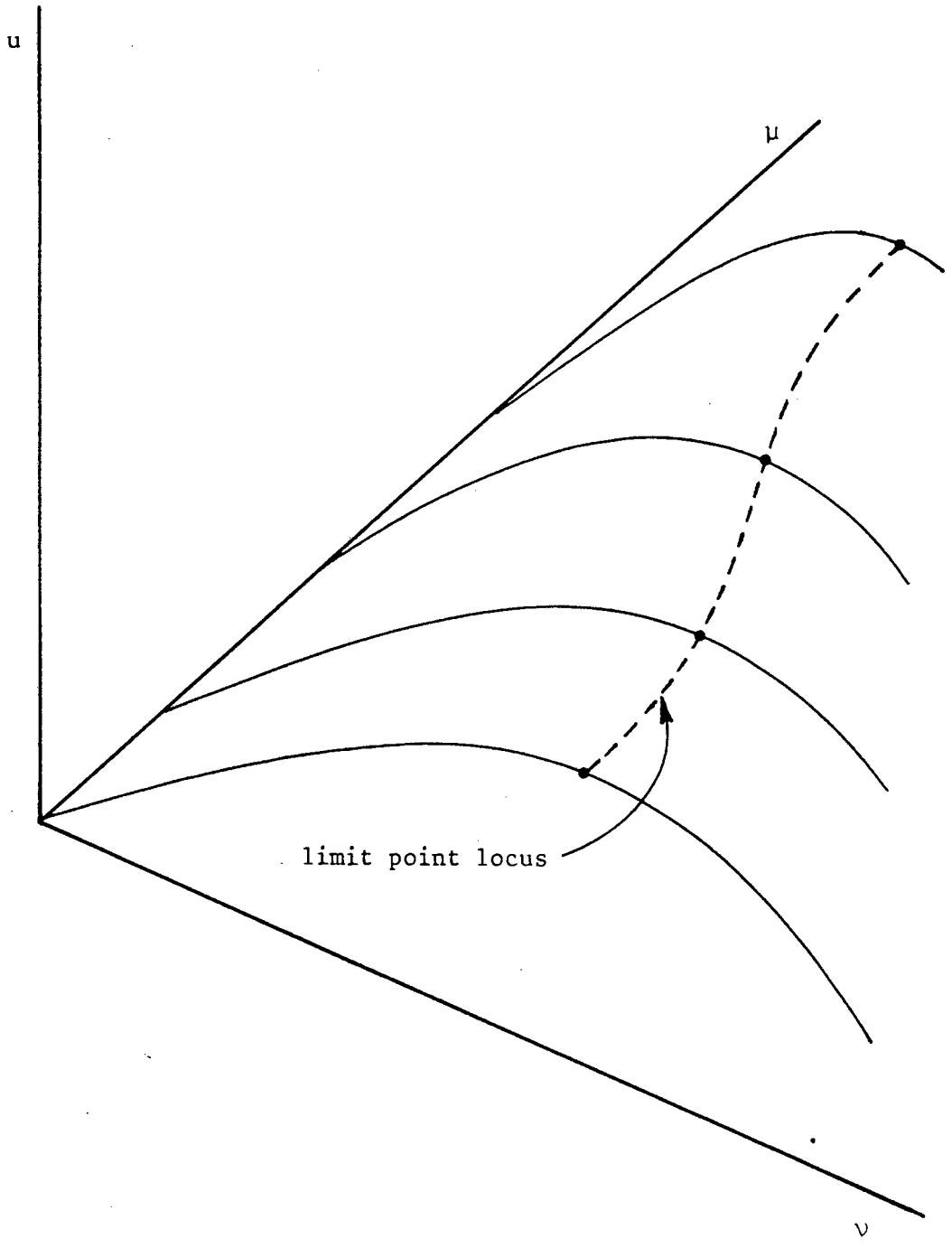

Figure 3.9 Locus of limit points in R^{n+2} (i.e. n=1,m=2) .

We can then write the derivatives as

$$\frac{\partial D}{\partial u_k} = \frac{\partial D}{\partial (f_u)_{ij}} \frac{\partial (f_u)_{ij}}{\partial u_k} = D(f_u^{-1})_{ij} \frac{\partial (f_u)_{ij}}{\partial u_k} \quad . \tag{3.57}$$

The computation of the terms in (3.57) will be described in the following chapter in section 4.4.1.

CHAPTER 4

SOLUTION OF NONLINEAR EQUATIONS

In previous chapters we have derived the equilibrium equations as well as the different constraint equations required for the various problems we wish to solve. In this chapter we now describe the numerical methods used to obtain the solutions to these problems.

In order to trace out solution arcs we use continuation methods (incrementation from step to step) together with the Newton-Raphson iteration method as described in section 4.1.1. To be able to use the Newton-Raphson method for our inflated systems of equations we need to compute derivatives of these equations with respect to the unknown parameters of the problem. The matrices and vectors resulting from these derivatives are obtained in section 4.1.2 and the equations required to compute them are described in appropriate parts of this chapter. Common to all the problems that will be discussed are the equilibrium equations and thus the coefficient matrices resulting from these equations are described in detail in section 4.1.3.

An important part of this study concerns singular points, and computations dealing with them are discussed in section 4.2. The derivatives of the arc-length constraint equation required by the Newton-Raphson method for our inflated system are described in section 4.2.1. In section 4.2.2 we then discuss methods for locating singular

points. The procedures used to branch onto bifurcation paths are discussed in section 4.2.3 as well as the method used to compute the approximate singular point. Generally the problems we are concerned with in section 4.2 are single parameter problems. In section 4.3, however, we consider multi-parameter problems and the associated piecewise-linear paths. The constraint equations required for these problems are derived from these piecewise-linear paths and their derivatives, which are required by the Newton-Raphson method, are described in section 4.3.1. A major consideration in these problems is that of ensuring that the solution follows the prescribed parameter path and the method used for this is described in detail in section 4.3.2. Apart from branching onto bifurcation paths and changing parameter paths at junctions we also wish to trace out loci of singular points. The computations required for this are discussed in section 4.4.

All the computations discussed in sections 4.2 to 4.4 are specific to the type of problem that is being considered. There are, however, many computational procedures that are common to all of these problems and these are described in section 4.5. Included here is the scaling of the solution space so that the dimensions of the quantities solved for are all approximately of the same magnitutde (section 4.5.1), and the algorithm that is used to obtain the solution to the non-symmetric system of equations produced by our inflation procedures (section 4.5.2). In order to improve the efficiency of the solution algorithm we use automatic incrementation techniques such as those discussed in section 4.6 for our continuation procedure.

4.1 Solution of inflated systems of equations

4.1.1 Newton-Raphson method

The Newton-Raphson method (or Newton's method) has been widely used for the computation of solution paths of systems of nonlinear equations of the form

$$f(x,\lambda) = 0 \quad , \tag{4.1}$$

where $x \in R^n$ is an unknown vector and λ is a scalar parameter. The standard Newton-Raphson method proceeds as follows : given a point (x_o,λ_o) on the solution path and an increment $\Delta\lambda$, we iterate on

$$\frac{\partial f}{\partial x}(x^{(t)},\lambda_o + \Delta\lambda)\ \Delta x^{(t)} = -f(x^{(t)},\lambda_o + \Delta\lambda) \quad , \tag{4.2a}$$

$$x^{(t+1)} = x^{(t)} + \Delta x^{(t)} \quad , \tag{4.2b}$$

until $\|f(x^{(t)},\lambda_o + \Delta\lambda)\|$ is less than some pre-assigned tolerance for some appropriate norm $\|\cdot\|$. We then repeat this process using $x^{(t+1)}$ to obtain the solution for the following point.

4.1.2 Application of the Newton-Raphson method to inflated systems of equations

The Newton-Raphson method as described above may be used to obtain solution paths for inflated systems of nonlinear equations with many parameters such as those described by equations (3.38). However, in this section we use the more general form of (3.38c) which is given by (3.25). Also, it is important to note that equation (3.38a) represents the set of equilibrium equations which are given by the equations (2.89). We are thus interested in the system of equations

$$G_a^i(\underset{\sim}{u}^r, p^c, \underset{\sim}{\lambda}) = 0 \quad , \tag{4.3a}$$

$$H_k(\underset{\sim}{u}^r) = 0 \quad , \tag{4.3b}$$

$$h(\underset{\sim}{u}^r, p^c, \underset{\sim}{\lambda}, s) = 0 \quad , \tag{4.3c}$$

$$g_b(\underset{\sim}{u}^r, p^c, \underset{\sim}{\lambda}) = 0 \quad . \tag{4.3d}$$

Here

$$i=1, \ \ldots \ , \text{ dimension of the problem ;} \tag{4.4a}$$

$$a,r = 1, \ \ldots \ , \text{ total number of nodes in the finite element model ;} \tag{4.4b}$$

$$k,c = 1, \ \ldots \ , \text{ total number of nodes in the model that have pressure degrees of freedom ;} \tag{4.4c}$$

$b = 1, \ldots, (m-1)$; m is the number of independent parameters in the model . (4.4d)

Note also that in equations (4.3) the independent parameter is the approximate arc-length s while $\underset{\sim}{u}^r$ and p^c are the unknown global displacement and pressure degrees of freedom respectively, with $\underset{\sim}{\lambda} \equiv (\nu, \underset{\sim}{\mu})$ the unknown vector of parameters.

Application of the Newton-Raphson iteration procedure to the system of equations (4.3) yields (for clarity we omit the iteration counter (t))

$$\frac{\partial G^i_a}{\partial u^r_\ell}\Delta u^r_\ell + \frac{\partial G^i_a}{\partial p^c}\Delta p^c + \frac{\partial G^i_a}{\partial \lambda_q}\Delta\lambda_q = -G^i_a \quad , \tag{4.5a}$$

$$\frac{\partial H_k}{\partial u^r_\ell}\Delta u^r_\ell = -H_k \quad , \tag{4.5b}$$

$$\frac{\partial h}{\partial u^r_\ell}\Delta u^r_\ell + \frac{\partial h}{\partial p^c}\Delta p^c + \frac{\partial h}{\partial \lambda_q}\Delta\lambda_q = -h \quad , \tag{4.5c}$$

$$\frac{\partial g_b}{\partial u^r_\ell}\Delta u^r_\ell + \frac{\partial g_b}{\partial p^c}\Delta p^c + \frac{\partial g_b}{\partial \lambda_q}\Delta\lambda_q = -g_b \quad . \tag{4.5d}$$

These equations may be written in matrix form as

$$\begin{bmatrix} \frac{\partial G_a^i}{\partial u_\ell^r} & \frac{\partial G_a^i}{\partial p^c} & \frac{\partial G_a^i}{\partial \lambda_q} \\ \frac{\partial H_k}{\partial u_\ell^r} & 0 & 0 \\ \frac{\partial h}{\partial u_\ell^r} & \frac{\partial h}{\partial p^c} & \frac{\partial h}{\partial \lambda_q} \\ \frac{\partial g_b}{\partial u_\ell^r} & \frac{\partial g_b}{\partial p^c} & \frac{\partial g_b}{\partial \lambda_q} \end{bmatrix} \begin{Bmatrix} \Delta u_\ell^r \\ \Delta p^c \\ \Delta \lambda_q \end{Bmatrix} = \begin{Bmatrix} -G_a^i \\ -H_k \\ -h \\ -g_b \end{Bmatrix} . \qquad (4.6)$$

Using equations (2.86) we see that

$$\frac{\partial}{\partial u_\ell^r} = \Lambda_r^{B(f)} \frac{\partial}{\partial u_\ell^{B(f)}} \quad , \quad \frac{\partial}{\partial p^c} = \Lambda_c^{K(f)} \frac{\partial}{\partial p^{K(f)}} \quad ; \qquad (4.7)$$

then using (4.7) together with equations (2.83) and (2.88) in equation (4.6) we obtain

$$\begin{bmatrix} \Lambda_a^{A(e)}\Lambda_r^{B(f)}\dfrac{\partial G^i_{A(e)}}{\partial u^{B(f)}_\ell} & \Lambda_a^{A(e)}\Lambda_c^{K(f)}\dfrac{\partial G^i_{A(e)}}{\partial p^{K(f)}} & \Lambda_a^{A(e)}\dfrac{\partial G^i_{A(e)}}{\partial \lambda_q} \\ \Lambda_k^{K(e)}\Lambda_r^{B(f)}\dfrac{\partial H_{K(e)}}{\partial u^{B(f)}_\ell} & 0 & 0 \\ \dfrac{\partial h}{\partial u^r_\ell} & \dfrac{\partial h}{\partial p^c} & \dfrac{\partial h}{\partial \lambda_q} \\ \Lambda_r^{B(f)}\dfrac{\partial g_b}{\partial u^{B(f)}_\ell} & \Lambda_c^{K(f)}\dfrac{\partial g_b}{\partial p^{K(f)}} & \dfrac{\partial g_b}{\partial \lambda_q} \end{bmatrix} \begin{Bmatrix} \Delta u^r_\ell \\ \Delta p^c \\ \Delta \lambda_q \end{Bmatrix} = \begin{bmatrix} -\Lambda_a^{A(e)} G^i_{A(e)} \\ -\Lambda_k^{K(e)} H_{K(e)} \\ -h \\ -g_b \end{bmatrix} \tag{4.8}$$

Summation is implied over <u>all</u> repeated indices, and we have

$A,B,C = 1, \ldots,$ number of nodes in an element ; (4.9a)

$K,L,M = 1, \ldots,$ number of nodes with pressure degrees of freedom in an element ; (4.9b)

$e,f = 1, \ldots,$ total number of elements in the finite element model ; (4.9c)

$\ell = 1, \ldots,$ dimension of the problem ; (4.9d)

$q = 1, \ldots,$ number of independent parameters in the model. (4.9e)

It can be seen from equation (4.8) that the coefficients in the iteration matrix and right-hand side vector can be computed for each element and the resulting element terms assembled via the transformations $A_a^{A(e)}, A_r^{B(f)}, A_c^{K(f)}$ and $A_k^{K(e)}$ into the global system of equations.

The computation of the terms appearing in equation (4.8) will be described in the following sections. Terms required for the equilibrium equations are dealt with in section 4.1.3 and those required for the arc-length constraint equation h, which is used for the analysis of singular problems, are dealt with in section 4.2. The terms for the equations g_b are dependent upon the type of analysis performed and are thus discussed in sections 4.3 and 4.4.

4.1.3 Element computations for the equilibrium equations

In this section we consider the computation of the equilibrium equation coefficients that are required for the iteration matrix in equation (4.8). We concern ourselves with the coefficients for a typical element Ω_h^e which are then assembled, together with the coefficients of all the other elements, into the global system of equations. Since the restrictions of $\underset{\sim}{u}_h$ and p_h to Ω_h^e are given by equations (2.79) and (2.80) we find that

$$\left.\begin{matrix} \dfrac{\partial G^i_{A(e)}}{\partial u^{B(f)}_{\ell}} \\ \\ \dfrac{\partial G^i_{A(e)}}{\partial p^{K(f)}} \\ \\ \dfrac{\partial H_{K(e)}}{\partial u^{B(f)}_{\ell}} \end{matrix}\right\} \quad \left\{\begin{matrix} = 0 \quad \text{if} \quad e \neq f \quad , \\ \\ \neq 0 \quad \text{if} \quad e = f \quad . \end{matrix}\right. \tag{4.10}$$

By using equations (2.83) and (2.84) together with equations (4.8) and (4.10) and omitting the indices (e) for clarity we obtain

$$\frac{\partial G^i_A}{\partial u^B_{\ell}} = \int_{\Omega_h} \left[N_{A,j} \frac{\partial \hat{S}_{ij}}{\partial u^B_{\ell}} - p^K M_K \frac{\partial \bar{F}^{-t}_{ij}}{\partial u^B_{\ell}} N_{A,j} \right] dV$$

$$+ \lambda_3 \int_{\bar{\Gamma}_{ph}} N_A \frac{\partial \bar{n}_i}{\partial u^B_{\ell}} \, d\bar{A} \quad , \tag{4.11a}$$

$$\frac{\partial G^i_A}{\partial p^K} = - \int_{\Omega_h} M_K \bar{F}^{-t}_{ij} N_{A,j} \, dV \quad , \tag{4.11b}$$

$$\frac{\partial G^i_A}{\partial \lambda_q} = - \delta_{2q} \int_{\Gamma_{th}} N_A b_i \, dA + \delta_{3q} \int_{\bar{\Gamma}_{ph}} N_A \bar{n}_i \, d\bar{A} \quad , \tag{4.11c}$$

$$\frac{\partial H_K}{\partial u_\ell^B} = \int_{\Omega_h} M_K \frac{\partial J}{\partial u_\ell^B}\, dV \quad . \tag{4.11d}$$

Using the fact that $\hat{\underset{\sim}{S}} = \hat{\underset{\sim}{\underset{\sim}{T}}}$ and the identities (2.10), (2.13), (2.29), (2.79), (2.80) with the chain rule of differentiation we can rewrite equations (4.11) in terms of quantities in the current configuration. Now suppose we choose the current configuration to be the reference configuration : then $\bar{V} = V$, $\bar{A} = A$, $\underset{\sim}{F} = \underset{\sim}{I}$ and $\hat{\underset{\sim}{T}} = \hat{\underset{\sim}{\sigma}}$ and by specialising the equations for plane problems we obtain

$$\left.\frac{\partial G_A^\alpha}{\partial u_\beta^B}\right|_o = \int_{\Omega_h} \Big\{ N_{A,\gamma}[N_{B,\kappa}\delta_{\alpha\beta}\hat{\sigma}_{\kappa\gamma} + C_{\alpha\gamma\beta\kappa}N_{B,\kappa} + p^K M_K \delta_{\gamma\beta}N_{B,\alpha}]$$

$$+ c\delta_{\alpha 1}\delta_{\beta 1}X_1^{-2}N_A N_B[\hat{\sigma}_{33} + C_{3333} + p^K M_K]\Big\}\, dV$$

$$+ (c-1)\lambda_3 \int_{\Gamma_{ph}} [\delta_{\alpha 1}\delta_{\beta 2}N_A\frac{\partial N_B}{\partial \zeta} + \delta_{\alpha 2}\delta_{\beta 1}N_B\frac{\partial N_A}{\partial \zeta}]\, t\, d\zeta$$

$$- c\lambda_3 \int_{\Gamma_{ph}} [(\delta_{\alpha 1}\delta_{\beta 2}N_A\frac{\partial N_B}{\partial \zeta} + \delta_{\alpha 2}\delta_{\beta 1}N_B\frac{\partial N_A}{\partial \zeta})X_1 + \delta_{\alpha 1}\delta_{\beta 1}N_A N_B\frac{\partial X_2}{\partial \zeta}]\, 2\pi d\zeta$$

$$- (c-1)\lambda_3\delta_{\alpha 2}\delta_{\beta 1}N_A N_B t\Big|_{\Gamma_{ph}^o} + c\lambda_3\delta_{\alpha 2}\delta_{\beta 1}N_A N_B X_1 2\pi\Big|_{\Gamma_{ph}^o} \quad , \tag{4.12a}$$

$$\left.\frac{\partial G_A^\alpha}{\partial p^K}\right|_o = -\int_{\Omega_h} M_K[N_{A,\alpha} + c\delta_{\alpha 1}X_1^{-1}N_A] \quad dV \quad , \tag{4.12b}$$

$$\left.\frac{\partial G_A^\alpha}{\partial \lambda_q}\right|_o = -\delta_{2q}\int_{\Gamma_{th}} N_A b_\alpha dA + \delta_{3q}\int_{\Gamma_{ph}} N_A n_\alpha dA \quad , \tag{4.12c}$$

$$\left.\frac{\partial H_K}{\partial u_\beta^B}\right|_o = \int_{\Omega_h} M_K[\delta_{\beta 1}N_{B,1} + \delta_{\beta 2}N_{B,2} + c\delta_{\beta 1}X_1^{-1}N_B] \quad dV \quad , \tag{4.12d}$$

where $|_o$ denotes evaluation when the current and reference configurations coincide, t is the element thickness for plane stress and plane strain and ζ is the coordinate along the boundary Γ_{ph}. Here and henceforth

$$c = \begin{cases} 1 & \text{for axisymmetric problems} \quad , \\ 0 & \text{for plane stress and plane strain problems} \quad . \end{cases} \tag{4.13}$$

In matrix form these equations are

$$[\Phi_{AB}] = \int_{\Omega_h}\left\{[B_A]^t[C^*][B_B] + [D_A]^t[\hat{\sigma}][D_B]\right\} \quad dV$$

$$+ \lambda_3 \int_{\Gamma_{ph}} [U_{AB}]\, d\zeta \quad , \tag{4.14a}$$

$$[\Psi_{AK}] = -\int_{\Omega_h} [B_A]^t [M_K] \, dV \quad , \tag{4.14b}$$

$$[\Lambda_{Aq}] = -\delta_{2q} \int_{\Gamma_{th}} [N_A]^t \{b\} \, dV + \delta_{3q} \int_{\Gamma_{ph}} [N_A]^t \{n\} \, dA \quad , \tag{4.14c}$$

and it can be shown from (4.12) that equation (4.12d) can be written as

$$[\Psi_{KA}] = -[\Psi_{AK}]^t \quad . \tag{4.14d}$$

All these matrices are described in detail in Appendix 4A. The boundary term in (4.12a) is zero if that part of the boundary with constant pressure loading lies between parts of the boundary that have prescribed displacements. This is a consequence of equation (2.36b). HIBBITT (1979) and ALY (1981) have also shown this result. Under these conditions, which prevail in our analyses, the matrix in equation (4.14a) is symmetric.

For each element (e) we need to evaluate

$$\begin{bmatrix} [\Phi_{AB}] & [\Psi_{AK}] & [\Lambda_{Aq}] \\ [\Psi_{KB}] & [\,0\,] & [\,0\,] \end{bmatrix}^{(e)} \quad , \quad \begin{Bmatrix} \{-G_A\} \\ \{-H_K\} \end{Bmatrix}^{(e)} \quad , \tag{4.15}$$

which is then assembled into the global system (4.8) . For plane stress problems the pressure can be computed directly from (2.21), (2.31) and (2.63) :

$$\sigma_{33} = 0 \quad \Rightarrow \quad p = \hat{\sigma}_{33} = \sum_n \mu_n (a_1 a_2)^{-\alpha_n} \quad . \tag{4.16}$$

This allows us to neglect the pressure degrees of freedom in equation (4.6); the corresponding matrices as well as the incompressible constraint matrix are then not required. By reworking equation (4.11a) through to (4.12a) for the special case of plane stress and using (4.16) we can show that the matrix $[C^*]$ in equation (4.14a) contains additional terms; these are given in Appendix 4A.

4.2 Computations for singular problems

4.2.1 Computations for the arc-length constraint equation

Inflation procedures are required to trace out solution paths for problems in which singular behaviour (see section 3.1.1) may occur. The different forms of the arc-length constraint equation as given in section 3.1.2 can be written more generally in terms of nodal quantities for plane problems as (see equation 4.3c)

$$h(\underset{\sim}{u}^r, p^c, \underset{\sim}{\lambda}, s) = 0 \quad , \tag{4.17}$$

where

$$h \equiv (\underset{\sim}{u}-\underset{\sim}{u}_o)^r.\dot{\underset{\sim}{u}}^r_o + (p-p_o)^c\dot{p}^c_o + (\underset{\sim}{\lambda}-\underset{\sim}{\lambda}_o).\dot{\underset{\sim}{\lambda}}_o - (s-s_o) \quad , \qquad (4.18a)$$

or

$$h \equiv \theta(\underset{\sim}{u}-\underset{\sim}{u}_o)^r.\dot{\underset{\sim}{u}}^r_o + \theta(p-p_o)^c\dot{p}^c_o + (1-\theta)(\underset{\sim}{\lambda}-\underset{\sim}{\lambda}_o).\dot{\underset{\sim}{\lambda}}_o - (s-s_o) \quad , \qquad (4.18b)$$

or

$$h \equiv \theta(\underset{\sim}{u}-\underset{\sim}{u}_o)^r.(\underset{\sim}{u}-\underset{\sim}{u}_o)^r + \theta(p-p_o)^c(p-p_o)^c + (1-\theta)(\underset{\sim}{\lambda}-\underset{\sim}{\lambda}_o).(\underset{\sim}{\lambda}-\underset{\sim}{\lambda}_o) - (s-s_o)^2 \quad . \qquad (4.18c)$$

Other modifications described in section 3.1.2 arise from simple substitutions into these equations and are thus not discussed here. The equations (4.18) are written in terms of the global degrees of freedom as this simplifies the computations considerably. Note that the summation convention still applies in equations (4.18).

It is now a simple matter to obtain the coefficients required for equation (4.8) for a particular constraint equation. The coefficients for the constraint equations (4.18) are thus

$$\frac{\partial h}{\partial u^r_\ell} = \dot{u}^r_{\ell o} \quad , \quad \frac{\partial h}{\partial p^c} = \dot{p}^c_o \quad , \quad \frac{\partial h}{\partial \lambda_m} = \dot{\lambda}_{mo} \quad ; \qquad (4.19a)$$

or

$$\frac{\partial h}{\partial u_{\ell}^{r}} = \theta \dot{u}_{\ell o}^{r} \quad , \quad \frac{\partial h}{\partial p^{c}} = \theta \dot{p}_{o}^{c} \quad , \quad \frac{\partial h}{\partial \lambda_{m}} = (1-\theta)\dot{\lambda}_{mo} \quad ; \text{ (4.19b)}$$

or

$$\frac{\partial h}{\partial u_{\ell}^{r}} = 2\theta(u_{\ell}^{r} - u_{\ell o}^{r}) \quad , \quad \frac{\partial h}{\partial p^{c}} = 2\theta(p^{c} - p_{o}^{c}) \quad ,$$

$$\frac{\partial h}{\partial \lambda_{m}} = 2(1-\theta)(\lambda_{m} - \lambda_{mo}) \quad . \qquad (4.19c)$$

In vector form we write

$$[\{\dot{u}\}^{t} , -\{\dot{p}\}^{t} , \{\dot{\lambda}\}^{t}] \begin{Bmatrix} \{\Delta u\} \\ -\{\Delta p\} \\ \{\Delta \lambda\} \end{Bmatrix} = \{-h\} \qquad (4.20)$$

which is then substituted into the global system (4.8).

4.2.2 Location of singular points

The location and computation of singular points is obviously required before we are able to compute any branches emanating from these points. Many methods are available for these computations : for example the methods proposed by SEYDEL (1979); MOORE and SPENCE (1980), SIMPSON (1975) and FUJIKAKE (1985). We, however, use a very simple yet effective method outlined by RIKS (1979) and also by KELLER (1977) for the location and later the computation of these singular points.

The location and characterisation of singular points on the solution arc is dependent upon the following quantities (Theorem 3.1, section 3.1.2) :

$$\det K = \det \begin{bmatrix} \dfrac{\partial G_a^i}{\partial u_\ell^r} & \dfrac{\partial G_a^i}{\partial p^c} \\ \dfrac{\partial H_k}{\partial u_\ell^r} & 0 \end{bmatrix} , \tag{4.21}$$

$$\det A = \det \begin{bmatrix} \dfrac{\partial G_a^i}{\partial u_\ell^r} & \dfrac{\partial G_a^i}{\partial p^c} & \dfrac{\partial G_a^i}{\partial \lambda_q} \\ \dfrac{\partial H_k}{\partial u_\ell^r} & 0 & 0 \\ \dfrac{\partial h}{\partial u_\ell^r} & \dfrac{\partial h}{\partial p^c} & \dfrac{\partial h}{\partial \lambda_q} \\ \dfrac{\partial g_b}{\partial u_\ell^r} & \dfrac{\partial g_b}{\partial p^c} & \dfrac{\partial g_b}{\partial \lambda_q} \end{bmatrix} . \tag{4.22}$$

These equations hold for multi-parameter problems in general, but (4.22) is easily specialised for the particular problem that is being solved. In this section junctions of the piecewise-linear paths required for the multi-parameter problems discussed in section 3.2.3 are excluded. The location of these junctions is dealt with in section 4.3.2.

Since det K is singular at limit points and both det K and det A are singular at bifurcation points we monitor these determinants at all steps t and seek changes in sign that characterise points on the solution arc as follows (Figure 4.1) :

$$\left.\begin{aligned} (\det K_t)(\det K_{t-1}) &> 0 \\ (\det A_t)(\det A_{t-1}) &> 0 \end{aligned}\right\} \quad \text{regular point} \quad , \qquad (4.23a)$$

$$\left.\begin{aligned} (\det K_t)(\det K_{t-1}) &< 0 \\ (\det A_t)(\det A_{t-1}) &> 0 \end{aligned}\right\} \quad \text{limit point between steps t and (t-1)} \quad , \qquad (4.23b)$$

$$\left.\begin{aligned} (\det K_t)(\det K_{t-1}) &< 0 \\ (\det A_t)(\det A_{t-1}) &< 0 \end{aligned}\right\} \quad \text{bifurcation point between steps t and (t-1)} \quad . \qquad (4.23c)$$

These determinants are easily obtainable as by-products of the Gauss elimination solution process but their magnitudes, for large systems of equations, can easily exceed the maximum range allowable by the computer being used. To avoid this the values of the determinants are scaled by some computed constant specific to each analysis. It is possible to monitor only the sign changes of these determinants, but this does not allow us to use bisection to compute the approximate singular point.

Once a singular point has been located the approximate singular point can be computed by using the simple method of bisection. We can then use this approximate singular point as our starting point for either tracing out bifurcation paths (section 4.2.3) or for tracing the locus of the singular point (section 4.4.2).

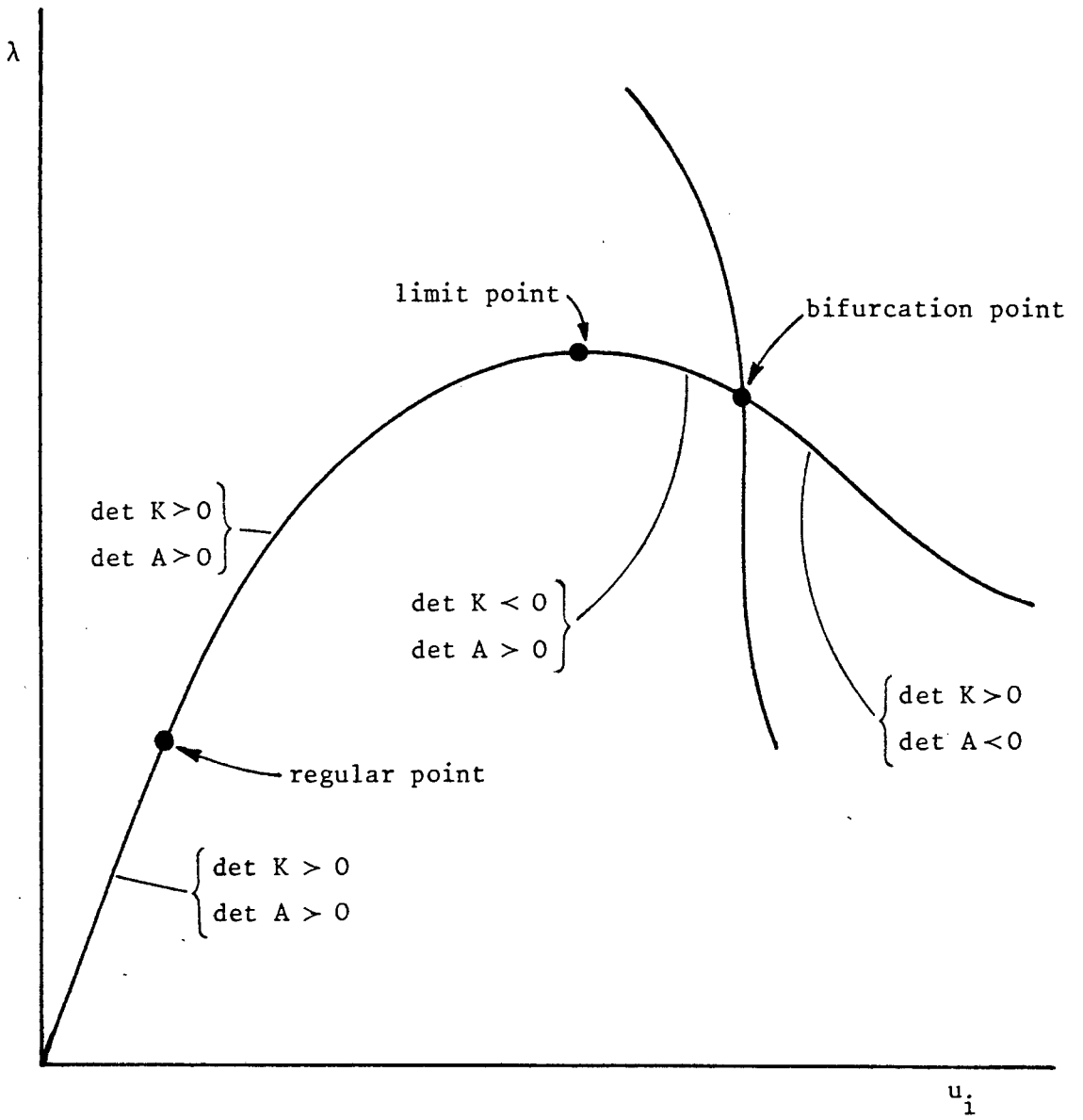

Figure 4.1 Characterisation of points on solution arc by detecting the determinants changing sign.

4.2.3 Branching onto secondary paths

Once a simple bifurcation point has been located on the primary solution path using the method described in the preceding section, it is possible to compute the secondary path passing through this point using the continuation methods described in this chapter. Continuation along any smooth path is possible if at least one regular point on that path is known in advance (see section 4.1.1). We discuss here methods of obtaining the initial regular point on the secondary path.

Assuming we have obtained the bifurcation point and the associated tangent to the primary path at this point we can proceed to obtain this initial regular point. We know, from section 3.1.1, that there are two non-tangential solution arcs passing through this point and thus it should be possible to compute the tangent, at this point, to the secondary path (Figure 4.2). However, this is neither practical from a computational point of view nor is it a necessary choice in obtaining the predictor for this regular point (RIKS (1979)). Any "tangent" may be used provided that the intersection between the solution curve and the intersecting surface remains reasonably well preserved (Figure 4.2). An effective choice for this "tangent" is thus (Figure 4.3)

$$\underset{\sim}{n} = \frac{\overset{\bullet *}{\underset{\sim}{p}} + \mu \underset{\sim}{a}}{\left\| \overset{\bullet *}{\underset{\sim}{p}} + \mu \underset{\sim}{a} \right\|} \quad , \tag{4.24a}$$

$$\mu = - k(\overset{\bullet *}{\underset{\sim}{p}} . \underset{\sim}{a})^{-1} \quad . \tag{4.24b}$$

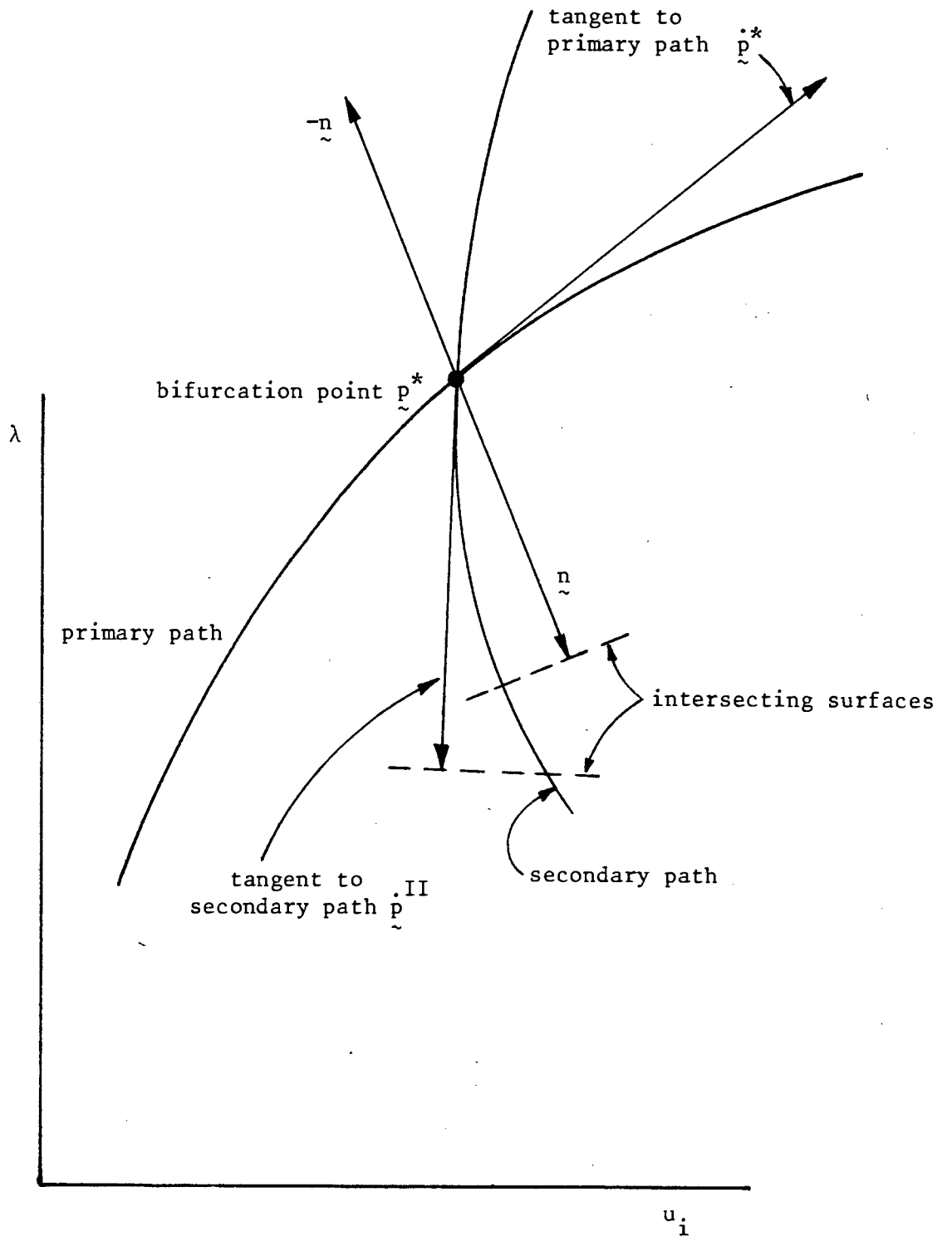

Figure 4.2 Tangents to branches at a bifurcation point (showing intersecting surfaces for initial regular point on secondary path).

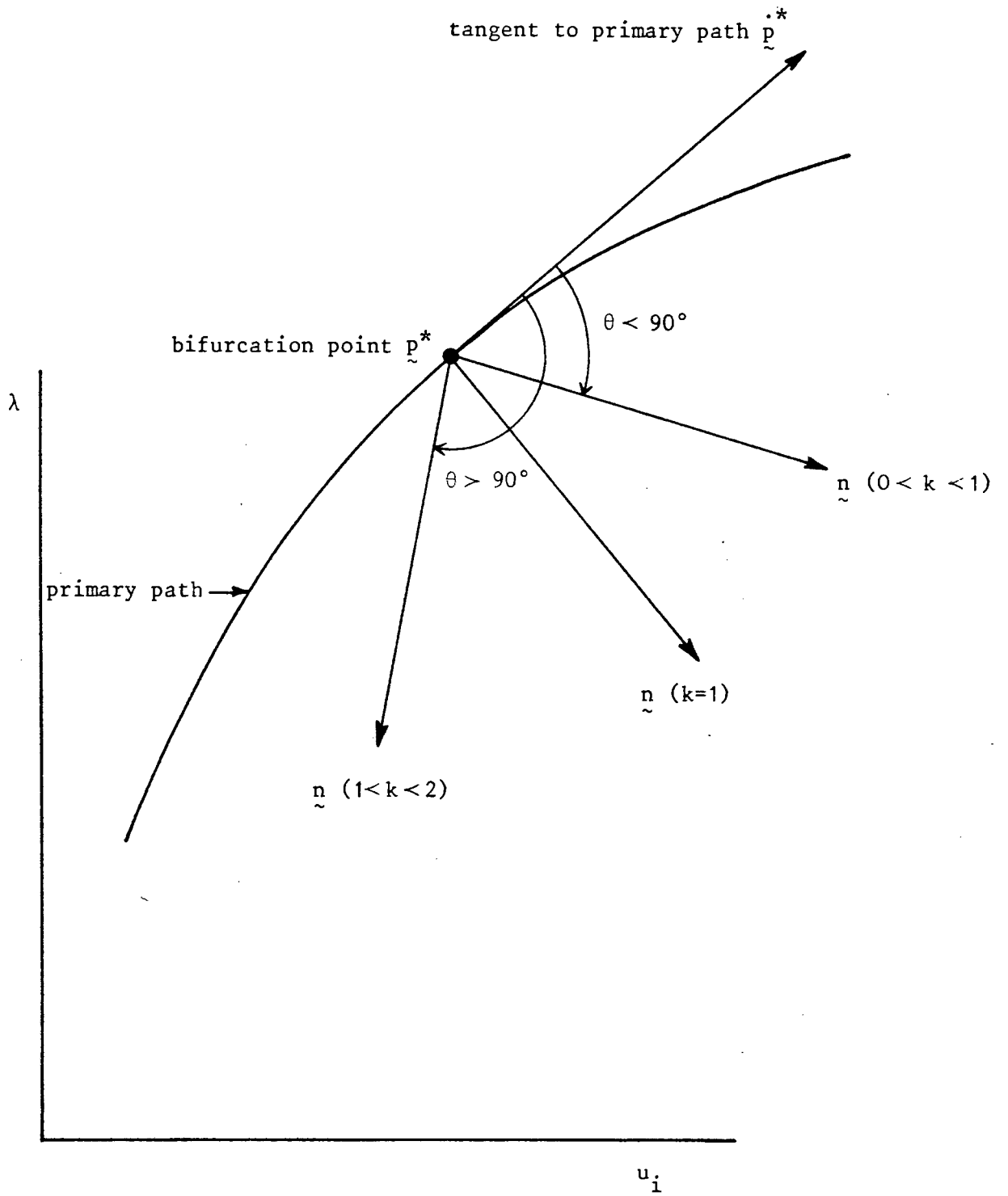

Figure 4.3 Choices for "tangent" to secondary curve.

Here $\underset{\sim}{\dot{p}}^{*} = (\dot{u}_{\ell}^{r}, \dot{p}^{c}, \dot{\lambda}_{q})^{*t}$ is the tangent to the primary path at the bifurcation point, $\underset{\sim}{a}$ is the eigenvector obtained at this point and k is a chosen constant. Equation (4.24) is a generalisation of the expression given by RIKS (1979) which may be obtained by setting $k = 1$.

The predictor for the initial regular point is then given by

$$\underset{\sim}{p}^{(1)} = \underset{\sim}{p}^{*} + \Delta s^{(1)} \underset{\sim}{n} \quad , \tag{4.25}$$

where $\Delta s^{(1)}$ is the initial step length onto the secondary path.

Remembering that the tangents and the eigenvector are all normalised vectors we obtain the scalar product

$$\underset{\sim}{\dot{p}}^{*} \cdot \underset{\sim}{n} = (1-k) / \| \underset{\sim}{\dot{p}}^{*} + \mu \underset{\sim}{a} \| \quad . \tag{4.26}$$

By considering the plane containing $\underset{\sim}{\dot{p}}^{*}$ and $\underset{\sim}{n}$ we find, by using $\underset{\sim}{\dot{p}}^{*} \cdot \underset{\sim}{n} = \| \underset{\sim}{\dot{p}}^{*} \| \| \underset{\sim}{n} \| \cos\theta$, that for a chosen value $0 \leq k \leq 2$ the vector $\underset{\sim}{n}$ makes an angle θ with the vector $\underset{\sim}{\dot{p}}^{*}$ (see Figure 4.3). Alternatively we could choose an angle θ and then compute the value of k which would give us the correct $\underset{\sim}{n}$. The use of equations (4.24) thus gives us the ability to compute a wide range of $\underset{\sim}{n}$ and thus find a vector which gives us an intersecting surface that has a reasonable intersection with the secondary path.

The advantage of RIKS' (1979) method with $k = 1$ is that the scalar product in equation (4.26) is zero. This means that the intersecting surface is parallel to the tangent $\overset{\bullet *}{\underset{\sim}{p}}$ and thus the computational process is prevented from returning to the primary path. This cannot be guaranteed with the general equation (4.24) and possible failures are anticipated when the angle between $\underset{\sim}{n}$ and $\overset{\bullet *}{\underset{\sim}{p}}$ is small (i.e. when k approaches 0 or 2).

It has been assumed here that the exact bifurcation point $\overset{*}{\underset{\sim}{p}}$ and its associated tangent to the primary path $\overset{\bullet *}{\underset{\sim}{p}}$ have been calculated. This is unnecessary since continuation onto secondary paths can easily be achieved by using approximations to these quantities (RHEINBOLDT (1978) and SEYDEL (1983)). Thus, if we locate a bifurcation point between steps $(t-1)$ and t of our analysis, we obtain the approximations (Figure 4.4)

$$\overset{\bullet *a}{\underset{\sim}{p}} = \frac{\underset{\sim}{p}_t - \underset{\sim}{p}_{t-1}}{\| \underset{\sim}{p}_t - \underset{\sim}{p}_{t-1} \|} \quad , \tag{4.27a}$$

$$\overset{*a}{\underset{\sim}{p}} = \underset{\sim}{p}_t + \Delta s^* \overset{\bullet *a}{\underset{\sim}{p}} \quad , \tag{4.27b}$$

where Δs^* is obtained using linear interpolation

$$\Delta s^* = (s_t - s_{t-1}) \frac{\det A_{t-1}}{\det A_{t-1} - \det A_t} \quad . \tag{4.28}$$

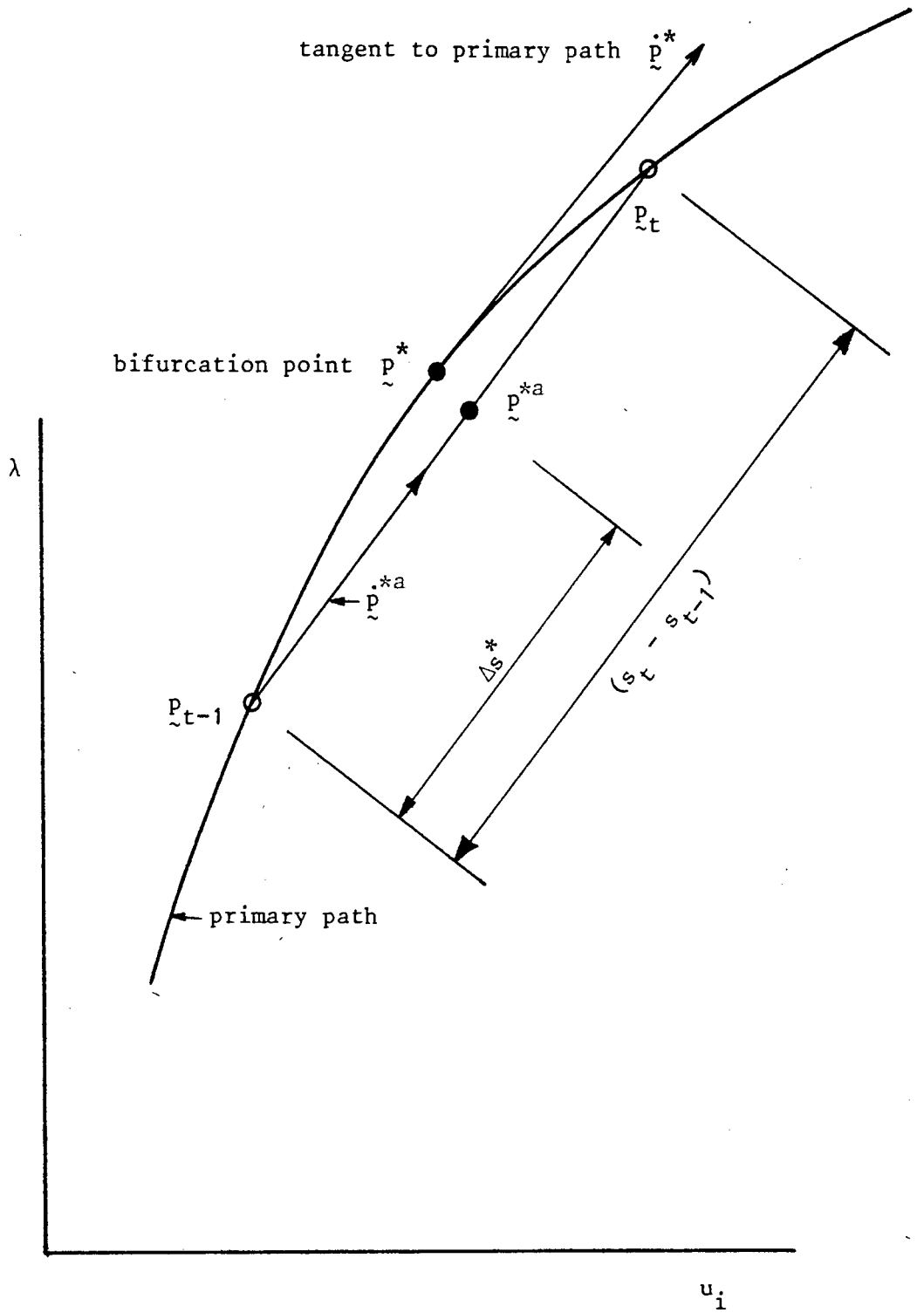

Figure 4.4 Computation of approximate bifurcation point p^{*a} and the approximate tangent at this point $\dot{p}^{*a}$.

We thus use the approximate bifurcation point $\underset{\sim}{p}^{*a}$ and the approximate tangent to the primary path $\underset{\sim}{\dot{p}}^{*a}$ at this point to obtain the first predictor and hence the initial regular point on the secondary path. We then use the continuation methods as described in this chapter to trace out our solution arc along this path. We note here also that since two paths intersect at the bifurcation point we can proceed along the secondary path on either side of the primary path (see Figure 4.2). Thus once the secondary arc has been traced out on one side of the primary path we can use the same methods to trace out the other side. To initiate this we merely restart at the approximate bifurcation point and use $-\underset{\sim}{n}$ instead of $\underset{\sim}{n}$ to obtain our first predictor.

DECKER and KELLER (1981), in dealing with single parameter problems, note that use of a "tangent" with $\dot{\lambda} = 0$ will in general allow a larger step size for convergence onto the initial regular point. This can easily be extended to our equation (4.24) : we compute the unnormed $\underset{\sim}{n}$, set all $\dot{\lambda}_q = 0$ and then compute the normalised vector $\underset{\sim}{n}$ which we use for our predictor in equation (4.25).

4.3 Computations for multi-parameter (piecewise-linear) problems

4.3.1 Computations for piecewise-linear parameter constraint equations

For problems where there are more than one parameter we require further constraint equations in order to solve the system of nonlinear equations. An application that has been discussed in section 3.2.3 is that of describing piecewise-linear paths in parameter space. To do this we require equations of the form (3.26). These equations are specialisations of the general equations (4.3d) and take the form

$$g_b(\underset{\sim}{\lambda}) \equiv g_b(\nu, \underset{\sim}{\mu}) = 0 \quad . \tag{4.29}$$

We note here that the range of b is from 1 to (m-1) where m is the number of independent parameters present in the problem. The coefficients required for the system (4.8) are easily obtainable from equations (3.50), (3.51) and (3.53); thus on piecewise-linear path (p)

$$\frac{\partial g_b}{\partial \nu} \equiv \frac{\partial g_b}{\partial \lambda_L}\bigg|^{(p)} = \frac{g_b}{g_b^{(p)}} \frac{e_b^{(p)}}{e_L^{(p)}} \quad , \tag{4.30a}$$

$$\frac{\partial g_b}{\partial \mu_j} \equiv \frac{\partial g_b}{\partial \lambda_q}\bigg|^{(p)}_{q \neq L} = - \frac{g_b}{g_b^{(p)}} \delta_{bj} \quad , \tag{4.30b}$$

where j has the same range as b. In matrix form we write

$$[\Omega]\{\Delta\lambda\} = \{-g\} \tag{4.31}$$

which is used in equation (4.8). Note that the matrix $[\Omega]$ is not a square matrix.

4.3.2 Changing paths at piecewise-linear junctions

For multi-parameter problems such as those discussed in sections 3.2 and 4.3.1 it is necessary to be able to ensure that the solution proceeds in the prescribed direction along the paths relating the parameters of the problem. Two stages are required to ensure this : firstly, we need to determine when a junction has been reached and, secondly, we need to guide the solution in the correct direction along the next path.

Location of the junctions is simplified by the parameterisation of the piecewise-linear path of interest by the length parameter τ : we compute the value of τ at each junction (p) as (see, for example, Figure 4.5)

$$\tau^{(p)} = \sum_{j=2}^{p} \| \underset{\sim}{\lambda}^{(j)} - \underset{\sim}{\lambda}^{(j-1)} \| \quad . \tag{4.32}$$

The same notation as that in section 3.2.3 is used here and $\|\cdot\|$ denotes the Euclidean norm (or length of the vector). It is now easy to monitor the parameter τ at all steps during the analysis and hence locate the junctions (p) . Once we have located a junction it is desirable to obtain the solution at this point. This is done simply by scaling the last incremental solution so that the total solution at this step corresponds to the values of the parameters at the junction, and

Junction coordinates :

$\underset{\sim}{\lambda}^{(1)} = (0,0,0)$

$\underset{\sim}{\lambda}^{(2)} = (0,1,0)$

$\underset{\sim}{\lambda}^{(3)} = (0,2,1)$

$\underset{\sim}{\lambda}^{(4)} = (1,3,1)$

$\underset{\sim}{\lambda}^{(5)} = (2,2,2)$

Parameter values :

$\tau^{(1)} = 0.$

$\tau^{(2)} = 1.$

$\tau^{(3)} = 2.414$

$\tau^{(4)} = 3.828$

$\tau^{(5)} = 5.560$

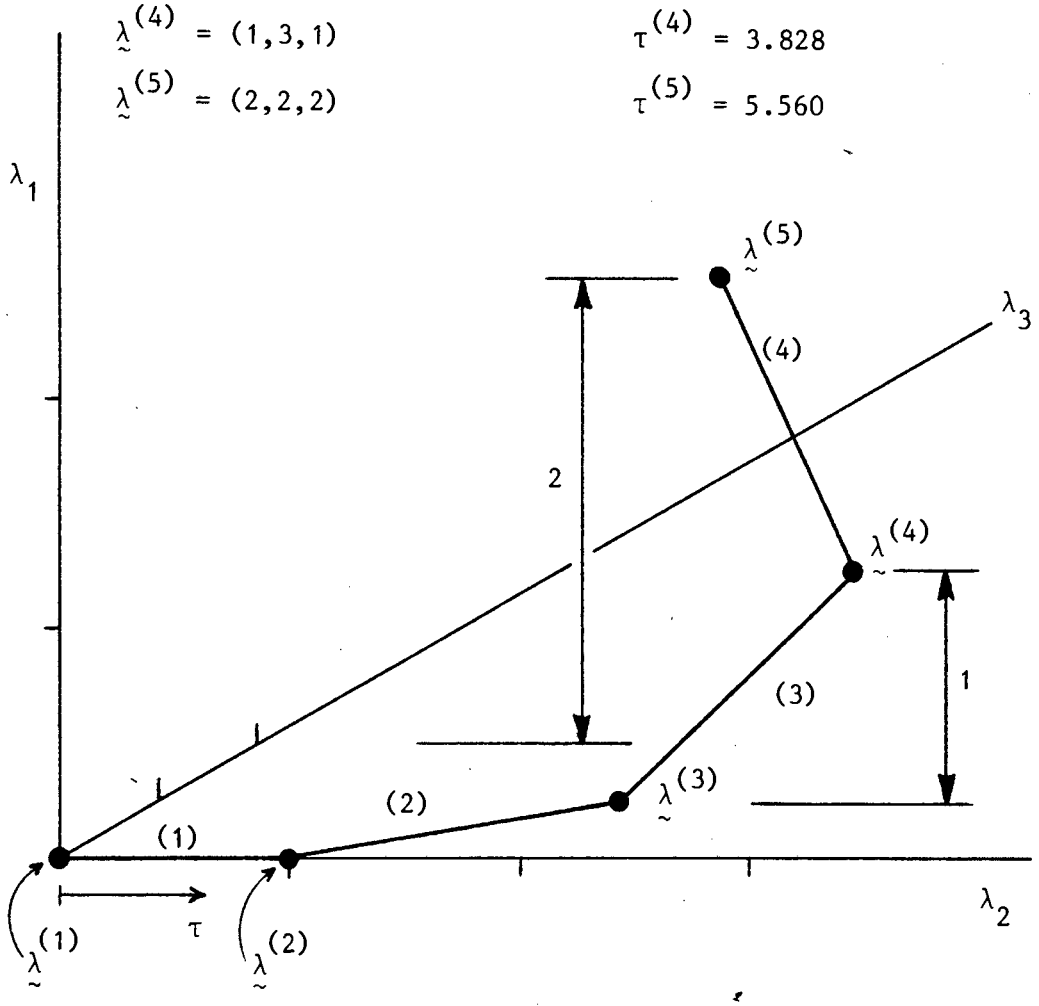

Figure 4.5 Parameterisation of piecewise-linear path for 3 parameter problem (m=3,N=4).

then fixing the parameters until convergence has been achieved. The next increment then proceeds along the path following this junction.

For problems with many parameters it is necessary to compute the predictor using the exact tangent at the previous point (see section 4.5) so that the correct tangent is obtained using the proper constraint equations. Use of the secant vector (section 3.1.2) as an approximate tangent will be incorrect for the increment immediately after a junction has been located for this very reason. Assuming we have located a junction (p) and obtained the solution at this point we now compute the tangent $\dot{\underset{\sim}{p}} = (\dot{u}_{\ell}^{r}, \dot{p}^{c}, \dot{\lambda}_{q})^{t}$ at this point using the constraint equations for the next path (p) (see Figure 4.6). Using the solution methods described in section 4.5 it is possible that we compute either one of two tangents that are directly opposite to each other (see Figure 4.6). To determine whether we have computed the correct tangent or its negative we evaluate the scalar product to determine (Figure 4.6)

$$\dot{\underset{\sim}{\lambda}} . \underset{\sim}{e}^{(p)} > 0 \quad \Rightarrow \quad \dot{\underset{\sim}{\lambda}} \text{ lies in direction } \underset{\sim}{e}^{(p)} , \qquad (4.33a)$$

$$\dot{\underset{\sim}{\lambda}} . \underset{\sim}{e}^{(p)} < 0 \quad \Rightarrow \quad \dot{\underset{\sim}{\lambda}} \text{ lies in direction } -\underset{\sim}{e}^{(p)} . \qquad (4.33b)$$

Note that if $\dot{\underset{\sim}{\lambda}}$ was a normalised vector the scalar products in equation (4.33a) and (4.33b) would be equal to +1 and -1 respectively.

Once the direction of the computed $\dot{\underset{\sim}{\lambda}}$ has been determined it remains only to alter the direction of $\dot{\underset{\sim}{p}}$ if necessary so as to be able to compute the correct predictor for the next point on the solution arc.

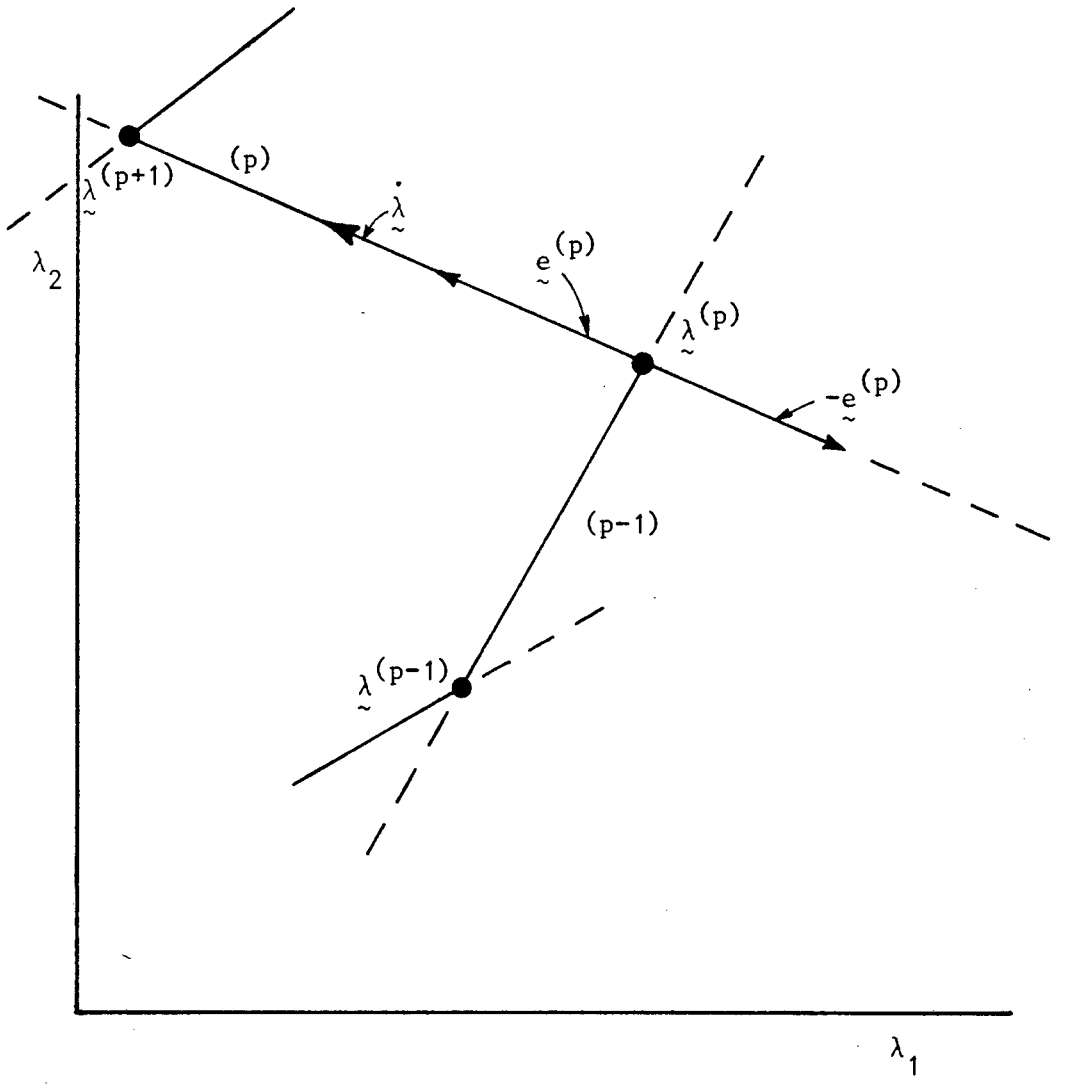

Figure 4.6 Directions in parameter space which solution path may follow for 2 parameter problem.

4.4 Computations for tracing loci of singular paths

4.4.1 Element computations for locus constraint equation

In order to trace the loci of singular points for problems where there are two load parameters we require the additional constraint equation as described in section 3.2.4. To be able to use the Newton-Raphson iteration scheme we require the derivatives as given in equation (3.57). We see from equations (4.6) and (3.57), that we require

$$\frac{\partial D}{\partial u_{\ell}^{r}} = D(K^{-1})_{ij} \frac{\partial K_{ij}}{\partial u_{\ell}^{r}} \quad , \tag{4.34a}$$

$$\frac{\partial D}{\partial p^{c}} = D(K^{-1})_{ij} \frac{\partial K_{ij}}{\partial p^{c}} \quad , \tag{4.34b}$$

$$\frac{\partial D}{\partial \lambda_{q}} = 0 \quad , \tag{4.34c}$$

where we have substituted D for g_b , and where

$$[K] = \begin{bmatrix} \dfrac{\partial G_a^i}{\partial u_m^s} & \dfrac{\partial G_a^i}{\partial p^d} \\ \dfrac{\partial H_k}{\partial u_m^s} & 0 \end{bmatrix} . \tag{4.35}$$

In equations (4.34a,b), we have, for a particular u^r_ℓ and p^c respectively, the scalar product of two tensors. The first part of the scalar products which involve the evaluation of the inverse and the determinant of a matrix, can be easily, although laboriously, computed. Our main aim in this section is thus to describe the computation of the second term in the scalar products in (4.34). Using equations (4.7) together with equations (4.8) we can write the coefficients in (4.34) in terms of element quantities : for example

$$\frac{\partial^2 G^i_a}{\partial u^r_\ell \partial u^s_m} = \Lambda^{B(f)}_r \Lambda^{A(e)}_a \Lambda^{C(g)}_s \frac{\partial^2 G^i_{A(e)}}{\partial u^{B(f)}_\ell \partial u^{C(g)}_m} \quad , \tag{4.36a}$$

$$\frac{\partial^2 G^i_a}{\partial u^r_\ell \partial p^d} = \Lambda^{B(f)}_r \Lambda^{A(e)}_a \Lambda^{L(g)}_d \frac{\partial^2 G^i_{A(e)}}{\partial u^{B(f)}_\ell \partial p^{L(g)}} \quad . \tag{4.36b}$$

The other coefficients can be written in similar fashion. Thus all quantities can be computed for each element and then assembled into the equations (4.34) using the correct transformations (2.85). We note here that equations (4.10) are also applicable in this section.

These element second derivatives are obtained by differentiating equations (4.11a,b,d) with respect to $\underset{\sim}{u}$ and p. We employ the identities as used in section 4.1.3 with the chain rule of differentiation to obtain the equations in terms of quantities in the current configuration. Again we choose the current configuration to be the reference configuration and specialising the equations for plane problems we obtain (omitting (e) for clarity)

$$\left.\frac{\partial^2 G_A^\alpha}{\partial u_\beta^B \partial u_\eta^C}\right|_o = \int_{\Omega_h} \Big\{ N_{A,\gamma} N_{B,\varepsilon} N_{C,\kappa} \mathcal{C}_{\alpha\gamma\eta\kappa\beta\varepsilon}$$

$$+ N_{A,\gamma}[\delta_{\alpha\eta} N_{B,\varepsilon} N_{C,\kappa} C_{\kappa\gamma\beta\varepsilon} + \delta_{\alpha\beta} N_{B,\kappa} N_{C,\varepsilon} C_{\kappa\gamma\eta\varepsilon}]$$

$$+ \tfrac{1}{2}\delta_{\eta\beta} N_{A,\gamma} C_{\alpha\gamma\kappa\varepsilon}[N_{B,\varepsilon} N_{C,\kappa} + N_{B,\kappa} N_{C,\varepsilon}]$$

$$- p^K M_K N_{A,\gamma}[\delta_{\gamma\beta} N_{B,\eta} N_{C,\alpha} + \delta_{\alpha\eta} N_{B,\alpha} N_{C,\beta}]$$

$$+ c\delta_{\alpha 1}\delta_{\beta 1}\delta_{\eta 1} X_1^{-3} N_A N_B N_C [\mathcal{C}_{333333} + 3C_{3333} - 2p] \Big\}\, dV$$

$$- c\lambda_3 \int_{\Gamma_{ph}} \Big\{ \delta_{\alpha 2}\delta_{\beta 1}\delta_{\eta 1} \frac{\partial N_A}{\partial \zeta} N_B N_C + \delta_{\alpha 1}\delta_{\beta 2}\delta_{\eta 1} N_A \frac{\partial N_B}{\partial \zeta} N_C$$

$$+ \delta_{\alpha 1}\delta_{\beta 1}\delta_{\eta 2} N_A N_B \frac{\partial N_C}{\partial \zeta} \Big\}\, 2\pi d\zeta$$

$$+ c\lambda_3 \delta_{\alpha 2}\delta_{\beta 1}\delta_{\eta 1} N_A N_B N_C 2\pi \Big|_{\Gamma_{ph}^o} , \qquad (4.37a)$$

$$\left.\frac{\partial^2 G_A^\alpha}{\partial u_\beta^B \partial p^L}\right|_o = \int_{\Omega_h} M_L [N_{A,\beta} N_{B,\alpha} + c\delta_{\alpha 1}\delta_{\beta 1} X_1^{-2} N_A N_B]\, dV , \qquad (4.37b)$$

$$\left.\frac{\partial^2 H_K}{\partial u^B_\beta \partial u^C_\eta}\right|_o = \int_{\Omega_h} \Big\{ M_K N_{B,\gamma} \delta_{\kappa\beta} N_{C,1} [\delta_{\kappa 2}\delta_{\gamma 2}\delta_{\eta 1} - \delta_{\kappa 1}\delta_{\gamma 2}\delta_{\eta 2}]$$

$$+ M_K N_{B,\gamma} \delta_{\kappa\beta} N_{C,2} [\delta_{\kappa 1}\delta_{\gamma 1}\delta_{\eta 2} - \delta_{\kappa 2}\delta_{\gamma 1}\delta_{\eta 1}]$$

$$+ c M_K N_{B,\gamma} \delta_{\kappa\beta} X_1^{-1} N_C [\delta_{\kappa 1}\delta_{\gamma 1}\delta_{\eta 1} + \delta_{\kappa 2}\delta_{\gamma 2}\delta_{\eta 1}]$$

$$+ c M_K \delta_{\beta 1} X_1^{-1} N_B [\delta_{\eta 1} N_{C,1} + \delta_{\eta 2} N_{C,2}] \Big\} \, dV \quad , \tag{4.37c}$$

$$\left.\frac{\partial^2 G^\alpha_A}{\partial p^K \partial u^B_\eta}\right|_o = \int_{\Omega_h} M_K [N_{A,\eta} N_{B,\alpha} + c\delta_{\alpha 1}\delta_{\eta 1} X_1^{-2} N_A N_B] \, dV \quad , \tag{4.37d}$$

$$\frac{\partial^2 G^\alpha_A}{\partial p^K \partial p^L} = 0 \quad , \tag{4.37e}$$

$$\frac{\partial^2 H_L}{\partial p^K \partial u^B_\eta} = 0 \quad , \tag{4.37f}$$

where c is given in equation (4.13). As expected, we see that equations (4.37b) and (4.37d) are equal. In matrix form these equations are

$$[\Phi^{(u)}_{AB(\beta)C}] = \int_{\Omega_h} [D_A]^t [\mathscr{C}^*_{B(\beta)}][D_C] \, dV + \int_{\Gamma_{ph}} [U^{(u)}_{AB(\beta)C}] \, d\zeta \,, \tag{4.38a}$$

$$[\Psi^{(u)}_{AB(\beta)L}] = \int_{\Omega_h} [D_A]^t [X_{B(\beta)}][M_L] \, dV \,, \tag{4.38b}$$

$$[\Psi^{(u)}_{KB(\beta)C}] = \int_{\Omega_h} [M_K]^t [Y_{B(\beta)}][D_C] \, dV \,, \tag{4.38c}$$

$$[\Phi^{(p)}_{AKB}] = \int_{\Omega_h} [D_A]^t [Z_K][D_B] \, dV \,, \tag{4.38d}$$

where the matrices are given in detail in Appendices 4A and 4B. The matrix $[\Phi^{(p)}_{AKB}]$ is symmetric but the matrix $[\Phi^{(u)}_{AB(\beta)C}]$ is only symmetric if the boundary term in equation (4.37a) is zero (i.e. if the conditions described after equation (4.14d) prevail).

For each element (e) these matrices are written in the following form (see equations (4.34) and (4.35))

$$\begin{bmatrix} [\Phi^{(u)}_{AB(\beta)C}] & [\Psi^{(u)}_{AB(\beta)L}] \\ [\Psi^{(u)}_{KB(\beta)C}] & [\;\;0\;\;] \end{bmatrix}^{(e)} , \tag{4.39a}$$

$$\begin{bmatrix} [\Phi^{(p)}_{AKB}] & [\ 0\ ] \\ [\ 0\ ] & [\ 0\ ] \end{bmatrix}^{(e)} , \qquad (4.39b)$$

which are then assembled into a "global system" in order for the scalar products in (4.34) to be evaluated (note that many terms in this scalar product are zero due to the sparseness of this "global system"). For each element (e) we then compute

$$\{\ \{\Delta^{(u)}_B\}^t\ ,\ -\{\Delta^{(p)}_K\}^t\ ,\ \{0\}^t\ \}^{(e)} \quad , \qquad (4.40)$$

which is assembled into the global system (4.8). For plane stress problems, where the pressures can be computed directly from (4.16), the matrices in equations (4.38b,c and d) as well as the vector $\{\Delta^{(p)}_K\}$ in (4.40) are not required. However, by reworking the equation (4.37a) for the special case of plane stress we can show that the matrix $[\mathcal{C}^*_{B(\beta)}]$ in (4.38a) has additional terms; these are shown in Appendix 4B.

4.4.2 Branching onto the locus of a singular point

In order to compute the locus of a singular point it is essential that we first locate at least one singular point on this locus. Once we have achieved this we can use our continuation methods to trace out the locus. There are thus two parts to this type of analysis.

Firstly, noting that we have two parameters, we compute the solution arc using the continuation methods described in this chapter. This analysis requires the use of a piecewise-linear path in parameter space which determines the relationship between the two parameters (usually one parameter is set to zero). We then locate the singular point using the methods described in section 4.2.2 and compute the approximate singular point using equations (4.27) and (4.28). This approximation is usually fairly accurate since the automatic incrementation schemes (section 4.6) produce large increments in regions of small curvature of the solution arc and small increments where there is greater curvature; the secant $(\underset{\sim}{p}_t - \underset{\sim}{p}_{t-1})$ in equation (4.27) is thus a close approximation to the actual solution arc. We are now able to continue with the second part of the analysis.

Immediately after we have obtained the approximate singular point we discard the piecewise-linear constraint equation and use the constraint equation described in sections 3.2.4 and 4.4.1 in order to trace the locus of this singular point. At the computed approximate singular point we compute the new tangent and thus obtain our predictor for the next singular point that lies on the locus. We then use continuation to trace out this locus. Note that the locus extends in two directions from any point that lies on it so that it is possible to trace out the locus in both of these directions. This method for branching onto a locus is similar to the method used in section 4.3.2 to change paths at junctions of the piecewise-linear paths.

4.5 General computational procedures

Various computational procedures are employed in obtaining the solution to the general set of nonlinear equations (4.3) and these are described in this section.

The integrals in equations (4.14) and (4.38) are evaluated using Gaussian quadrature (see DAHLQUIST and BJORCK (1974) and STROUD and SECREST (1966)). It follows that the principal stretches and the directions of the principal axes at the Gauss points have to be found so that the matrices $[C^*]$ and $[\mathcal{C}^*]$ may be formulated using equations (2.65), (2.66) and (2.68) where appropriate. These principal directions are obtained by using equations (2.16b) and (2.17). Once the integrations have been performed and all the terms in equation (4.6) have been evaluated we can solve for our incremental quantities. The new values of deformation gradient at the Gauss points are then found, and the updated values of stress may be obtained using (2.31) and (2.63), after evaluating the new principal stretches. We also see from these two equations that the pressure p is not zero in the undeformed state. Since it is preferable to have in the program a pressure variable p^* which vanishes in the undeformed state, we define

$$p^* = \sum_n \mu_n - p \quad ; \tag{4.41}$$

then

$$\underset{\sim}{\sigma} = \underset{\sim}{0} \quad \Rightarrow \quad p^* = 0 \quad . \tag{4.42}$$

In the computer program we thus wish to solve for $\Delta p^* = -\Delta p$.

Nine-noded isoparametric quadrilateral elements are used in the program with displacement degrees of freedom being interpolated quadratically. The pressures are only interpolated linearly though, with four degrees of freedom, one at each corner node. Higher order interpolation is used on the displacements than on the pressures so as to have the same order of approximation for the multiples of strain and the pressures which are added to obtain the stresses (see equations (2.30) and (2.31) and also BATHE (1982)).

The incremental solution is obtained from the global system of equations (4.8) which comprises the assembled element matrices (4.15) together with the arc-length constraint coefficients (4.20) and the constraint coefficients from either (4.31) or (4.40); in general we thus solve

$$\begin{bmatrix} \frac{\partial G}{\partial u} & \frac{\partial G}{\partial p} & \frac{\partial G}{\partial \lambda} \\ \frac{\partial H}{\partial u} & 0 & 0 \\ \frac{\partial h}{\partial u} & \frac{\partial h}{\partial p} & \frac{\partial h}{\partial \lambda} \\ \frac{\partial g}{\partial u} & \frac{\partial g}{\partial p} & \frac{\partial g}{\partial \lambda} \end{bmatrix} \begin{Bmatrix} \Delta u \\ \Delta p^* \\ \Delta \lambda \end{Bmatrix} = \begin{Bmatrix} -G \\ -H \\ -h \\ -g \end{Bmatrix} , \qquad (4.43)$$

where all terms shown are either matrices or vectors. We see here that as a consequence of equations (4.12), (4.14d) and (4.41) we have

$$[\frac{\partial G}{\partial p}] = [\frac{\partial H}{\partial u}]^t \quad ; \tag{4.44}$$

we thus have symmetry in the upper left-hand corner of the matrix in equation (4.43).

The predictor $\underset{\sim}{p}_t^{(1)}$ for step t of the solution arc is obtained by using the equation

$$\underset{\sim}{p}_t^{(1)} = \underset{\sim}{p}_{t-1} + \Delta s \, \dot{\underset{\sim}{p}}_{t-1} \quad , \tag{4.45}$$

where Δs is the approximate arc-length that is either chosen or computed using the methods of section 4.6. Here $\dot{\underset{\sim}{p}}_{t-1}$ is either the exact tangent at step $(t-1)$ or an approximate tangent obtained by using the secant vector $\dot{\underset{\sim}{p}}_{t-1} = \underset{\sim}{p}_{t-1} - \underset{\sim}{p}_{t-2}$ (see Figures 3.2 and 3.3 in Chapter 3). The exact tangent at a point is obtained by solving equation (4.43) with the following <u>substitutions into the right-hand side</u>

$$\begin{aligned} &\underset{\sim}{G} = \underset{\sim}{0} \quad , \quad \underset{\sim}{H} = \underset{\sim}{0} \quad , \quad \underset{\sim}{g} = \underset{\sim}{0} \quad , \\ &\underset{\sim}{h} = (-1, 0, \ldots, 0)^t \quad . \end{aligned} \tag{4.46}$$

The equation (4.43) with substitutions (4.46) is obtained by taking derivatives of equations (4.3) with respect to the arc-length parameter s.

Once the predictor has been computed we use Newton-Raphson iterations to obtain the converged solution point on the curve. This solution point together with the tangent which is computed at this point is then used to compute the predictor for the next point. Using this continuation we are able to trace out the complete primary solution arc as well as locating and characterising all singular points. We then return to these singular points to either begin continuation along secondary branches (section 4.2) or to trace the locus of the singular point (section 4.4).

4.5.1 Scaling the system of equations

We see in equation (4.43) that Δu has displacement units, Δp^* has pressure units and $\Delta\lambda$ can have either displacement or load or pressure units depending on which (and how) boundary conditions (2.26) are specified. It is thus desirable to scale the solution space to make the dimensions of all quantities approximately of the same magnitude. To do this we define

$$\mu = \sum_n \mu_n \quad , \tag{4.47}$$

as well as

$$\alpha = \max_i |u_i| \quad , \tag{4.48a}$$

$$\beta = \max_j |p_j^*/\mu| \quad , \tag{4.48b}$$

$$\gamma = \max_k |\lambda_k| \quad , \tag{4.48c}$$

where max ≡ maximum value in the initial (linear) iteration at the first step of the solution path. The scaled system of equations that we solve is then

$$\begin{bmatrix} \frac{\partial G}{\partial u} & \frac{\mu\beta}{\alpha}\frac{\partial G}{\partial p} & \frac{\gamma}{\alpha}\frac{\partial G}{\partial \lambda} \\ \frac{\mu\beta}{\alpha}\frac{\partial H}{\partial u} & 0 & 0 \\ \alpha\frac{\partial h}{\partial u} & \mu\beta\frac{\partial h}{\partial p} & \gamma\frac{\partial h}{\partial \lambda} \\ \alpha\frac{\partial g}{\partial u} & \mu\beta\frac{\partial g}{\partial p} & \gamma\frac{\partial g}{\partial \lambda} \end{bmatrix} \begin{Bmatrix} \frac{\Delta u}{\alpha} \\ \frac{\Delta p^*}{\mu\beta} \\ \frac{\Delta\lambda}{\gamma} \end{Bmatrix} = \begin{Bmatrix} -\frac{1}{\alpha}G \\ \frac{-\mu\beta}{\alpha^2}H \\ -h \\ -g \end{Bmatrix} . \quad (4.49)$$

Notice that extra multiplications have been carried out in the top two rows in order to preserve symmetry in part of the matrix : equation (4.44) thus still holds.

4.5.2 Solution of equations

In order to solve equations (4.49) we use Gauss elimination with partitioning, extending a scheme proposed by KELLER (1977) which exploits the symmetry in (4.49). In order to explain the procedure let us rewrite (4.49) as

$$\begin{bmatrix} A & B \\ C & E \end{bmatrix} \begin{Bmatrix} \Delta x \\ \Delta\lambda \end{Bmatrix} = \begin{Bmatrix} -r \\ -s \end{Bmatrix} , \quad (4.50)$$

where capital letters denote matrices and lower case letters denote vectors. Note that the matrix A is symmetric (see (4.44) and (4.49)). From (4.50) we obtain

$$(E - CA^{-1}B)\Delta\lambda = -s + CA^{-1}r \quad , \tag{4.51a}$$

$$\Delta x = -A^{-1}r - A^{-1}B\Delta\lambda \quad . \tag{4.51b}$$

We now define the vectors b_p and c_q by

$$b_p \in R^n \quad , \quad b_p = (B_{1p}, B_{2p}, \ldots, B_{np})^t \quad , \quad p=1,\ldots,m \quad , \tag{4.52}$$

$$c_q \in R^n \quad , \quad c_q = (C_{q1}, C_{q2}, \ldots, C_{qn})^t \quad , \quad q=1,\ldots,m \quad ; \tag{4.53}$$

then, with $d = -A^{-1}r$ and $e_p = A^{-1}b_p$ we have, from (4.51) ,

$$\sum_p \{E_{qp} - c_q.e_p\}\Delta\lambda_p = -s - c_q.d \quad , \tag{4.54a}$$

$$\Delta x = d - \sum_p e_p \Delta\lambda_p \quad . \tag{4.54b}$$

In practice the dimension of the vector Δx is generally much larger than that of $\Delta\lambda$ so that it is very simple to solve (4.54a) . This scheme takes full advantage of the symmetry of A and requires that the elimination procedure need only be done once since the vectors e_p can be obtained by performing successive resolutions.

4.6 Automatic incrementation

The selection of proper increment sizes is essential in an efficient solution procedure : strong motivation for incrementation techniques that try to make the increment size as large as possible with suitable convergence is given by SCHWETLICK (1984). It is believed that near optimum variable increments are obtained when the truncation error, which is a measure of the linearisation error for one step, remains nearly constant for all steps (BERGAN (1980) and BERGAN, HORRIGMOE, KRAKELAND and SOREIDE (1978)). Based on this criteron increment sizes should be automatically adjusted so that the number of iterations at each step remains nearly constant. Thus we would have large increments in regions of small curvature of the solution arc and small increments where there is greater curvature. Many methods have been proposed in order to try and achieve this : they include very simple methods which are based on numerical experience (ABAQUS Theoretical Manual (1982)), the methods proposed by CRISFIELD (1980,1981), BERGAN et al (1978) and BERGAN (1980) as well as the more complex methods proposed by SCHMIDT (1978), RHEINBOLDT (1980), DEN HEIJER and RHEINBOLDT (1981) and DEUFLHARD (1979). Some of these methods will be discussed here.

The method that is used in the program ABAQUS (see ABAQUS Theoretical Manual (1982)) is based on the maximum force residuals following each iteration. By comparing consecutive values of these quantities, the program determines whether convergence is likely within the maximum number of iterations, I_m , specified by the user. If convergence appears unlikely, the increment is adjusted to 25% of its size and the solution is then started over again from the end of the

previous increment. If convergence appears likely, I_m is ignored and a solution for that increment is obtained. However, if convergence is achieved in less than $I_m/2$ iterations for two successive increments, the increment size is increased by 25% for the following increment. The variable incrementation scheme here is very empirical, but the procedure used when convergence is unlikely is very useful if convergence is not achieved when using one of the following incrementation methods.

CRISFIELD (1980,1981) monitors the number of iterations per increment and compares it with the desired number of iterations to obtain

$$\Delta s_{t+1} = \Delta s_t (I_d / I_t) \quad . \tag{4.55}$$

Here t describes the number of the increment, Δs is the arc-length control parameter, I_t is the number of iterations required to achieve equilibrium in the t-th increment and I_d is the desired number of iterations. RAMM (1981) has found that the use of equation (4.55) results in oscillations in the number of iterations required from step to step, and has advocated instead the use of

$$\Delta s_{t+1} = \Delta s_t (I_d / I_t)^{1/2} \quad . \tag{4.56}$$

BATHE and DVORKIN (1983) use a further variation of this expression by multiplying the right-hand side by a ratio of allowable over actual displacement norms.

The method proposed by BERGAN (1980) uses a scalar stiffness parameter, which attempts to characterise the overall behaviour of nonlinear problems, to predict increment sizes. The current stiffness parameter relates the scalar stiffness at some equilibrium point to the initial scalar stiffness of the problem; hence

$$\theta_t = (\Delta\lambda_t/\Delta\lambda_o)\|\Delta\underset{\sim}{x}_o\|/\|\Delta\underset{\sim}{x}_t\| \quad . \tag{4.57}$$

Here $\underset{\sim}{x} = (u_\ell^r, p^c)^t$ and $\Delta\lambda_t, \Delta\underset{\sim}{x}_t$ are the total increments required for the t-th increment, $\|\cdot\|$ denotes the Euclidean norm and $\Delta\lambda_o, \Delta\underset{\sim}{x}_o$ are the initial increments required for the linear problem (i.e. the initial iteration at the first increment). Note that equation (4.57) is written for single parameter problems only; for multi-parameter problems, instead of (4.57), we use

$$\theta_t = (\|\Delta\underset{\sim}{\lambda}_t\|/\|\Delta\underset{\sim}{\lambda}_o\|)(\|\Delta\underset{\sim}{x}_o\|/\|\Delta\underset{\sim}{x}_t\|) \quad . \tag{4.58}$$

BERGAN et al (1978) give an alternative form of equation (4.57) but, although they do not give identical values, either expression can be used to obtain very similar results (BERGAN (1980)). Another definition of the scalar stiffness parameter may be obtained by replacing the finite increments in equations (4.57) and (4.58) with the corresponding tangents. Thus we have

$$\theta_t = (\dot{\lambda}_t/\dot{\lambda}_o)\|\dot{\underset{\sim}{x}}_o\|/\|\dot{\underset{\sim}{x}}_t\| \tag{4.59}$$

and

$$\theta_t = (\|\dot{\underset{\sim}{\lambda}}_t\| / \|\dot{\underset{\sim}{\lambda}}_o\|)(\|\dot{\underset{\sim}{x}}_o\| / \|\dot{\underset{\sim}{x}}_t\|) \quad . \tag{4.60}$$

However, for reasons of efficiency, use of these equations should be limited to procedures where the tangent is already required. Any of these expressions can be used to predict the increment size (BERGAN (1980))

$$\Delta s_{t+1} = \Delta s_t (\Delta\theta_d / |\Delta\theta_t|) \quad , \tag{4.61}$$

where $\Delta\theta_d$ is a prescribed constant (the desired change in stiffness parameter) and $\Delta\theta_t = \theta_t - \theta_{t-1}$ is the change in stiffness parameter between the t-th and (t-1)th increments. This extrapolation based on the previous steps will have some "inertia" built into it which can, to a certain extent, be corrected for by using (BERGAN (1980))

$$\Delta s_{t+1} = \Delta s_t (\Delta\theta_d / |\Delta\theta_t|)^2 \tag{4.62}$$

instead of equation (4.61).

The current stiffness parameter as given in equations (4.57) and (4.59) for single parameter problems changes sign when the solution passes through limit points; it can thus be used as an alternative method to locate such points (see section 4.2.2). It can be seen from equations (4.58) and (4.60), however, that the current stiffness parameter is always positive for multi-parameter problems. Thus the

current stiffness parameter cannot be used for the location of bifurcation points in single parameter problems nor for the location of all singular points in multi-parameter problems; other methods such as those in section 4.2.2 will then have to be used.

RHEINBOLDT (1980) has suggested various step length algorithms which are obtained by using a quadratic approximation to the solution arc together with an Euler predictor. He also makes use of results on the convergence behaviour of the corrector together with the constraint that the number of iterations remains constant at some pre-assigned number. Further discussion of step length algorithms and their relationship to convergence of the corrector process is given by DEN HEIJER and RHEINBOLDT (1981).

APPENDIX 4A

The matrices in equations (4.14) are :

$$[N_A] = \begin{bmatrix} N_A & 0 \\ 0 & N_A \end{bmatrix}, \quad [M_K] = \begin{bmatrix} M_K \\ M_K \\ M_K \\ M_K \end{bmatrix}, \quad [B_A] = \begin{bmatrix} N_{A,1} & 0 \\ 0 & N_{A,2} \\ N_{A,2} & N_{A,1} \\ X_1^{-1} N_A & 0 \end{bmatrix}, \quad [D_A] = \begin{bmatrix} N_{A,1} & 0 \\ N_{A,2} & 0 \\ 0 & N_{A,1} \\ 0 & N_{A,2} \\ X_1^{-1} N_A & 0 \end{bmatrix}$$

$$[C^*] = [C] + [Q] + \xi[C^{ps}] \quad ,$$

$\xi = 1$ for plane stress, $\xi = 0$ otherwise

$$[C] = \begin{bmatrix} C_{1111} & C_{1122} & C_{1112} & 0 \\ & C_{2222} & C_{1222} & 0 \\ & & C_{1212} & 0 \\ \text{sym} & & & cC_{3333} \end{bmatrix} \quad , \quad [Q] = \begin{bmatrix} p & 0 & 0 & 0 \\ & p & 0 & 0 \\ & & 0 & 0 \\ \text{sym} & & & cp \end{bmatrix} \quad , \quad [C^{ps}] = (C_{3333} + 2p) \begin{bmatrix} 1 & 1 & 0 & 0 \\ & 1 & 0 & 0 \\ & & 0 & 0 \\ \text{sym} & & & 0 \end{bmatrix}$$

$$[\hat{\sigma}] = \begin{bmatrix} \hat{\sigma}_{11} & \hat{\sigma}_{12} & 0 & 0 & 0 \\ & \hat{\sigma}_{22} & 0 & 0 & 0 \\ & & \hat{\sigma}_{11} & \hat{\sigma}_{12} & 0 \\ & & & \hat{\sigma}_{22} & 0 \\ \text{sym} & & & & c\hat{\sigma}_{33} \end{bmatrix} \quad , \qquad [U_{AB}] = \lambda_3 \begin{bmatrix} -c2\pi N_A N_B \dfrac{\partial X_2}{\partial \zeta} & N_A \dfrac{\partial N_B}{\partial \zeta}[(c-1)t - c2\pi X_1] \\ N_B \dfrac{\partial N_A}{\partial \zeta}[(c-1)t - c2\pi X_1] & 0 \end{bmatrix}$$

$$\{b\} = \begin{Bmatrix} b_1 \\ b_2 \end{Bmatrix} \quad , \qquad \{n\} = \begin{Bmatrix} n_1 \\ n_2 \end{Bmatrix}$$

APPENDIX 4B

The matrices in equations (4.38) are :

$$[\mathscr{C}^{*}_{B(\beta)}] = [\mathscr{C}_{B(\beta)}] + [\hat{C}_{B(\beta)}] + [\hat{Q}_{B(\beta)}] - \xi[\mathscr{C}^{ps}_{B(\beta)}] \quad ,$$

$\xi = 1$ for plane stress, $\xi = 0$ otherwise

$$[\mathscr{C}_{B(\beta)}] = \begin{bmatrix} \mathscr{C}_{1111\beta\gamma}N_{B,\gamma} & \mathscr{C}_{1112\beta\gamma}N_{B,\gamma} & \mathscr{C}_{1112\beta\gamma}N_{B,\gamma} & \mathscr{C}_{1122\beta\gamma}N_{B,\gamma} & 0 \\ & \mathscr{C}_{1212\beta\gamma}N_{B,\gamma} & \mathscr{C}_{1212\beta\gamma}N_{B,\gamma} & \mathscr{C}_{1222\beta\gamma}N_{B,\gamma} & 0 \\ & & \mathscr{C}_{1212\beta\gamma}N_{B,\gamma} & \mathscr{C}_{2212\beta\gamma}N_{B,\gamma} & 0 \\ \text{sym} & & & \mathscr{C}_{2222\beta\gamma}N_{B,\gamma} & 0 \\ & & & & \delta_{1\beta}cX_1^{-1}\mathscr{C}_{333333} \end{bmatrix}$$

$$
[\hat{C}_{B(\beta)}] = \begin{bmatrix}
(3\delta_{1\beta}C_{111\gamma}N_{B,\gamma} + \delta_{2\beta}C_{112\gamma}N_{B,\gamma}) & (2\delta_{1\beta}C_{211\gamma}N_{B,\gamma} + \delta_{1\beta}C_{112\gamma}N_{B,\gamma} + \delta_{2\beta}C_{122\gamma}N_{B,\gamma}) & (\delta_{1\beta}C_{121\gamma}N_{B,\gamma} + \delta_{2\beta}C_{111\gamma}N_{B,\gamma}) & (\delta_{1\beta}C_{221\gamma}N_{B,\gamma} + \delta_{2\beta}C_{112\gamma}N_{B,\gamma}) & 0 \\
 & (2\delta_{1\beta}C_{122\gamma}N_{B,\gamma} + \delta_{1\beta}C_{2221\gamma}N_{B,\gamma} + \delta_{2\beta}C_{222\gamma}N_{B,\gamma}) & (\delta_{1\beta}C_{122\gamma}N_{B,\gamma} + \delta_{2\beta}C_{121\gamma}N_{B,\gamma}) & (\delta_{1\beta}C_{222\gamma}N_{B,\gamma} + \delta_{2\beta}C_{121\gamma}N_{B,\gamma}) & 0 \\
 & & (\delta_{1\beta}C_{111\gamma}N_{B,\gamma} + 2\delta_{2\beta}C_{211\gamma}N_{B,\gamma} + \delta_{2\beta}C_{112\gamma}N_{B,\gamma}) & (\delta_{1\beta}C_{121\gamma}N_{B,\gamma} + 2\delta_{2\beta}C_{122\gamma}N_{B,\gamma} + \delta_{2\beta}C_{2221\gamma}N_{B,\gamma}) & 0 \\
 & & & (\delta_{1\beta}C_{221\gamma}N_{B,\gamma} + 3\delta_{2\beta}C_{222\gamma}N_{B,\gamma}) & \\
\text{sym} & & & & 3\delta_{1\beta}cX_1^{-1}C_{3333}
\end{bmatrix}
$$

$$[\hat{Q}_{B(\beta)}] = \begin{bmatrix} -2p\delta_{1\beta}\delta_{1\gamma}N_{B,\gamma} & -p\delta_{2\beta}\delta_{1\gamma}N_{B,\gamma} & -p\delta_{1\beta}\delta_{2\gamma}N_{B,\gamma} & 0 & 0 \\ & 0 & -pN_{B,\beta} & -p\delta_{2\beta}\delta_{1\gamma}N_{B,\gamma} & 0 \\ & & 0 & -p\delta_{1\beta}\delta_{2\gamma}N_{B,\gamma} & 0 \\ & & & -2p\delta_{2\beta}\delta_{2\gamma}N_{B,\gamma} & 0 \\ \text{sym} & & & & -2cp\delta_{1\beta}X_1^{-1} \end{bmatrix}$$

$$[\mathcal{C}^{ps}_{B(\beta)}] = \begin{bmatrix} (\varepsilon+\tau)N_{B,\beta} + \delta_{1\beta}\tau N_{B,1} & 0 & 0 & \varepsilon N_{B,\beta} + \delta_{1\beta}\tau N_{B,1} & 0 \\ \delta_{2\beta}\tau N_{B,1} & 0 & \tau N_{B,\beta} & \delta_{2\beta}\tau N_{B,1} & 0 \\ \delta_{1\beta}\tau N_{B,2} & \tau N_{B,\beta} & 0 & \delta_{1\beta}\tau N_{B,2} & 0 \\ \varepsilon N_{B,\beta} + \delta_{2\beta}\tau N_{B,2} & 0 & 0 & (\varepsilon+\tau)N_{B,\beta}+\delta_{2\beta}\tau N_{B,2} & 0 \\ 0 & 0 & 0 & 0 & 0 \end{bmatrix}$$

where $\varepsilon = \mathcal{C}_{333333} + 5C_{3333} + 2p$

$\tau = C_{3333} + 2p$

$$[U^{(u)}_{AB(\beta)C}] = \lambda_3 \begin{bmatrix} -c2\pi\delta_{2\beta} N_A N_C \dfrac{\partial N_B}{\partial \zeta} & -c2\pi\delta_{1\beta} N_B N_A \dfrac{\partial N_C}{\partial \zeta} \\ -c2\pi\delta_{1\beta} N_B N_C \dfrac{\partial N_A}{\partial \zeta} & 0 \end{bmatrix}$$

$$, \quad [X_{B(\beta)}] = \begin{bmatrix} \delta_{1\beta} N_{B,1} & 0 & 0 & 0 \\ \delta_{2\beta} N_{B,1} & 0 & 0 & 0 \\ \delta_{1\beta} N_{B,2} & 0 & 0 & 0 \\ 0 & \delta_{2\beta} N_{B,2} & 0 & 0 \\ 0 & 0 & 0 & \delta_{1\beta} c X_1^{-1} N_B \end{bmatrix}$$

$$[Y_{B(\beta)}] = \begin{bmatrix} (\delta_{1\beta} c X_1^{-1} N_B + \delta_{2\beta} N_{B,2}) & -\delta_{2\beta} N_{B,2} & 0 & 0 & c\delta_{2\beta} N_{B,2} \\ 0 & 0 & -\delta_{1\beta} N_{B,2} & \delta_{1\beta} N_{B,1} & 0 \\ 0 & 0 & 0 & 0 & 0 \\ 0 & 0 & 0 & \delta_{1\beta} c X_1^{-1} N_B & c\delta_{1\beta} N_{B,1} \end{bmatrix}$$

$$[Z_K] = \begin{bmatrix} M_K & 0 & 0 & 0 & 0 \\ & 0 & M_K & 0 & 0 \\ & & 0 & 0 & 0 \\ & & & M_K & 0 \\ \text{sym} & & & & cM_K \end{bmatrix}$$

CHAPTER 5

EXAMPLES AND DISCUSSION

In this chapter we apply the methods discussed previously to the study of a circular cylinder of an incompressible elastic material subjected to axial extension and internal radial pressure. This example contains two identifiable loading parameters and also exhibits complex limit point and bifurcation behaviour. Thus, if we choose our parameters correctly, we are able to locate singular points while tracing out the primary solution paths on the equilibrium surface. This allows us to study the characteristics of these points and also to study the bifurcation behaviour in more detail. HAUGHTON and OGDEN (1979b) have presented an extensive analytical study of the primary equilibrium behaviour of this example, including the location of limit and bifurcation points, and their closed-form results are used as a basis for comparison. The complete analysis is done in three parts and each is discussed under a separate heading.

5.1 Finite element model

The dimensions of the cylinder are chosen to be $L/B = 10$, $A/B = .85$ where L, A and B are the undeformed length, inner radius and outer radius respectively; all results will be given in terms of these dimensionless quantities. A finite element model consisting of two axisymmetric nine-noded elements was chosen for the analysis; this

model is shown in Figure 5.1. The model approximates the behaviour on the primary surface very well and saves on computational effort, especially when doing the computer-intensive computations required for the tracing of the loci of singular points. Further refinement of this finite element model improves the results marginally. It must be borne in mind, though, that this model may not allow for the detection of bifurcation points that have associated complex bifurcation modes since such modes may possibly not be approximated closely enough by the piecewise quadratic approximation.

The three-term form of the strain-energy function in equation (2.62) is used with material constants

$$\begin{aligned} &\alpha_1 = 1.3 \quad , \quad \alpha_2 = 5.0 \quad , \quad \alpha_3 = -2.0 \quad , \\ &\mu_1^* = 1.491 \quad , \quad \mu_2^* = 0.003 \quad , \quad \mu_3^* = -0.023 \quad , \end{aligned} \tag{5.1}$$

where $\mu_n^* = \mu_n/\mu$, $\mu = \frac{1}{2}\sum \mu_n \alpha_n$ being the ground-state shear modulus. The strain-energy function having these constants is a good model for a vulcanised natural rubber (OGDEN (1972a)).

5.2 Primary equilibrium surface using piecewise-linear paths

In order to obtain an idea of the primary equilibrium surface it is necessary to trace various solution paths and to depict them in a diagram of some form (usually a three-dimensional diagram or a family of parameterised paths drawn in two-dimensions). For a multi-parameter

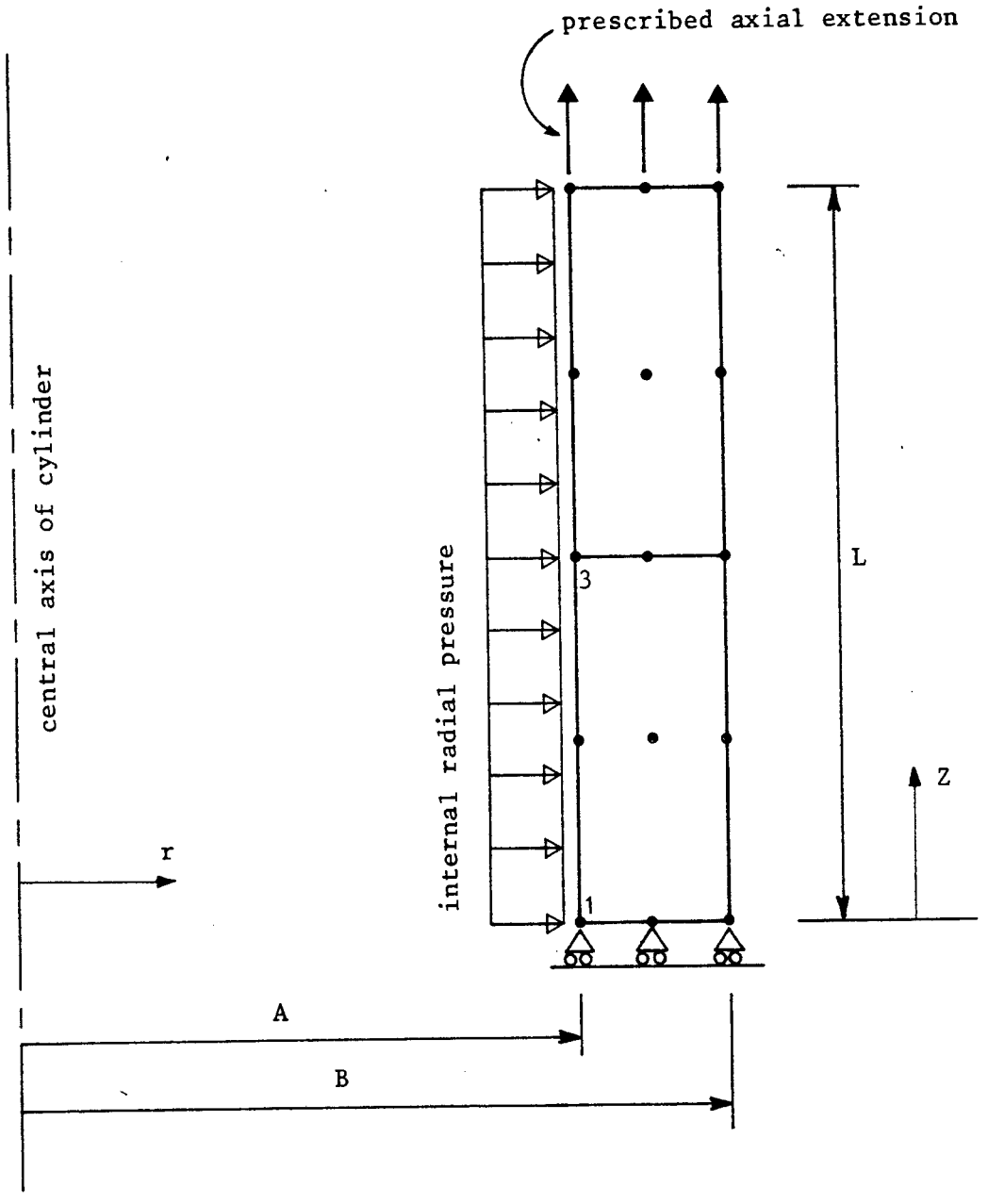

Figure 5.1 Finite element model.

problem we thus require the use of piecewise-linear paths to prescribe the path which the solution must follow.

For our example we may plot the behaviour of pressure and axial extension versus radial displacement at any node since, for the primary solution paths, all nodes behave in a very similar manner. We can thus obtain a three-dimensional diagram of the primary equilibrium surface, the vertices being the internal radial pressure, the axial stretch and the inner circumferential stretch. Of course, we now have the possibility of choosing any two of the three variables as the parameters of the problem, the other variable being the unknown. We must emphasise, however, that depending on which variables are parameters, singular points may or may not be detected. For example, for a fixed axial stretch (one parameter) if we choose the second parameter to be the pressure we detect a limit point, but if we choose the radial extension (equivalent to the inner circumferential stretch) as a parameter, so that we have a prescribed radial displacement on the inner surface, no limit point is detected. This is due to the fact that, in the first case, a point on the solution curve of pressure versus displacement is found at which the derivative of the nonlinear equation with respect to the pressure vanishes. In the second case, however, the curve of pressure versus displacement is monotonically increasing.

By prescribing a family of piecewise-linear paths such as those shown in Figure 5.2 we are able to trace out a series of solution paths; using these results in a graphics package we can then draw the three-dimensional primary equilibrium surface (Figure 5.3) as well as the corresponding contour diagram (Figure 5.4) for the case of positive

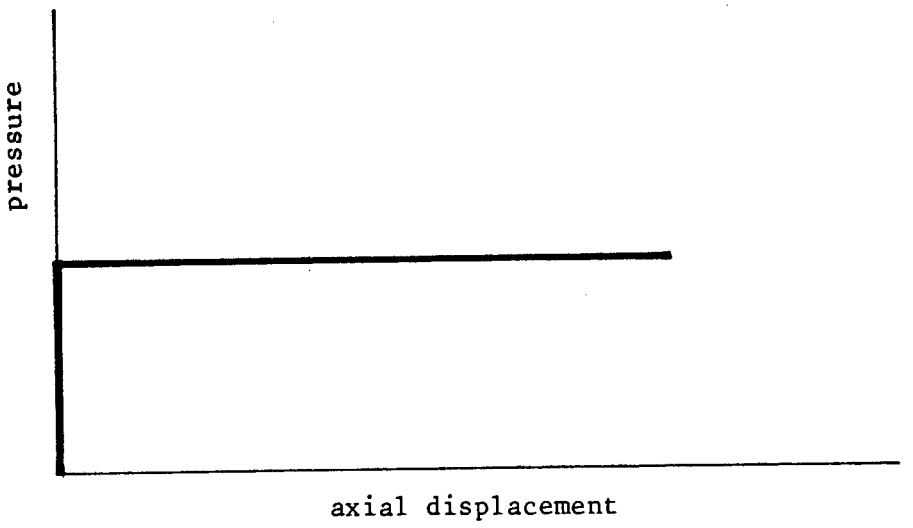

(a) Piecewise-linear path with pressure and axial displacement as parameters.

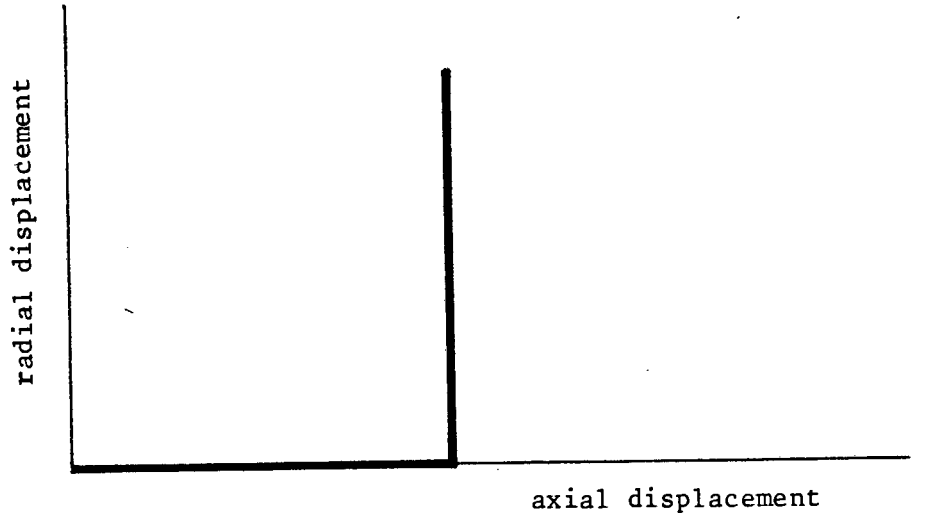

(b) Piecewise-linear path with radial and axial displacements as parameters.

Figure 5.2 Typical piecewise-linear paths used for tracing solution paths on the equilibrium surface.

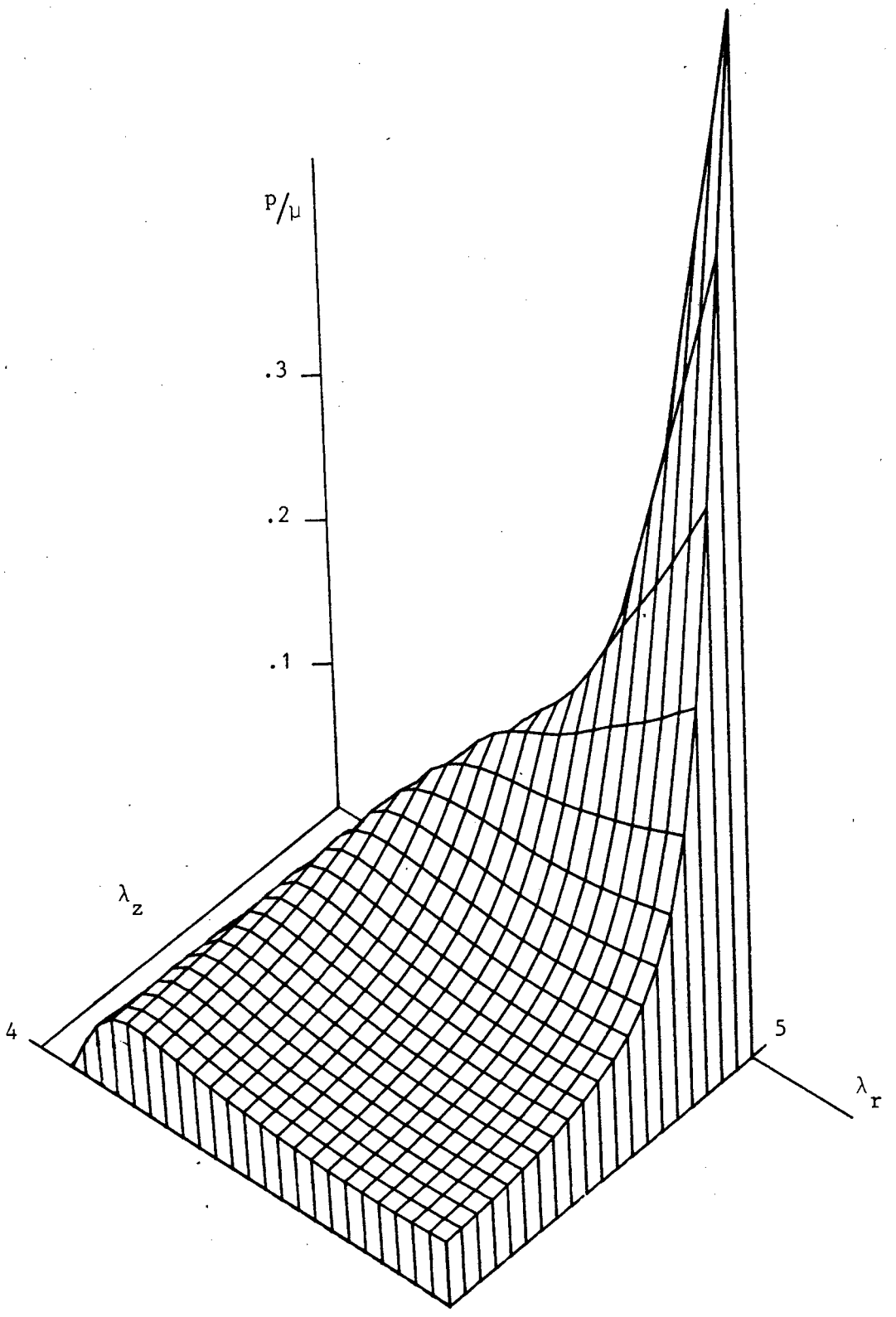

Figure 5.3 Three-dimensional primary equilibrium surface.

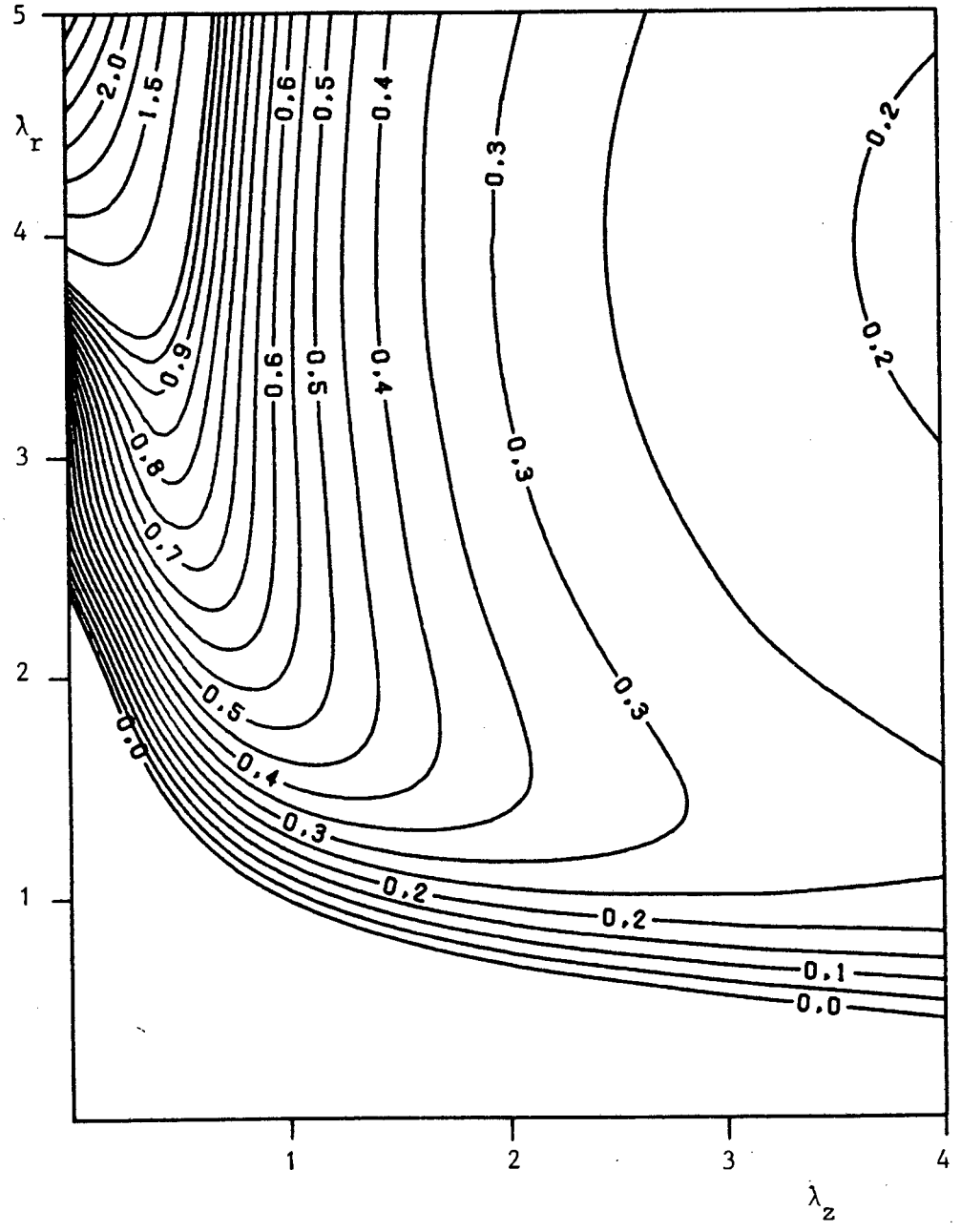

Figure 5.4 Contour diagram of primary equilibrium surface (contours of equal pressure).

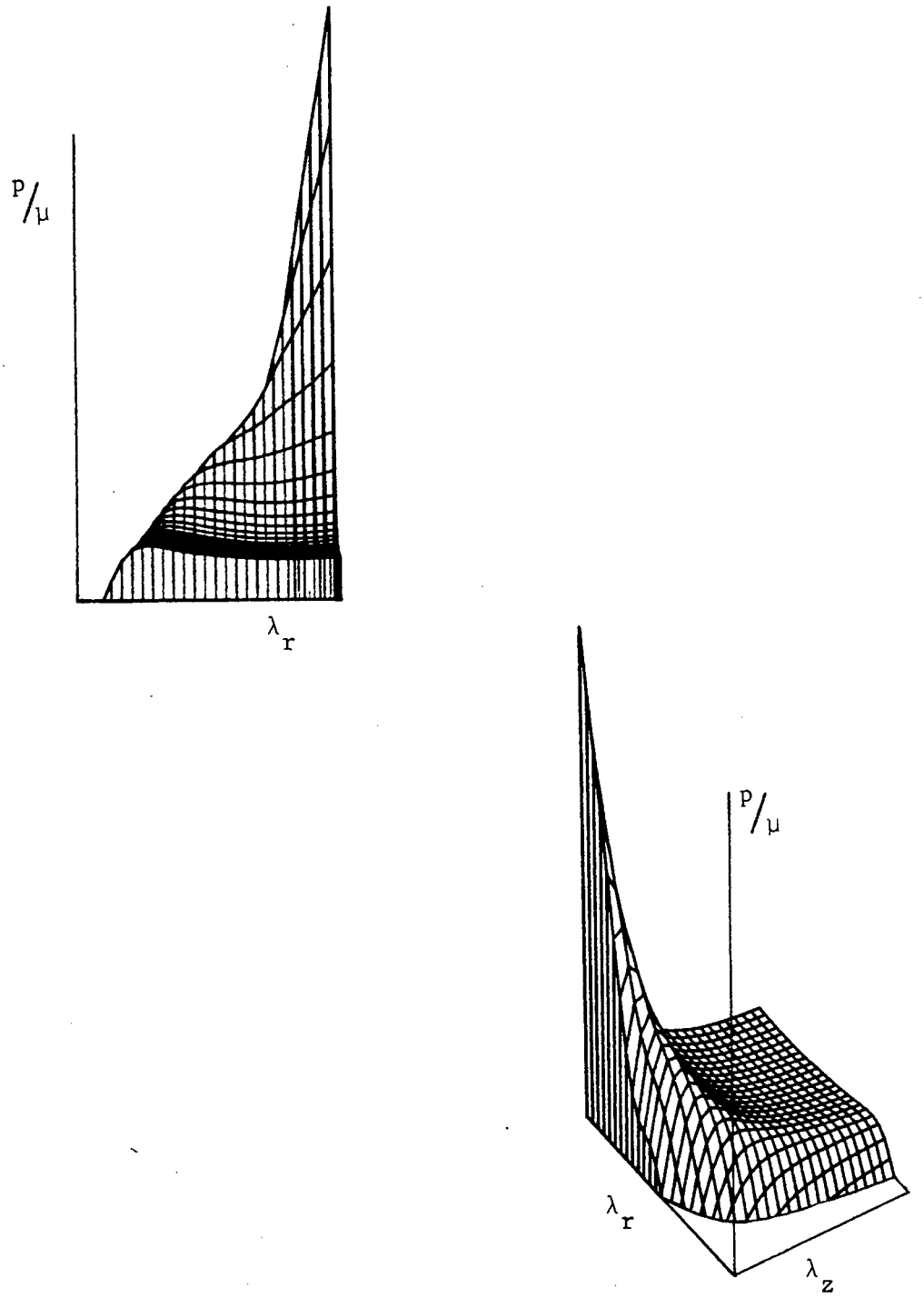

Figure 5.5 Other three-dimensional views of primary equilibrium surface.

pressure (i.e. inflation). It must be noted that the zero pressure contour should be asymptotic to the λ_r axis. Inaccuracies along this axis are due to the interpolation and smoothing techniques used in the graphics package and not due to erroneous results from the analysis. Except for this region of "graphical" error the equilibrium surface agrees very well with results obtained by HAUGHTON and OGDEN (1979b). The crest and trough that indicate lines of limit points are clearly seen in Figures 5.3 and 5.4. Note that the crest and trough join together at approximately $\lambda_z = 0.6$. Different views of this surface are shown in Figure 5.5.

To obtain the solution paths that combine to create this equilibrium surface we use the continuation methods described in chapter 4. It was found that these paths could be obtained using any one of the arc-length constraint equations described in section 3.1.2 and that for this example no particular arc-length constraint equation had any advantage over the others. For this reason results and discussion pertaining to this aspect of the solution procedure are not given here. The automatic incrementation techniques (section 4.6), which were found to be very useful in obtaining these results, produce similar results and very little advantage is gained from choosing any particular method over another.

An example of a solution path that can be obtained is shown in Figure 5.6. The prescribed piecewise-linear path is given in Figure 5.6(a) and the resulting solution path is depicted on the primary equilibrium surface in Figure 5.6(b).

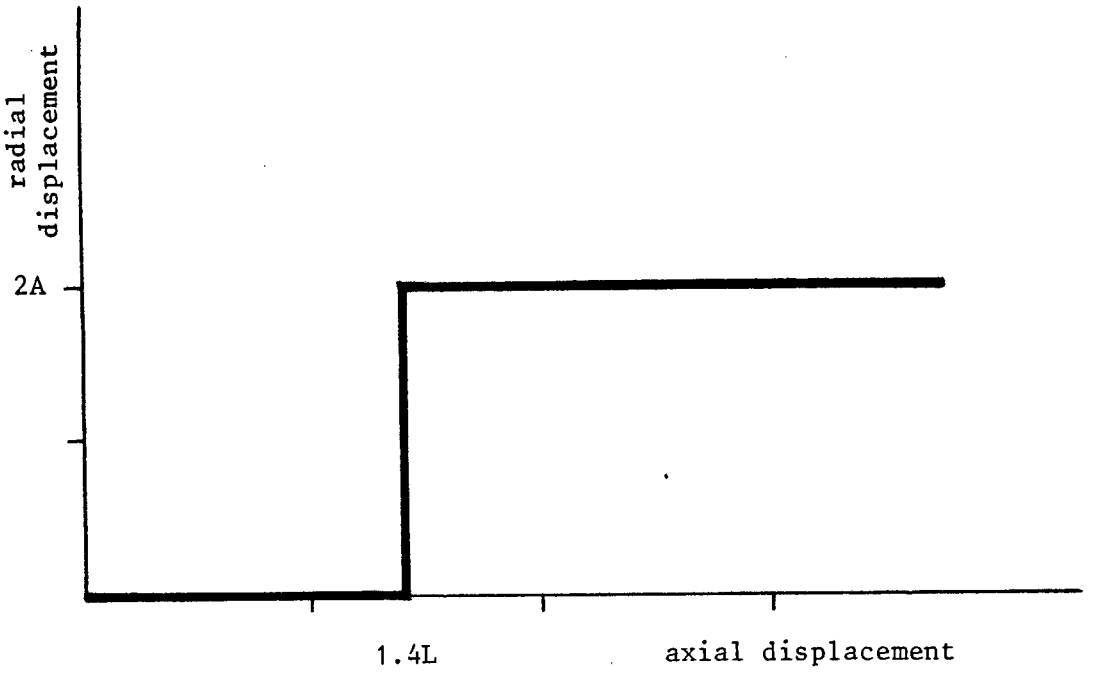

(a) Piecewise-linear path

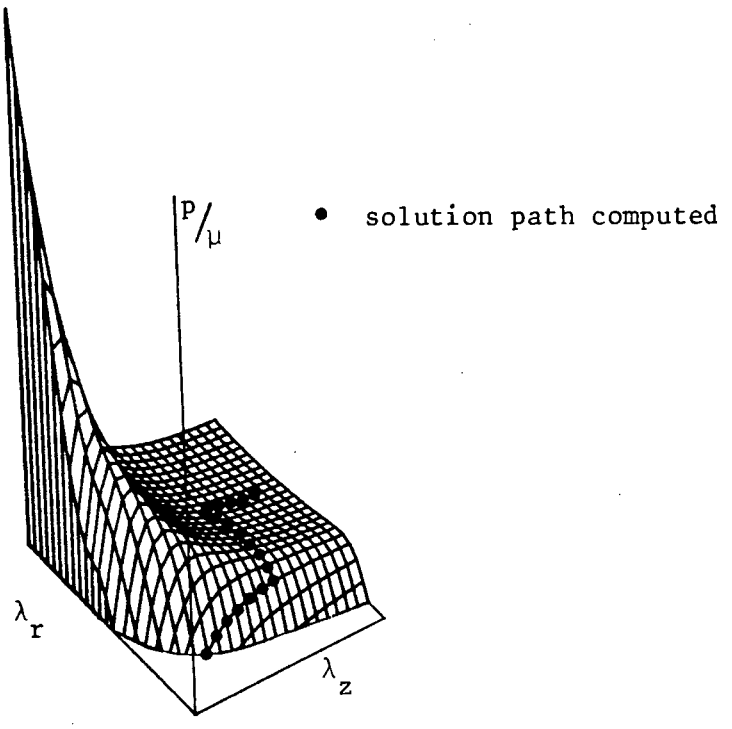

(b) Three-dimensional equilibrium surface showing required solution path

Figure 5.6 Tracing a particular solution path on the primary equilibrium surface.

5.3 Bifurcation analysis

The object of this part of the analysis is to investigate the post-bifurcation behaviour of the pressurised cylinder subject to various axial extensions. This is done so that we may obtain a description of the shape of the secondary (or bifurcated) surface. The analysis thus requires us to trace out solution paths (possibly piecewise-linear paths) and to locate bifurcation points along these paths. Then, changing paths at these bifurcation points we are able to trace out the secondary paths. Because of the location of the bifurcation points and the nature of the secondary paths (see the figures in this section) reasonable results could only be obtained by using Euler chord continuation (incrementation along the paths without corrector iterations). This process obviously introduces some error, which is normally a function of the step size, into the solution. A brief investigation of these likely errors is thus necessary.

We consider a pressurised cylinder with no axial extension which we use as a model for this error investigation. The closed-form result obtained by HAUGHTON AND OGDEN (1979b) for this example is easily duplicated using the predictor-corrector method and we use this for our comparisons. Using the Euler chord continuation method with different step lengths we obtain the results shown in Figure 5.7. From these results we see that although the "convergence ratio", which is a percentage measure of the error in the norm given after equation (4.2), gets fairly large the general behaviour is the same as that of the

Convergence ratios :

step	at limit point	at bifurcation point	at point A
1.0	37%	41%	52%
.5	37%	41%	53%
.1	37%	41%	52%

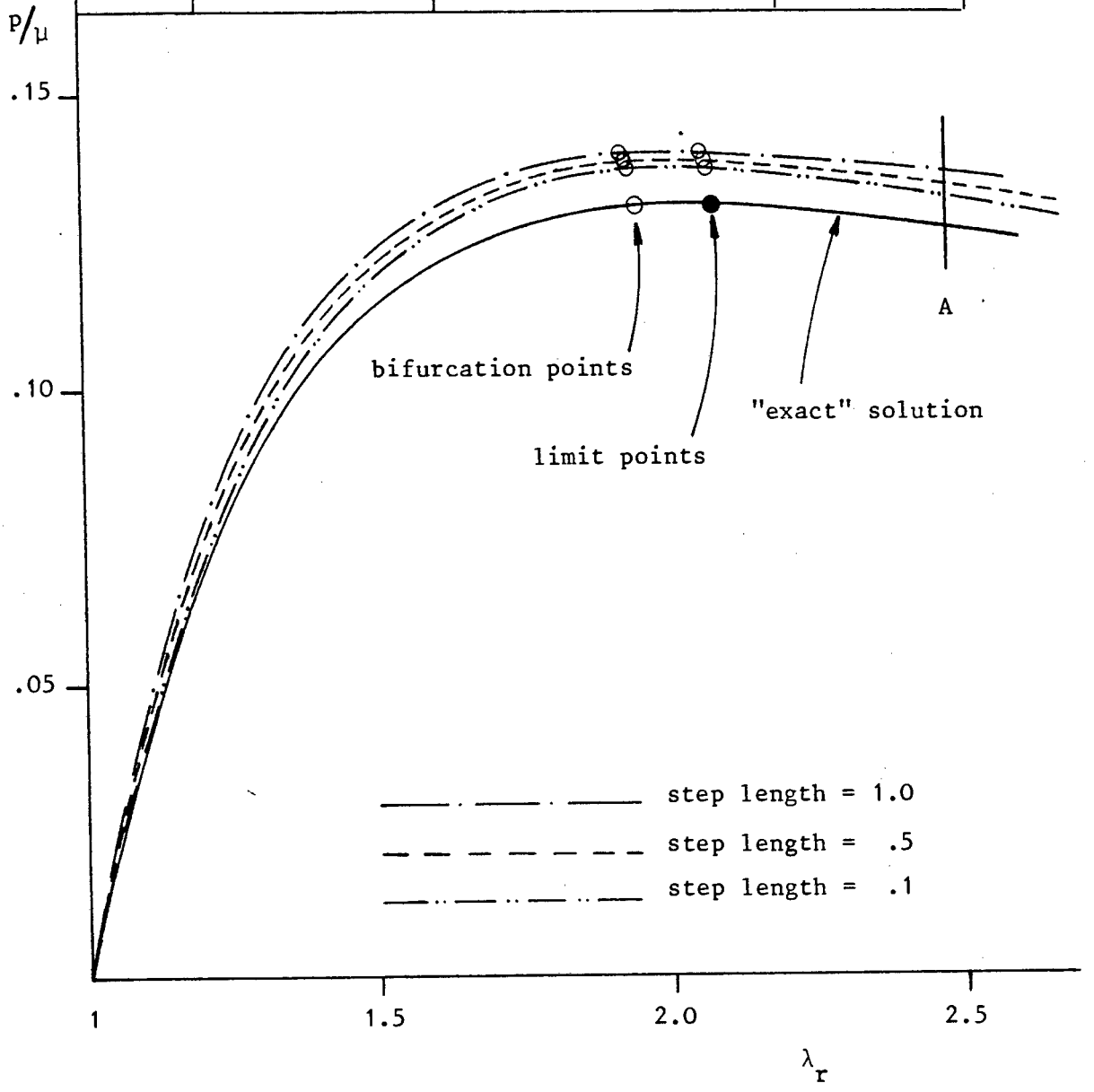

Figure 5.7 Solution paths using Euler chord continuation.

"exact" result and the location of the bifurcation (and limit) points is accurate enough for our purposes. With these results in mind we investigate the bifurcation behaviour and characteristics of the example.

The bifurcation points together with the secondary paths are shown in Figures 5.8 and 5.9 for various values of axial stretch; the primary paths in these figures agree with the solutions obtained by HAUGHTON and OGDEN (1979b). Notice in Figure 5.9 that $w/\lambda_z L = 0$ for all primary paths (w is the axial displacement of a point). It must be noted that these figures only depict the behaviour of a particular point (node) of the model and that while the behaviour at other points may be similar the numerical values will not be the same. The displaced shape of the cylinder along the secondary paths, henceforth called the bifurcated mode, is different to that of the cylinder along the primary path, and the particular points used in Figures 5.8 and 5.9 were chosen so as to give a clearer picture of what the overall bifurcated behaviour will be like. The bifurcated mode for a cylinder with no axial extension is shown in Figure 5.10; this mode is typical for all the secondary paths shown in Figures 5.8 and 5.9 and agrees with the results of HAUGHTON and OGDEN (1979b) who considered modes of the form

$$u(r,z) = f(r)\cos(\pi z/\ell) \quad , \tag{5.2a}$$

$$w(r,z) = g(r)\sin(\pi z/\ell) \quad , \tag{5.2b}$$

where u and w are the radial and axial displacements, f and g are functions of r, ℓ is the current length and the other quantities are

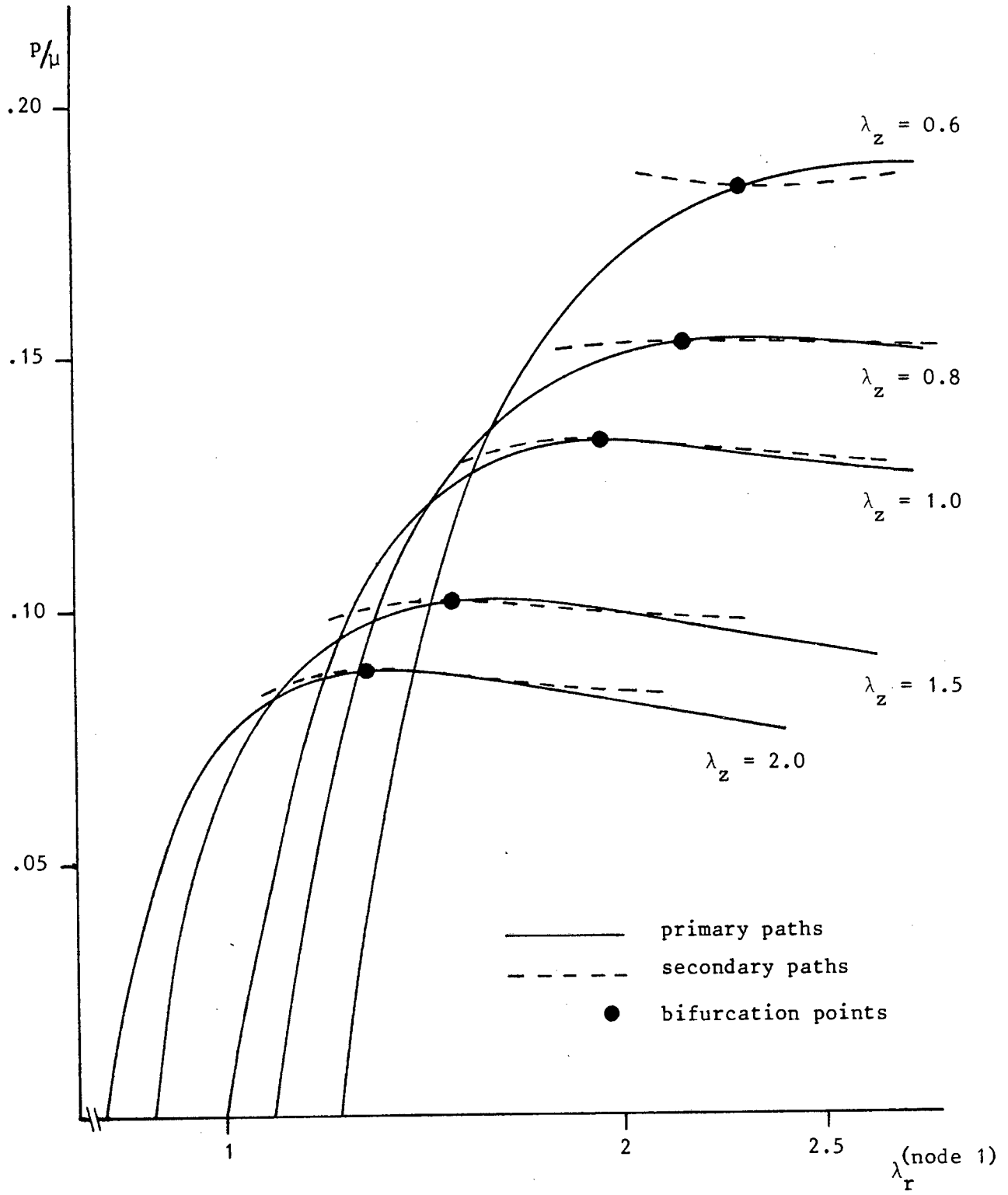

Figure 5.8 Secondary paths (circumferential stretch at node 1) for bifurcation mode described by equations (5.2).

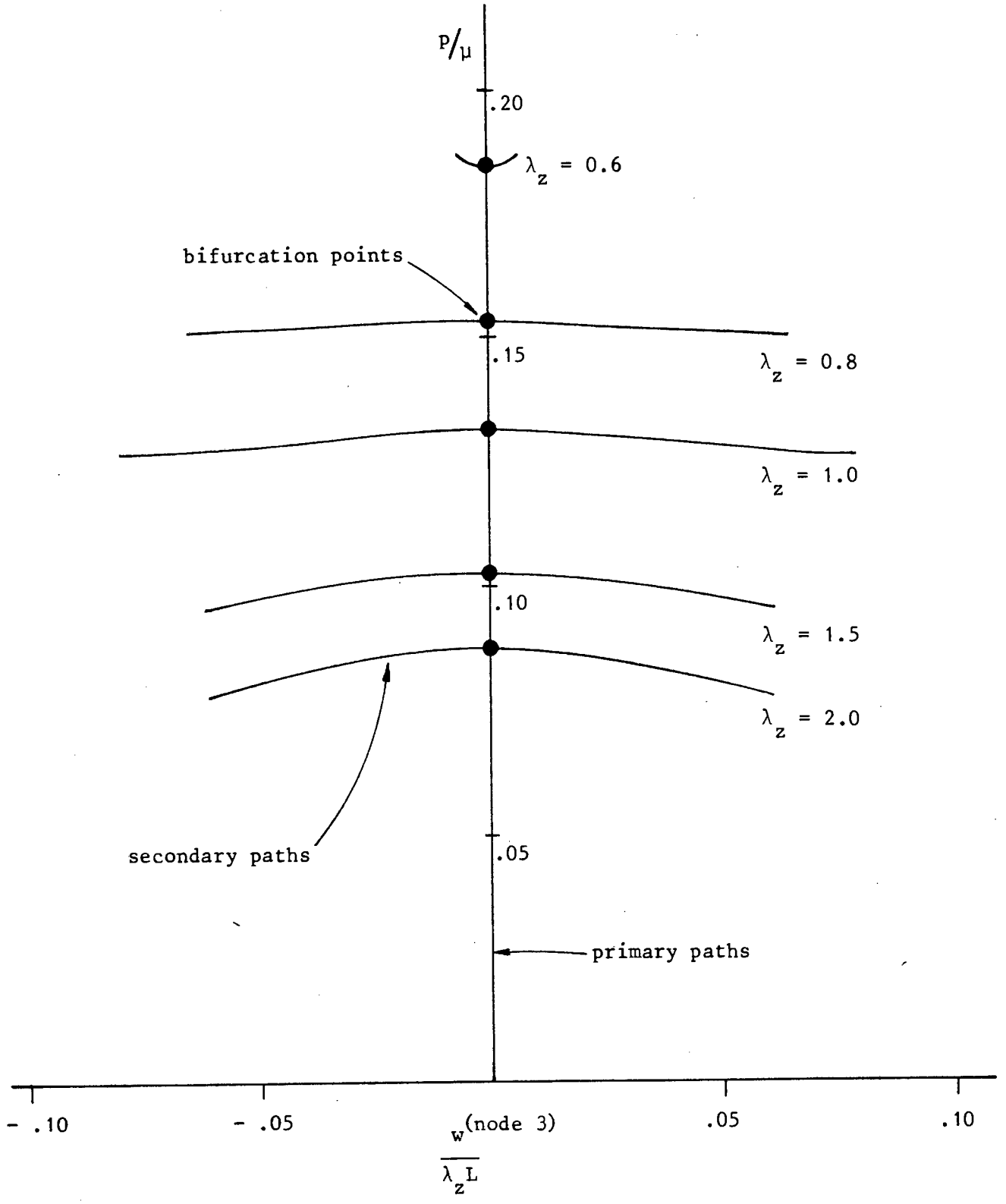

Figure 5.9 Secondary paths (vertical displacement at node 3) for bifurcation node described by equations (5.2).

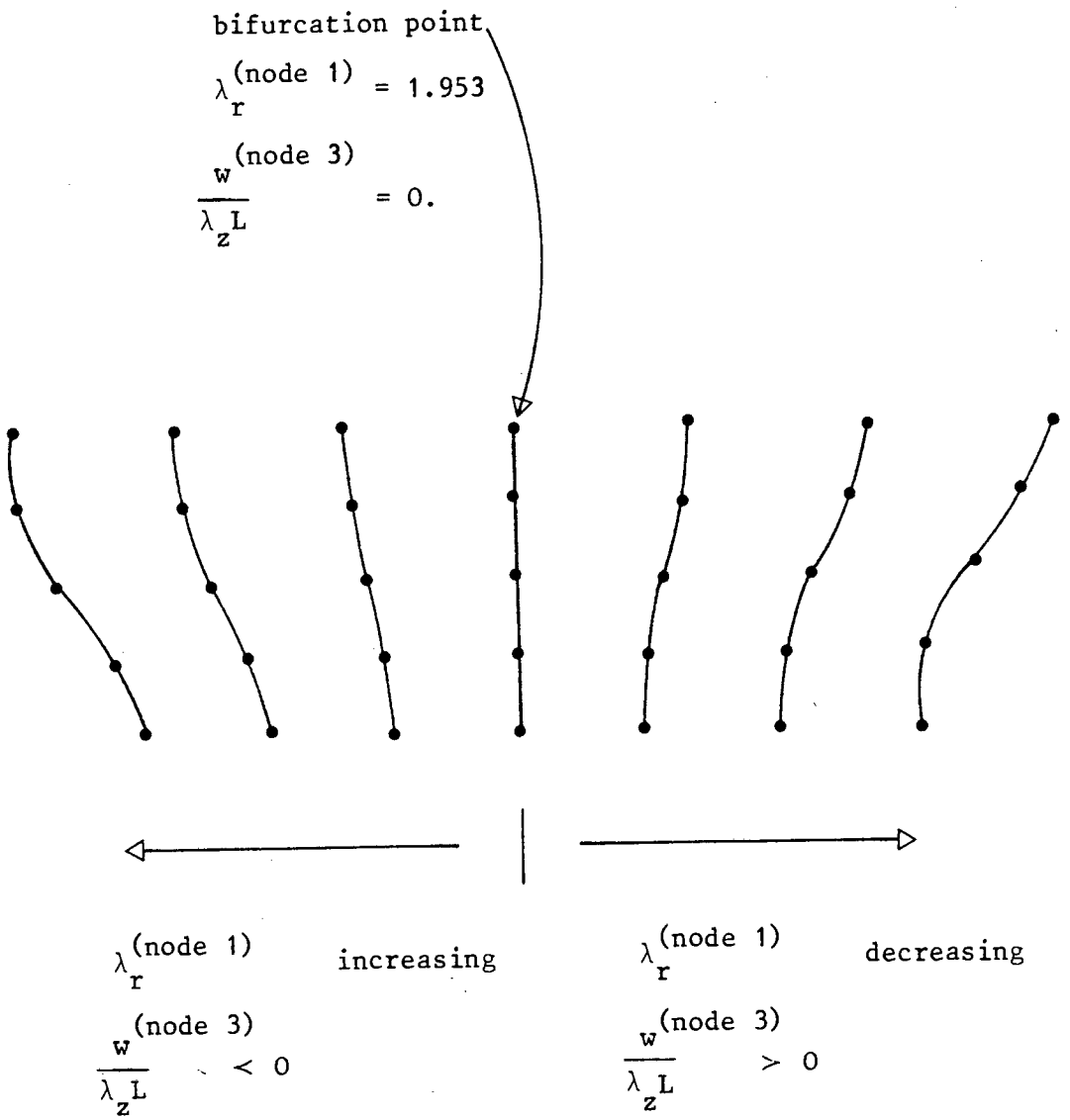

Figure 5.10 Bifurcated mode along secondary path for $\lambda_z = 1.0$.

shown in Figure 5.1. The behaviour of a particular point is depicted in Figure 5.8 and thus points of intersection between the primary and secondary paths, other than the located bifurcation point, are not singular points; for this reason we do not depict the intersection of a primary and a bifurcated surface.

The method of branching onto the secondary paths as described in section 4.2.3 was used with reasonable success. It was found, though, that the choice of the parameter k is critical (see equation (4.24)). Often the solution would tend towards the primary path and trace that path instead. This is due, in part, to the nature of the bifurcation path in this example and also due to the value of k being close to 0 or 2. The best way of ensuring that the secondary path is followed and that no doubling back onto the primary path occurs is to use the method proposed by RIKS (1979), that is, to set $k = 1$. This was used successfully to branch onto all the secondary paths shown here.

An interesting aspect in this bifurcation analysis is the detection of another bifurcation point for the case when $\lambda_z = 2.0$ and $\lambda_z = 0.6$. The bifurcation points and the secondary paths branching from them are shown in Figure 5.11. The bifurcation mode for these paths corresponds to a barrelling of the cylinder and can be seen in part of Figure 5.12. The case when $\lambda_z = 0.6$ requires further attention.

For this case the bifurcation point corresponding to this mode occurs at a much lower value of pressure than the bifurcation point corresponding to the mode assumed by HAUGHTON and OGDEN (1979b). This barrelling seems reasonable for cylinders that are compressed axially

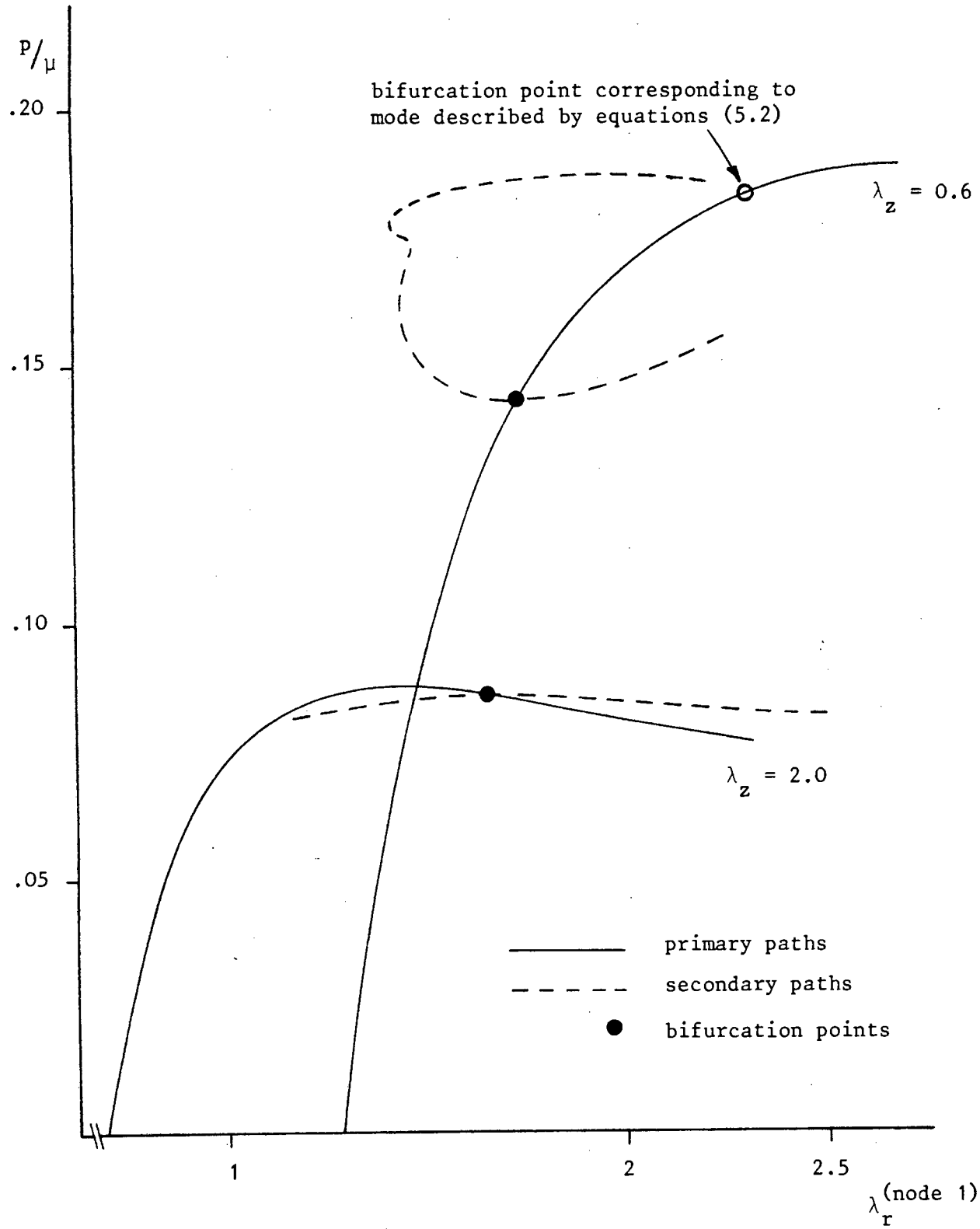

Figure 5.11 Secondary paths (circumferential stretch at node 1) for barrelling bifurcation mode.

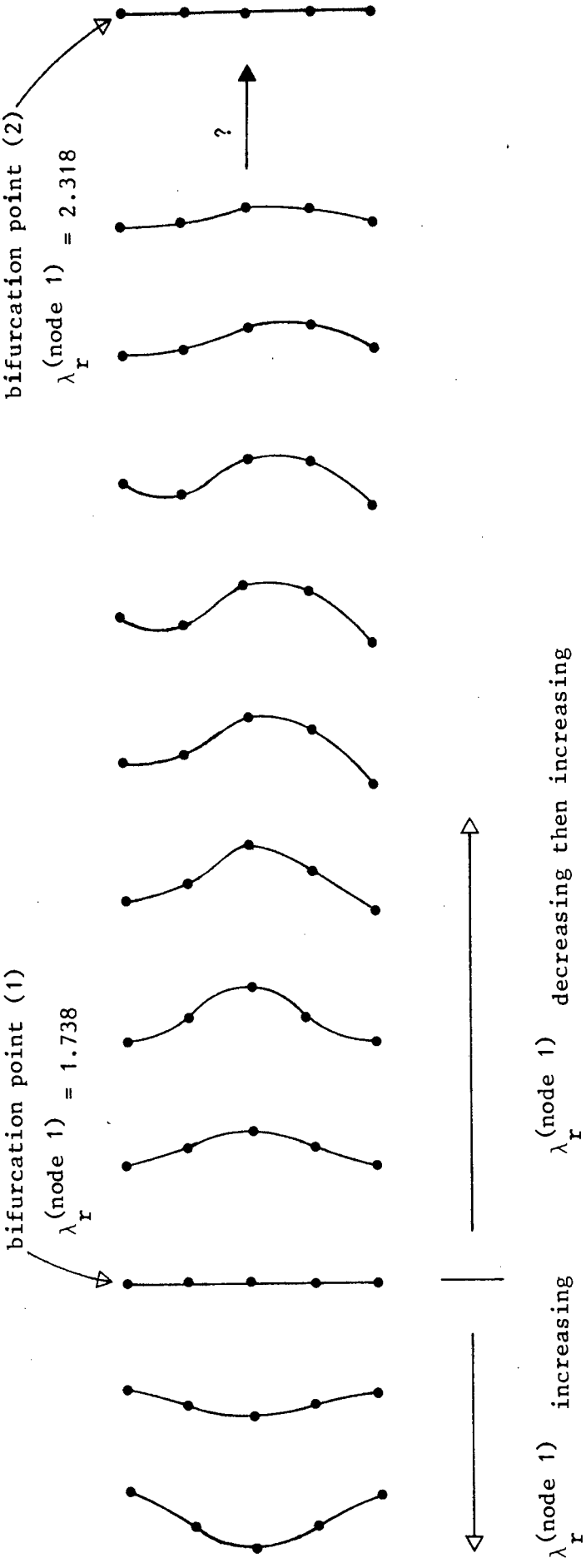

Figure 5.12 Bifurcated mode along secondary path for $\lambda_z = 0.6$.

but this result seems to indicate that bifurcations will occur earlier than expected by HAUGHTON and OGDEN (1979b). In their analysis HAUGHTON and OGDEN (1979b) cannot locate this bifurcation mode because of their assumed bifurcation mode given in equation (5.2). However, the bifurcation behaviour appears to be stable and in fact the mode changes shape (see Figure 5.12) and approaches the mode of the upper bifurcation point as shown in Figure 5.11. This seems to indicate a similar type of behaviour to that found by HAUGHTON (1980) in his analysis of the post-bifurcation behaviour of spherical elastic membranes : the first bifurcation point indicates the initiation of a bifurcation mode while the second bifurcation point indicates the return to the primary path configuration. Thus it appears that while inflating the cylinder either of the paths shown in Figure 5.11 may be followed. A stability analysis of each path would be required to determine which path would actually be followed.

Use of the Euler chord method of obtaining this path obviously introduces errors which are difficult to evaluate. The existence of the "bump" along the secondary path seems to indicate some error in that region and thus casts some doubt on the accuracy of the results along the path. However, repeating the analysis with half the step length produced almost identical results. This would seem to indicate that either the results obtained are reasonably accurate or that a much smaller step length is required to compute these paths accurately. A complete investigation into the nature and characteristics of this bifurcation mode as well as its interaction with the other mode is thus required.

5.4 Loci of limit and bifurcation points

We have seen in section 5.2 that we can locate singular points (both limit and bifurcation points) while we are tracing out solution paths on the primary equilibrium surface. It is possible then, if we want to determine the loci of these singular points, to do this by prescribing various piecewise-linear parameter paths and computing the singular points on each. This is obviously a tedious process and an alternative is the method described in section 4.4. Using this method we trace one solution path, locate the singular points on it and then trace out the loci of these points. This requires that the solution procedure must change paths at the particular singular point and the equation constraining solution points to lie on the locus must be used (see section 4.4).

The computation required for derivatives of this constraint equation is substantial and for this reason the two element model has been chosen. To decrease computer time still further the Euler chord method of continuation was again used and although errors are introduced into the solution the method has proved to be successful. Our example has two independent parameters and is thus ideally suited to this type of analysis. Loci of limit and bifurcation points are shown for regions of axial extension and axial compression in Figure 5.13. Also shown in the diagram are computed values of limit and bifurcation points as well as the results obtained by HAUGHTON and OGDEN (1979b). There appears to be some discrepancy in HAUGHTON and OGDEN'S (1979b) results for the curve of bifurcation points in the axial compression region; this region shown on a large scale (HAUGHTON and OGDEN (1979b), Figure 5(a)) does

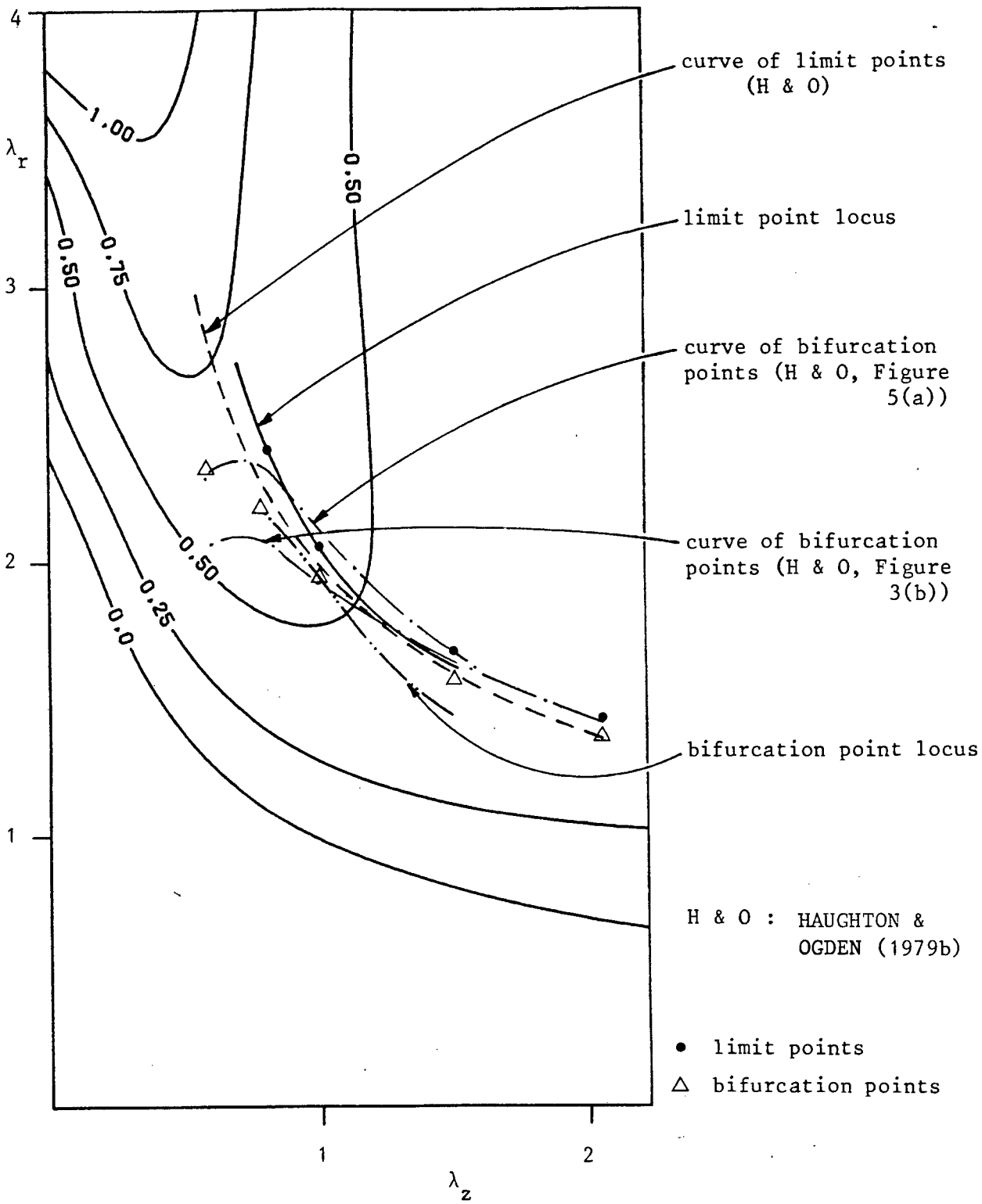

Figure 5.13 Loci of limit and bifurcation points.

not agree very closely with the diagram showing the complete curve of bifurcation points (HAUGHTON and OGDEN (1979b), Figure 3(b)). We thus show both curves in Figure 5.13. It is interesting to note that the curves of limit points and bifurcation points intersect in HAUGHTON and OGDEN'S (1979b) results; at this point we thus have a bifurcation point coincident with a limit point. DECKER and KELLER (1980) discuss the location and characteristics of such points.

The locus of the limit point agrees closely with the result of HAUGHTON and OGDEN (1979b) as well as with the computed values and thus requires no further discussion. The locus of the bifurcation point in the axial extension region is not as good as expected; the reason for this discrepancy lies in the fact that the locus of the bifurcation point runs along the "steep" side of the equilibrium surface where the Euler chord method is more prone to inaccuracies. The locus of the limit point, however, runs along a "ridge" in the equilibrium surface where there is no severe curvature. Smaller step lengths may improve the accuracy but the computational time would be prohibitive. A point to note is that, although our computed values of the limit and bifurcation points agree quite closely with those of HAUGHTON and OGDEN (1979b) they indicate that the curves of these points do not intersect in our analysis; this is shown by the computed loci as well.

An important aspect of this analysis is the extensive computational effort that is required to compute these loci. The method is successful but further investigation into decreasing the computational effort is required. One solution to this problem would be to trace the locus for a few steps using the predictor-corrector method and then use a secant-

type method to compute the approximate derivatives of the constraint equation. No doubt other approximate methods can also be used but further research in this direction is required.

5.5 Concluding remarks

All the analyses in this chapter have been carried out automatically with the minimum of user input and "intelligence". This includes the tracing of any of the paths required, be they primary paths, secondary paths or loci of singular points, the branching onto these paths as well as the automatic selection of step sizes. In general the methods used to compute the results in this chapter have been found to be quite successful and thus provide a useful tool for the analysis of problems which have more than one parameter. There is, however, the necessity for more robust and efficient algorithms to be developed so that analyses of this type will become more economical.

The computation of the primary solution paths along prescribed piecewise-linear parameter paths was done using the predictor-corrector method with full Newton-Raphson iteration. This was found to be very efficient but tended to break down at times due to the inter-dependence of the optimum parameter for the automatic incrementation techniques (see section 4.6) and the maximum allowable step length (a parameter input by the user). Generally, though, the arc-length procedures combined with the automatic incrementation was found to be efficient. The Euler chord method of continuation which was used to trace the secondary paths and the loci of the singular points is not efficient

generally but, for reasons discussed previously, it was justifiable to use these methods here. For tracing secondary paths that are very distinct from the primary path (see for example RIKS (1979)) the predictor-corrector method is obviously superior, but this is not the case in this example. Attempts were made to trace the secondary paths using the Newton-Raphson method but much difficulty was experienced. Unfortunately there are no reports of similar studies in the literature so it is difficult to say if this is typical of all genuine large strain bifurcation problems. Most studies of secondary paths have been confined to shallow arch and plate buckling problems which are not genuine large strain problems (see for example RIKS (1979)).

Further research is thus required in the general area of efficiency, especially for the method used to trace loci of singular points. Also, further investigation into the bifurcation behaviour of the cylinder in the region of axial compression is needed in order to evaluate the results obtained in this chapter.

REFERENCES

ABAQUS Theoretical Manual (1982). Hibbitt, Karlsson and Sorenson, Inc., Providence, Rhode Island.

ABBOTT, J.P. (1980). Computing solution arcs of nonlinear equations with a parameter, The Computer Journal, v23, n1, pp.85-89.

ALLGOWER, E. and GEORG, K. (1980). Simplical and continuation methods for approximating fixed points and solutions to systems of equations, SIAM Review, v22, n1, pp.28-85.

ALY, A.S. (1981). A finite element analysis for problems of large strain and large displacement, TICOM Report 81-14, University of Texas at Austin.

BABUSKA, I. and RHEINBOLDT, W.C. (1982). Computational error estimates and adaptive processes for some nonlinear structural problems, Comp. Meth. Appl. Mech. Engng., v34, pp.895-937.

BAPAT, C.N. and BATRA, R.C. (1984). Finite plane strain deformations of nonlinear viscoelastic rubber-covered rolls, Int. J. Num. Meth. Engng., v20, pp.1911-1927.

BATHE, K-J. (1982). Finite Element Procedures in Engineering Analysis. Prentice-Hall Inc., Englewood Cliffs, New Jersey.

BATHE, K-J. and CIMENTO, A.P. (1980). Some practical procedures for the solution of nonlinear finite element equations, Comp. Meth. Appl. Mech. Engng., v22, pp.59-85.

BATHE, K-J. and DVORKIN, E.N. (1983). On the automatic solution of nonlinear finite element equations, Comp. & Struct., v17, n5-6, pp.871-879.

BATOZ, J-L. and DHATT, G. (1979). Incremental displacement algorithms for nonlinear problems, Int. J. Num. Meth. Engng., v14, pp.1262-1267.

BATRA, R.C. (1980). Finite plane strain deformations of rubberlike materials, Int. J. Num. Meth. Engng., v15, pp.145-160.

BERGAN, P.G. (1980). Solution algorithms for nonlinear structural problems, Comp. & Struct., v12, pp.497-509.

BERGAN, P.G., HORRIGMOE, G., KRAKELAND, B. and SOREIDE, T.H. (1978). Solution techniques for non-linear finite element problems, Int. J. Num. Meth. Engng., v12, pp.1677-1696.

BREZZI, F., RAPPAZ, J. and RAVIART, P.A. (1980). Finite dimensional approximation of nonlinear problems; Part I : Branches of nonsingular solutions, Numer. Math., v36, pp.1-25.

BREZZI, F., RAPPAZ, J. and RAVIART, P.A. (1981a). Finite dimensional approximation of nonlinear problems; Part II : Limit points, Numer. Math., v37, pp.1-28.

BREZZI, RAPPAZ, J. and RAVIART, P.A. (1981b). Finite dimensional approximation of nonlinear problems; Part III : Simple bifurcation points, Numer. Math., v38, pp.1-30.

BROCKMAN, R.A. (1984). Economical stiffness formulations for nonlinear finite elements, Comp. & Struct., v18, n1, pp.15-22.

CAREY, G.F. and ODEN, J.T. (1983). Finite Elements: A Second Course; Volume II, The Texas Finite Element Series. Prentice-Hall Inc., Englewood Cliffs, New Jersey.

CESCOTTO, S. and FONDER, G. (1979). A finite element approach for large strains of nearly incompressible rubber-like materials, Int. J. Solids Structs., v15, pp.589-605.

CESCOTTO, S., FREY, F. and MASSONNET, Ch. (1980). On the effective finite element analysis of engineering structures in the nonlinear range, Theoretical and Applied Mechanics, 15th International Congress of Theoretical and Applied Mechanics - ICTAM - Toronto; North-Holland Publishing Company, pp.67-78.

CRISFIELD, M.A. (1979). A faster modified Newton-Raphson iteration, Comp. Meth. Appl. Mech. Engng., v20, pp.267-278.

CRISFIELD, M.A. (1980). The automatic nonlinear analysis of stiffened plates and shallow shells using finite elements, Proc. Inst. Civ. Engrs., Part 2, v69, pp.891-909.

CRISFIELD, M.A. (1981). A fast incremental/iterative solution procedure that handles "snap-through", Comp. & Struct., v13, pp.55-62.

CRISFIELD, M.A. (1982). Accelerated solution techniques and concrete cracking, Comp. Meth. Appl. Mech. Engng., v33, pp.585-607.

CRISFIELD, M.A. (1983). An arc-length method including line searches and accelerations, Int. J. Num. Meth. Engng., v19, pp.1269-1289.

CRISFIELD, M.A. (1984). Accelerating and damping the modified Newton-Raphson method, Comp. & Struct., v18, n3, pp.395-407.

CHADWICK, P., CREASY, C.F.M. and HART, V.G. (1977). The deformation of rubber cylinders and tubes by rotation, J. Austral. Math. Soc., v20 (Series B), pp.62-96.

CHADWICK, P. and OGDEN, R.W. (1971a). On the definition of elastic moduli, Arch. Rat. Mech. Anal., v44, pp.41-53.

CHADWICK, P. and OGDEN, R.W. (1971b) A theorem of tensor calculus and its application to isotropic elasticity, Arch. Rat. Mech. Anal., v44, pp.54-68.

DAHLQUIST, G. and BJORCK, A. (1974). Numerical Methods. Prentice-Hall Inc., Englewood Cliffs, New Jersey.

DECKER, D.W. and KELLER, H.B. (1980). Multiple limit point bifurcation, J. Math. Anal. Appl., v75, n2, pp.417-430.

DECKER, D.W. and KELLER, H.B. (1981). Path following near bifurcation, Comm. Pure Appl. Math., v XXXIV, pp.149-175.

DEN HEIJER, C. and RHEINBOLDT, W.C. (1981). On steplength algorithms for a class of continuation methods, SIAM J. Numer. Anal., v18, n5, pp.925-948.

DEUFLHARD, P. (1979). A stepsize control for continuation methods and its special application to multiple shooting methods, Numer. Math., v33, pp.115-146.

DUFFETT, G. and REDDY, B.D. (1983). The analysis of incompressible hyperelastic bodies by the finite element method, Comp. Meth. Appl. Mech. Engng., v41, pp.105-120.

ENDO, T., ODEN, J.T., BECKER, E.B. and MILLER, T. (1984). A numerical analysis of contact and limit-point behaviour in a class of problems of finite elastic deformation, Comp. & Struct., v18, n5, pp.899-910.

FINK, J.P. and RHEINBOLDT, W.C. (1984). Solution manifolds and submanifolds of parameterized equations and their discretization errors, Numer. Math., v45, pp.323-343.

FRIED, I. (1984). Orthogonal trajectory accession to the nonlinear equilibrium curve, Comp. Meth. Appl. Mech. Engng., v47, pp.283-297.

FUJIKAKE, M. (1985). A simple approach to bifurcation and limit point calculations, Int. J. Num. Meth. Engng., v21, pp.183-191.

GLOWINSKI, R. and LE TALLEC, P. (1982). Numerical solution of problems in incompressible finite elasticity by augmented Lagrangian methods I. Two-dimensional and axisymmetric problems, SIAM J. Appl. Math., v42, n2, pp.400-429.

GLOWINSKI, R. and LE TALLEC, P. (1984). Numerical solution of problems in incompressible finite elasticity by augmented Lagrangian methods II. Three-dimensional problems, SIAM J. Appl. Math., v44, n4, pp.710-733.

GURTIN, M.E. (1981). An Introduction to Continuum Mechanics. Academic Press, New York.

HAGGBLAD, B. and SUNDBERG, J.A. (1983). Large strain solutions of rubber components, Comp. & Struct., v17, n5-6, pp.835-843.

HAUGHTON, D.M. (1980). Post-bifurcation of perfect and imperfect spherical elastic membranes, Int. J. Solids Structs., v16, pp.1123-1133.

HAUGHTON, D.M. and OGDEN, R.W. (1978a). On the incremental equations in non-linear elasticity - I. Membrane theory, J. Mech. Phys. Solids, v26, pp.93-110.

HAUGHTON, D.M. and OGDEN, R.W. (1978b). On the incremental equations in non-linear elasticity - II. Bifurcation of pressurized spherical shells, J. Mech. Phys. Solids, v26, pp.111-138.

HAUGHTON, D.M. and OGDEN, R.W. (1979a). Bifurcation of inflated circular cylinders of elastic material under axial loading - I. Membrane theory for thin-walled tubes, J. Mech. Phys. Solids, v27, pp.179-212.

HAUGHTON, D.M. and OGDEN, R.W. (1979b). Bifurcation of inflated circular cylinders of elastic material under axial loading - II. Exact theory for thick-walled tubes, J. Mech. Phys. Solids, v27, pp.489-512.

HIBBITT, H.D. (1979). Some follower forces and load stiffness, Int. J. Num. Meth. Engng., v14, pp.937-941.

IOOSS, G. and JOSEPH, D.D. (1980). Elementary Stability and Bifurcation Theory. Springer, Berlin.

JANKOVICH, E., LEBLANC, F., DURAND, H. and BERCOVIER, M. (1981). A finite element method for the analysis of rubber parts, experimental and analytical assessment, Comp. & Struct., v14, n5-6, pp.385-391.

KAMAT, M.P., WATSON, L.T. and VENKAYYA, V.B. (1983). A quasi-Newton versus a homotopy method for nonlinear structural analysis, Comp. & Struct., v17, n4, pp.579-585.

KARAMANLIDIS, D., HONECKER, A. and KNOTHE, K. (1981). Large deflection finite element analysis of pre- and postcritical response of thin elastic frames, Nonlinear Finite Element Analysis in Structural Mechanics, ed. Wunderlich, W., Stein, E. and Bathe, K-J., Springer-Verlag, pp.217-235.

KELLER, H.B. (1977). Numerical solution of bifurcation and nonlinear eigenvalue problems, Applications of Bifurcation Theory, ed. Rabinowitz, P.H., Academic Press, New York, pp.359-384.

KELLER, H.B. (1981). Geometrically isolated nonisolated solutions and their approximation, SIAM J. Numer. Anal., v18, n5, pp.822-838.

KIKUCHI, F. (1978). Finite element approximation of bifurcation problems, Theoretical and Applied Mechanics, v26, Proceedings of 26th Japanese National Congress for Applied Mechanics, Tokyo; North-Holland Publishing Company, pp.37-51.

KLINGBEIL, W.W. and SHIELD, R.T. (1966). Large deformation analysis of bonded elastic mounts, Z. Angew. Math. Phys., v17, pp.281-305.

KUBICEK, M. and KLIC, A. (1983). Direction of branches bifurcating at a bifurcation point. Determination of starting points for a continuation algorithm, Appl. Math. and Comp., v13, pp.125-142.

MALKUS, D.S. (1980). Finite elements with penalties in nonlinear elasticity, Int. J. Num. Meth. Engng., v16, pp.121-136.

MEHRA, R.K. and CARROLL, J.V. (1978). Global stability and control analysis of aircraft at high angles-of-attack, Report ONR-CR215-248-2, Scientific Systems Inc., Cambridge, MA.

MOORE, G. and SPENCE, A. (1980). The calculation of turning points of nonlinear equations, SIAM J. Numer. Anal., v17, n4, pp.567-576.

ODEN, J.T. (1972). Finite Elements of Nonlinear Continua. McGraw-Hill, New York.

ODEN, J.T. and CAREY, G.F. (1983). Finite Elements: Mathematical Aspects; Volume IV, The Texas Finite Element Series. Prentice-Hall Inc., Englewood Cliffs, New Jersey.

ODEN, J.T. and KEY, J.E. (1970). Numerical analysis of finite axisymmetric deformations of incompressible elastic solids of revolution, Int. J. Solids Structs., v6, pp.497-518.

ODEN, J.T. and KEY, J.E. (1972). On the effect of the form of the strain energy function on the solution of a boundary-value problem in finite elasticity, Comp. & Struct., v2, pp.585-592.

ODEN, J.T. and KIKUCHI, N. (1982). Finite element methods for constrained problems in elasticity, Int. J. Num. Meth. Engng., v18, pp.701-725.

ODEN, J.T. and REDDY, J.N. (1976). An Introduction to the Mathematical Theory of Finite Elements, Wiley-Interscience, New York.

OGDEN, R.W. (1972a). Large deformation isotropic elasticity - on the correlation of theory and experiment for incompressible rubberlike solids, Proc. R. Soc. Lond., A326, pp.565-584.

OGDEN, R.W. (1972b). Large deformation isotropic elasticity : on the correlation of theory and experiment for compressible rubberlike solids, Proc. R. Soc. Lond., A328, pp.567-583.

OGDEN, R.W. (1974). On stress rates in solid mechanics with application to elasticity theory, Proc. Camb. Phil. Soc., v75, pp.303-319.

OGDEN, R.W. (1976). Volume changes associated with the deformation of rubber-like solids, J. Mech. Phys. Solids, v24, pp.323-338.

OGDEN, R.W. (1978). Nearly isochoric elastic deformations: application to rubberlike solids, J. Mech. Phys. Solids, v26, pp.37-57.

OGDEN, R.W. (1982). Elastic deformations of rubberlike solids, in Mechanics of Solids (R. Hill Anniversary Volume), ed. Hopkins, H.G. and Sewell, M.J., Pergamon Press, pp.499-537.

OGDEN, R.W. and CHADWICK, P. (1972). On the deformation of solid and tubular cylinders of incompressible isotropic elastic material, J. Mech. Phys. Solids, v20, pp.77-90.

OGDEN, R.W., CHADWICK, P. and HADDON, E.W. (1973). Combined axial and torsional shear of a tube of incompressible isotropic elastic material, Quart. J. Mech. Appl. Math., v XXVI, Part 1, pp.23-41.

ORTEGA, J.M. and RHEINBOLDT, W.C. (1970). Iterative Solution of Nonlinear Equations in Several Variables. Academic Press, New York.

PADOVAN, J. and TOVICHAKCHAIKUL, S. (1982). Self-adaptive predictor-corrector algorithms for static nonlinear structural analysis, Comp. & Struct., v15, n4, pp.365-377.

POWELL, G. and SIMONS, J. (1981). Improved iteration strategy for nonlinear structures, Int. J. Num. Meth. Engng., v17, pp.1455-1467.

RALL, L.B. (1969). Computational Solution of Nonlinear Operator Equations. Wiley, New York.

RAMM, E. (1981). Strategies for tracing the nonlinear response near limit points, Nonlinear Finite Element Analysis in Structural Mechanics, ed. Wunderlich, W., Stein, E. and Bathe, K-J., Springer-Verlag, pp.63-89.

RHEINBOLDT, W.C. (1978). Numerical methods for a class of finite dimensional bifurcation problems, SIAM J. Numer. Anal. v15, n1, pp.1-11.

RHEINBOLDT, W.C. (1980). Solution fields of nonlinear equations and continuation methods, SIAM J. Numer. Anal., v17, n2, pp.221-237.

RHEINBOLDT, W.C. (1981). Numerical analysis of continuation methods for nonlinear structural problems, Comp. & Struct., v13, pp.103-113.

RHEINBOLDT, W.C. (1982). Computation of critical boundaries on equilibrium manifolds, SIAM J. Numer. Anal., v19, n3, pp.653-669.

RIKS, E. (1972). The application of Newton's method to the problem of elastic stability, J. Appl. Mech., v39, pp.1060-1065.

RIKS, E. (1979). An incremental approach to the solution of snapping and buckling problems, Int. J. Solids Structs., v15, pp.529-551.

RIKS, E. (1984). Some computational aspects of the stability analysis of nonlinear structures, Comp. Meth. Appl. Mech. Engng., v47, pp.219-259.

RUAS, V. (1981). A class of asymmetric simplical finite element methods for solving finite incompressible elasticity problems, Comp. Meth. Appl. Mech. Engng., v27, pp.319-343.

SANDIDGE, D.W. and ODEN, J.T. (1974). Stability and postbuckling behaviour of hyperelastic bodies at finite strain by the finite element method, Developments in Mechanics, v7. Proceedings of the 13th Midwestern Mechanics Conference, pp.305-320.

SCHARNHORST, T. and PIAN, T.H.H. (1978). Finite element analysis of rubber-like materials by a mixed model, Int. J. Num. Meth. Engng., v12, pp.665-676.

SCHMIDT, W.F. (1978). Adaptive step size selection for use with a continuation method, Int. J. Num. Meth. Engng., v12, pp.677-694.

SCHWETLICK, H. (1984). On the choice of steplength in path following methods, Z. Agnew. Math. Mech., v64, n9, pp.391-396.

SEYDEL, R. (1979). Numerical computation of branch points in nonlinear equations, Numer. Math., v33, pp.339-352.

SEYDEL, R. (1983). Branch switching in bifurcation problems for ordinary differential equations, Numer. Math., v41, pp.93-116.

SHIELD, R.T. (1983). Equilibrium solutions in finite elasticity, J. Appl. Mech., v50, pp.1171-1180.

SIMO, J.C. and TAYLOR, R.L. (1982). Penalty function formulations for incompressible nonlinear elastostatics, Comp. Meth. Appl. Mech. Engng., v35, pp.107-118.

SIMPSON, R.B. (1975). A method for the numerical determination of bifurcation states of nonlinear systems of equations, SIAM J. Numer. Anal., v12, n3, pp.439-451.

STRANG, G. (1980). Linear Algebra and its Applications, 2nd Edition. Academic Press, New York.

STRICKLIN, J.A., HAISLER, W.E. and VON RIESEMANN, W.A. (1973). Evaluation of procedures for material and/or geometrically nonlinear structural analysis, AIAA Journal, v11, n3, pp.292-299.

STROUD, A.H. and SECREST, D. (1966). Gaussian Quadrature Formulas. Prentice-Hall Inc., Englewood Cliffs, New Jersey.

THOMPSON, E.G. (1975). Average and complete incompressibility in the finite element method, Int. J. Num. Meth. Engng., v9, pp.925-932.

THURSTON, G.A. (1969). Continuation of Newton's method through bifurcation points, J. Appl. Mech., v36, pp.425-430.

TRELOAR, L.R.G. (1973). The elasticity and related properties of rubbers, Rep. Prog. Phys., v36, pp.755-826.

WASZCZYSZYN, Z. (1983). Numerical problems of nonlinear stability analysis of elastic structures, Comp. & Struct., v17, n1, pp.13-24.

WATSON, L.T. and HOLZER, S.M. (1983). Quadratic convergence of Crisfield's method, Comp. & Struct., v17, n1, pp.69-72.

WATSON, L.T., HOLZER, S.M. and HANSEN, M.C. (1983). Tracking nonlinear equilibrium paths by a homotopy method, Nonlinear Analysis Theory Methods and Applications, v7, n11, pp.1271-1282.

WATSON, L.T., KAMAT, M.P., and REASER, M.H. (1985). A robust hybrid algorithm for compluting multiple equilibrium solutions, Eng. Comput., v2, pp.30-34.

WEBER, H. (1985). Multigrid bifurcation iteration, SIAM J. Numer. Anal., v22, n2, pp.262-279.

WELLFORD, L.C. and DIB, G.M. (1976). Finite element methods for nonlinear eigenvalue problems and the postbuckling behavior of elastic plates, Comp. & Struct., v6, pp.413-418.

WELLFORD, L.C. and DIB, G.M. (1980). Post-buckling behaviour of structures using a finite element-nonlinear eigenvalue technique, Int. J. Num. Meth. Engng., v15, pp.955-980.

WEMPNER, G.A. (1971). Discrete approximations related to nonlinear theories of solids, Int. J. Solids Structs., v7, pp.1581-1599.

ZHANG, L. and OWEN, D.R.J. (1982). A modified secant Newton method for non-linear problems, Comp. & Struct., v15, n5, pp.543-547.